Modeling Feedback Loops in the Mammalian Circadian Oscillator

D I S S E R T A T I O N

zur Erlangung des akademischen Grades

doctor rerum naturalium
(Dr. rer. nat.)
im Fach Biophysik

eingereicht an der
Mathematisch-Naturwissenschaftlichen Fakultät I
Humboldt-Universität zu Berlin

von
Frau Dipl.-Biol. Sabine Becker-Weimann
geboren am 22.09.1976 in Karlsruhe

Präsident der Humboldt-Universität zu Berlin:
Prof. Dr. Dr. h.c. Christoph Markschies

Dekan der Mathematisch-Naturwissenschaftlichen Fakultät I:
Prof. Dr. Lutz-Helmut Schön

Gutachter:
1. Prof. Dr. Hanspeter Herzel
2. Prof. Dr. Achim Kramer
3. Prof. Dr. Peter Ruoff

eingereicht am: 4. September 2008
Tag der mündlichen Prüfung: 7.Juli 2009

Abstract

In many organisms the circadian clock ticks with a period of approximately 24 hours and enables the organisms to keep track of time even without any environmental time cues. Numerous physiological and cellular processes underly circadian regulation. The molecular clock is a network of intracellular feedback loops: The clock gene products directly or indirectly regulate their own transcription, which results in molecular oscillations.

In this thesis, existing and new mathematical models of the circadian oscillator are used to investigate the meaning of structural features — in particular the design of the feedback loops — for fundamental circadian characteristics. In a simple model ('Goodwin model') which consists of one negative feedback loop, the introduction of saturating kinetics in a degradation term, but not in a production term, supports oscillations.

With a new model that additionally contains a positive feedback loop, circadian oscillations with the correct phases between the clock components are obtained. The phenotype of several clock mutants can be reproduced. The model synchronizes with the light/dark cycle. Its phase can be fixed to either light onset or light offset with different lengths of the day, if circadian restriction of light-input ('gating') is assumed. In this model, the positive feedback has only a minor influence on the robustness of the circadian oscillations towards parameter variations. This explains the rhythmic phenotype of *Rev-erbα*$^{-/-}$ mutant mice that lack a positive feedback. The model can also explain the unexpected regeneration of circadian oscillations in *Per2*^{Brdm1}/*Cry2*$^{-/-}$ double mutant mice. The regeneration of circadian oscillations in the arrhythmic *Per2*^{Brdm1} by additional mutation of *Rev-erbα* is predicted.

By including *Rev-erbα* explicitly into the model, another negative feedback loop is added: This model reproduces circadian dynamics and the phenotypes of several clock mutants.

Finally, models describing different molecular oscillators and general models containing positive or negative feedback loops of varying chain length are compared with respect to their robustness towards parameter variation. The structural design and in particular the kind of feedback underlying the oscillator seems important for the robustness of the model. A correlation between the robustness and temperature compensation in a system is observed. Further analysis of circadian features with these and other models will give insight into underlying principles of the circadian oscillator.

Zusammenfassung

In den meisten Organismen tickt eine zirkadiane Uhr, die eine Periode von ungefähr 24 Stunden aufweist. Sie ermöglicht ihnen die Zeitmessung auch ohne äußere Signale. Zahlreiche physiologische und zelluläre Prozesse unterliege zirkadianer Regulation. Die molekulare Uhr besteht aus gekoppelten intrazellulären Rückkopplungen: Die Produkte der Uhrgene regulieren ihre eigene Bildung direkt oder indirekt und erzeugen so molekulare Oszillationen.
In dieser Arbeit werden bestehende und neue mathematische Modelle des zirkadianen Oszillators verwendet, um die Bedeutung struktureller Merkmale — insbesondere der Art der Rückkopplungen — für grundlegende zirkadiane Eigenschaften zu untersuchen. In einem einfachen Modell ('Goodwin-Modell'), das eine negative Rückkopplung enthält, erleichtert der Einbau von sättigender Kinetik in einen Abbauterm, nicht aber in einen Produktionsterm, Oszillationen.
Ein neues Modell, das außerdem eine positive Rückkopplung enthält, erzeugt korrekte Phasen zwischen den Komponenten. Es reproduziert die Phänotypen von zirkadianen Mutanten. Das Modell synchronisiert mit dem Licht/Dunkel-Rhythmus. Seine Phase bei verschiedenen Photoperioden kann auf den Sonnenaufgang oder Sonnenuntergang stabilisiert werden unter der Annahme von zirkadian reguliertem Lichteinfluß ('gating'). Die positive Rückkopplung hat nur geringen Einfluß auf die Robustheit der Oszillationen gegenüber Parametervariationen. Dies erklärt den rhythmischen Phänotyp von *Rev-erbα*$^{-/-}$ Mäusen, die die positive Rückkopplung nicht besitzen. Die überraschende Wiederherstellung von zirkadianen Oszillationen in der *Per2*^{Brdm1}/*Cry2*$^{-/-}$ Doppelmutante kann mit dem Modell erklärt werden. Die Wiederherstellung zirkadianer Oszillationen in der arhythmischen *Per2*^{Brdm1} Mutante durch zusätzliche Mutation von *Rev-erbα*$^{-/-}$ wird vorausgesagt.
Durch das Einfügen von *Rev-erbα* in das Modell entsteht eine weitere Rückkopplung. Mit diesem neuen Modell koennen dynamische Eigenschaften und Phänotypen von Mutanten reproduziert werden.
Zuletzt werden Modelle verschiedener molekularer Oszillatoren und allgemeine Modelle, die aus eine positiven oder negativen Rückkopplung unterschiedlicher Kettenlänge bestehen, bezüglich ihrer Robustheit bei Parametervariationen verglichen. Die strukturelle Anordnung und speziell die Art der Rückkopplung ist wichtig für die Robustheit der Modelle. Eine Beziehung zwischen der Robustheit und der Fähigkeit zur Temperaturkompensation wird beobachtet. Die weitere Untersuchung zirkadianer Eigenschaften mit diesen und anderen Modellen wird zum Verständnis der zugrundeliegenden Prinzipien des zirkadianen Oszillators beitragen.

Contents

List of Figures

List of Tables

1 The circadian clock

The behavior and physiology of organisms as diverse as plants, the fruit fly and humans varies with a period of approximately 24 hours even if the environment is kept constant and therefore no time cues are available to the organisms. This is due to the circadian clock — an intracellular clock, that enables even single cells to keep track of time independently of external time cues (lat.: *circa diem*: approximately one day).
The circadian clock influences the organisms on all levels of organization: It regulates physiological and behavioral phenomena such as activity patterns and body temperature in homeotherms (Fig. 1.1, [142]) or leave movement in plants [22]. Moreover, it affects cellular processes: about 10% of all mRNAs are transcribed with a circadian pattern, including transcripts involved in processes as diverse as cell cycle and metabolism [85, 122].

An experiment that illustrates the advantage of a circadian clock for an organism is based on the observation of competing cell strains of Cyanobacteria: Strains whose circadian clock had a period close to the external period had a better chance of survival than strains with a deviating period [88]. This advantage can be explained by the ability of such organisms to coordinate the timing of different biological processes. This enables them to anticipate environmental changes that lead to varying needs and conditions at different times of the day. An example for this anticipation is the stress-activated p38-type MAPK in *Neurospora crassa* that is rhythmically activated by the circadian clock. Thereby, the organism gets prepared for the hyperosmotic stress that begins with sunrise [136].
Another advantage for an organism that has an independent internal clock is the ability to measure the time between external events: If the clock is synchronized to one external event, the phase of the clock can be compared with the phase of other external events. Thereby, an organism can determine the length of the day and by that estimate the time of the year. This is of major importance for the time-keeping of seasonal events like the flowering in plants [52]. It is also needed for time-compensated spatial orientation if the sun is used as a compass as by migratory birds or butterflies. With a non-functional circadian clock, for example, the navigation of the monarch butterfly to its overwintering site is disrupted [28].

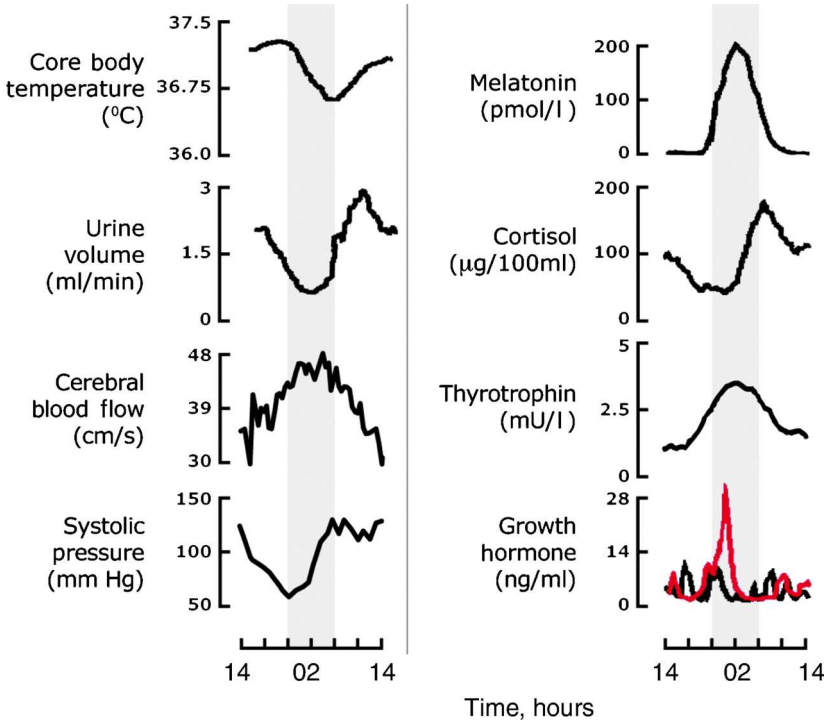

Figure 1.1: Representative physiological (left) and endocrine (right) circadian rhythms measured in suspects under constant dim light conditions. The shaded area depicts the normal sleeping time of the suspects. In the case of growth hormone, levels are not rhythmic in the absence of sleep (black line) but if sleep is permitted a clear circadian cycle emerges (red line). Taken form [48].

Circadian terminology

freerunning period	length of an average circadian cycle in a constant environment
circadian time (CT)	subjective time of an organism; one circadian day (i.e. one cycle of the circadian rhythm) is divided into 24 circadian hours; CT0 represents subjective dawn, CT12 subjective dusk
Zeitgeber	any daily environmental cue to which the circadian system can synchronize or entrain [73]
Zeitgeber time (ZT)	time given by the environment
entrainment	synchronization of the circadian clock by environmental cues
phase response curve	plot of the phase shift that occurs after a light-pulse over the phase when the light-pulse was administered
T-cycle	cycle given by a Zeitgeber with variable length
LL	permanent light
DD	permanent darkness
LD	alternating light and darkness
photoperiod	duration of an organism's daily exposure to light

1.1 Features of the circadian clock

At least three features seem to be characteristic for the circadian clock and necessary for a proper functioning [21].

Circadian period of about 24h

The circadian period is always close to, but not equal to 24h under constant conditions. In mice, for example, the period usually deviates less than 30min from 24h [92]. This supports good synchronization with a fixed phase between external time and internal clock [94].

Synchronization

The circadian clock is able to synchronize with the external light/dark cycle. Therefore it needs to be responsive to light or other stimuli, that vary daily. Indeed, the circadian rhythm of mice kept in conditions of constant darkness can be phase-shifted by a light-pulse and other synchronizing agents. The extent of the phase-shift and its direction depends on the phase of the circadian clock (circadian time) at which the light-pulse occurs. This correlation can be depicted by a so-called phase-response curve (Fig. 1.2). In the case of synchronization (entrainment) of the clock to the external 24 h rhythm, the varying responsiveness of the clock at different circadian times determines the phase of entrainment between the LD cycle and the inner clock in the synchronized state.
Seasonally changing day lengths (i.e., photoperiods) require mechanisms that adapt the phase of processes regulated by the circadian clock to the changing times of sunrise and sunset. Such mechanisms lead to a constant phase of entrainment between the external events sunrise or sunset and clock-controlled internal events such as activity onset under different photoperiods [93].

Temperature compensation/Robustness

The circadian period remains stable in a wide temperature range. While usually the Q10 value of an enzymatic reaction is in the range of 2 to 3 (which means the reaction rate rises with a factor of 2 to 3 at an increase of the temperature of 10C), the period in most circadian systems hardly changes ($Q_{10} \approx 1$) or even is overcompensated ($Q_{10} < 1$) (Fig. 1.3). It is believed that this is due to temperature compensation. In general, the period of a reliable clock has to be robust towards changes in the environment.

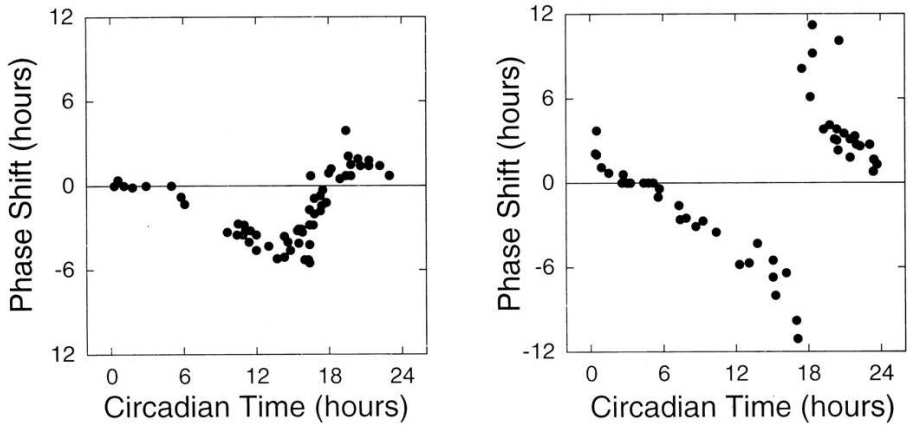

Figure 1.2: Phase-response curve for wildtype (left) and *Clock*/+ (right) mice. The x-axis of the phase-response curve indicates the circadian time at which a light pulse is given, the y-axis indicates the phase-shift following the light pulse. In these particular PRCs, in the wildtype only a phase-shift (advance or delay) of a few hours is possible, while in the mutant an advance or delay of up to 12 h can occur. (Taken from [139])

1.2 Mechanism of the circadian clock

In rats it was found that the lesion of the suprachiasmatic nucleus (SCN) in the brain leads to a loss of the circadian rhythm of behavior [121]. The SCN is a small region of the Hypothalamus that is located above the optic chiasm on either side of the third ventricle [100]. Later it was found, that without the SCN, clocks that are present in many organs go out of phase and show different circadian periods [150](see below how they show it). The SCN is the organ that receives light input via nerves coming from the eyes and sends out humoral and electric signals that control circadian output pathways. Because of this ability to function as a time-giver and synchronizer, the SCN is considered the master clock in mice.
The molecular mechanism of the circadian clock was revealed in several mutants in mice, fruit flies and other species. In those mutants a loss of the circadian rhythmicity or an altered circadian period was observed (Fig. 1.4, [152, 59]). They also show an altered rhythm on the molecular level: While the amount of transcript of most of those genes oscillates with a period of approximately 24h in many tissues of the wildtype, in mutants the oscillations have an altered period or no oscillations occur (Fig. 1.5). The sustained oscillations of mRNA concentrations of about 24h period have even been observed in isolated cells of the Suprachiasmatic Nucleus (SCN) [143] and in single fibroblasts [144]. This indicates that a molecular intracellular clock that is based on a set of so-called clock genes is present in diverse body cells. The circadian clock on the organismic level can only function if the cells containing the circadian oscillators are synchronized to each other and/or the 24h day, since the period of the cells and tissues deviate to different

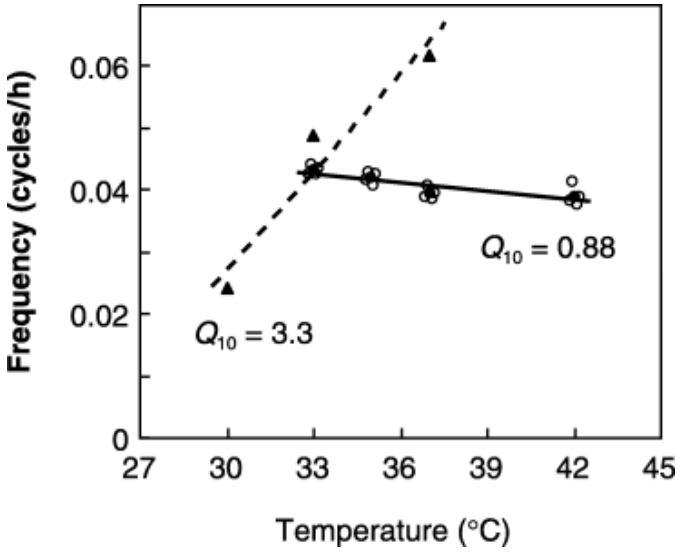

Figure 1.3: Temperature compensation in the circadian oscillator: The period of the circadian rhythm (circles) and the cell cycle (triangles) of NIH3T3 fibroblasts was estimated for different temperatures of the environment. Circadian oscillations were detected by measuring the amount of clock-gene transcripts using quantitative RT-PCR, the period of the cell-cycle was determined by counting the cells. While the period of the cell cycle depends considerably on the temperature, the period of the circadian rhythm is not much effected by it. (Taken from [130])

degrees from 24h [144].
Among the clock-gene mutants that have been found there are also some that show a higher temperature sensitivity compared to the wildtype. However compared to calcium or glycolytic oscillations the circadian oscillations of these mutants are still to a good degree temperature compensated.
A change of the temperature in the environment is only one of many kinds of change that the circadian oscillator has to cope with: It is also exposed to variations in the metabolic state of the cell or to changes of the protein composition, e.g. due to signaling events. Under all circumstances the circadian period has to remain stable for a proper functioning of the clock. At the same time, the system has to be sensitive towards external stimuli that entrain the clock. How robustness and sensitivity can be achieved at the same time, is not known. Besides the robustness of the circadian period, the robustness of phases as well as of the shape of oscillations might be important. Phase relations that might play a role for the clock include those between different components of the clock and those between the circadian clock and an external zeitgeber.

We see that all the characteristic features of the circadian clock — the circadian period, synchronization and temperature compensation/robustness — play an important role even on the cellular level. The origin of those features can probably be found in the

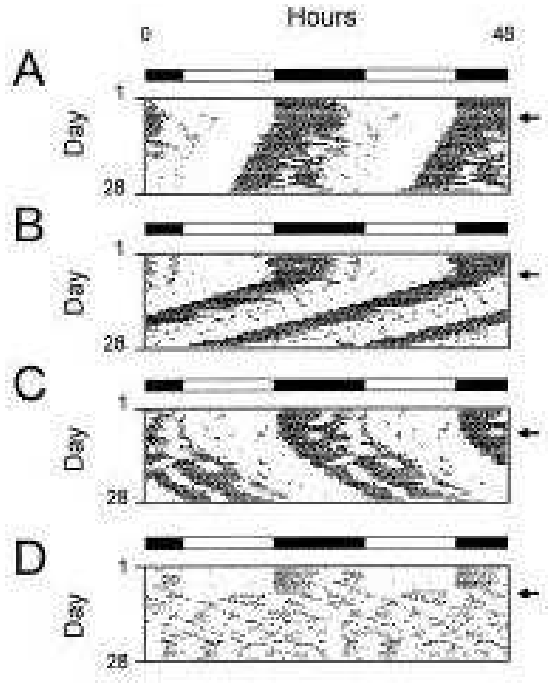

Figure 1.4: Circadian rhythm of locomotor activity in wildtype and mutant mice. Dark areas mark high activity, light areas low activity. A: In a light-dark cycle (LD) of 12h light and 12h darkness the activity of the mouse is synchronized with the external light-dark cycle. When the light is switched off (arrow) and the mouse is kept in permanent darkness (DD), the activity remains periodic, but the period is slightly shorter than 24h. B,C,D: Different mutations of clock genes and their effect on the circadian rhythm. The period can get shorter or longer or the circa 24h period can disappear completely. Taken from [137].

molecular mechanism that leads to the circadian oscillations, that will be explained in the following.

The molecular oscillator

The circadian oscillations are the result of a complex intracellular regulatory network of feedback loops in which the proteins encoded by the clock genes activate or inhibit their own expression directly and/or indirectly (Fig. 1.6, [100]). A list of the most important clock genes in mice and the phenotypes of found mutations is given in table 1.2.
The circadian oscillators of the various species differ in the molecular details. More complex organism tend to have a more complex clock. In this thesis, I will focus on the description of the circadian oscillator in mice, as this is the mammal with the highest amount of data available.

Proteins		Mutations[1]	
Family	Member	Gene(s)	Behavioral phenotype[2]
bHLH-PAS	CLOCK[3]	*Clock*[4]	Long period, then arrhythmic
	BMAL1 (MOP3)	*Bmal1 (Mop3)*	Arrhythmic
PER-PAS	PER1	*Per1* or *Per1 + Per3*	Short period, then arrhythmic
	PER2	*Per2* or *Per2 + Per3*	Short period, then arrhythmic
	PER3	*Per3*	Short period
		Per1 + Per2	Arrhythmic
Flavoproteins	CRY1	*Cry1*	Short period
	CRY2	*Cry2*	Long period
		Cry1 + Cry2	Arrhythmic
Casein kinase	CKIϵ	*CkI*ϵ[5]	Short period
Orphan nuclear receptor	REV-ERBα	*Rev-erb*α	Short Period

Table 1.1: Components of the mouse clock mechanism and the effect of their mutation (Taken from [100])

[a] Unless otherwise noted, the mutations listed are deletion mutations induced by targeted mutagenesis

[b] The most severe phenotypes of homozygous mutant animals studied under constant conditions are listed

[c] A CLOCK-like role has been described for MOP4 (also known as NPAS2) — a bHLH-PAS transcription factor closely related to CLOCK — in the cerebral cortex and in the vasculature [77].

[d] Ethylnitrosourea-induced semidominant autosomal mutation. The mutation is a nucleotide transversion in a splice donor site causing exon skipping and deletion of part of the transactivation domain [138].

[e] Spontaneous semidominant autosomal mutation described in the Syrian hamster (the *tau* mutation). The mutant enzyme is deficient in its ability to phosphorylate PER [97].

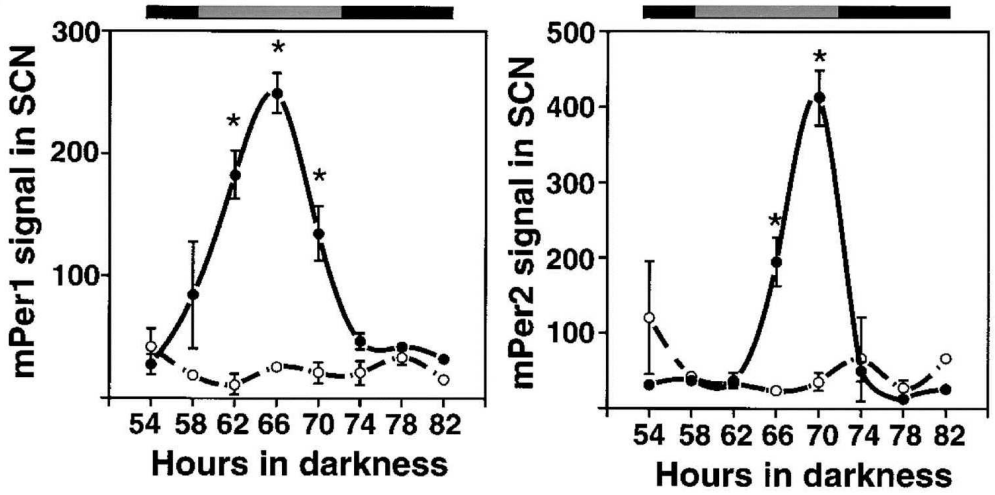

Figure 1.5: Oscillations of clock gene encoded mRNA transcripts in wildtype and clock mutant. Time course of *mPer1* (left) and *mPer2* (right) expression in the SCN of wild-type (filled circles) and $Bmal1^{-/-}$ (open circles) mice held in constant darkness. The bar at the top indicates subjective night in black and subjective day in gray. Asterisks indicate significant differences between wild-type and $Bmal1^{-/-}$ mice at the times shown. Taken from [14]

The negative feedback loop that can be considered the core of the circadian oscillator consists of the clock gene products BMAL1 (also called MOP3), CLOCK, PERIOD1 (PER)1 and PER2, CRYPTOCHROME (CRY)1 and CRY2. BMAL1 and CLOCK are both transcription factors that contain basic helix-loop-helix (bHLH)-PAS (Period-Arnt-Single-minded) domains. As a heterodimer, they activate the transcription of the *Per* and *Cry* genes (*Per3* seems to have a minor role in the core oscillator) [14, 31, 153]. As a consequence, the mRNA levels of *Per* and *Cry* rise, which after a delay also leads to an increase of PER1, PER2, CRY1 and CRY2 protein concentrations. Several hours after the mRNA concentration has reached its maximum, those proteins accumulate in the nucleus, where they inhibit their own transcription by binding to BMAL1/CLOCK [54, 113]. As a result, the levels of *Per* and *Cry* mRNA decrease again, followed by the inhibitory protein concentrations, and the process starts all over again. Posttranslational processes like phosphorylation, nuclear transport and complex formation seem to play an important role for the delay between transcription and nuclear accumulation that is necessary for the oscillations[1].
While the mRNA level of *Clock* can be regarded as constant [75], the BMAL1 protein concentration is oscillating with a circadian period [126]. Moreover, the mRNA level of *Bmal1* has been shown to be decreased in the $Per2^{Brdm1}$ mutant, that is considered to be a null-mutant. This indicates that PER2 is activating *Bmal1* transcription, either directly or indirectly. This suggests that PER2 and BMAL1 form a positive feedback loop in addition to the negative feedback loop: In this case, PER2 would be activating

its own transcription by increasing the amount of its transcriptional activator BMAL1 [113].
Another clock-gene, *Rev-erbα*, might be involved in this positive feedback loop, making it a negative-negative feedback loop: REV-ERBα is a transcription factor, that inhibits the transcription of *Bmal1* [95]. Activation of *Bmal1* transcription by PER2 could therefore be the result of the inhibition of *Rev-erbα* transcription by PER2. As the transcription of *Rev-erbα* is activated by BMAL1, those two proteins form another feedback loop: BMAL1 inhibits its own transcription by increasing the concentration of the transcriptional inhibitor REV-ERBα. An overview of those feedback loops is given in Fig. 1.6.

With the rising number of known clock genes and new experiments the view of the circadian clock becomes more complex, containing an increasing number of feedback loops. For example, RORα, which is activated by BMAL1/CLOCK, activates *Bmal1* transcription by competing for the same binding site as *Rev-erbα* [42].

1.3 Mathematical modeling of the circadian oscillator

Today more and more molecular details about the circadian oscillator are known, and many recent models represent the molecular processes underlying the clock to some degree. Such processes can be described mathematically by differential equations. The variables of the equations represent the molecular components, the parameters their attributes like half-lives, time constants, etc. The couplings between the differential equations represent the interactions between the components. The kinetics of the molecular processes can be included by usage of the corresponding mathematical term for each process.
With such a model, an interesting set of questions and problems can be addressed: How do specific proteins, processes and feedback loops function and what do they mean for the clock? And how can they contribute to the three basic features of the circadian clock? In the following, I summarize the achievements of former models and open questions regarding those features. In 1.4, I will show how some of these questions are addressed in this thesis.

Oscillations with a period of about 24h

Generally, in a feedback system that is dominated by a negative feedback, such as the circadian clock, the appearance of oscillations depends on the phase between the components as well as the presence of sufficient amplification of the signal that is feeding back. As it is not known which processes cause the phase-shift or amplification *in vivo*, many different approaches have been made in modeling the circadian oscillator: In some models a large phase shift is achieved either by using a high number of feedback components [26] or — to keep the model simple — by including a delay like in [116] (model for the *Drosophila* circadian oscillator). A high amplification is achieved by using non-linear

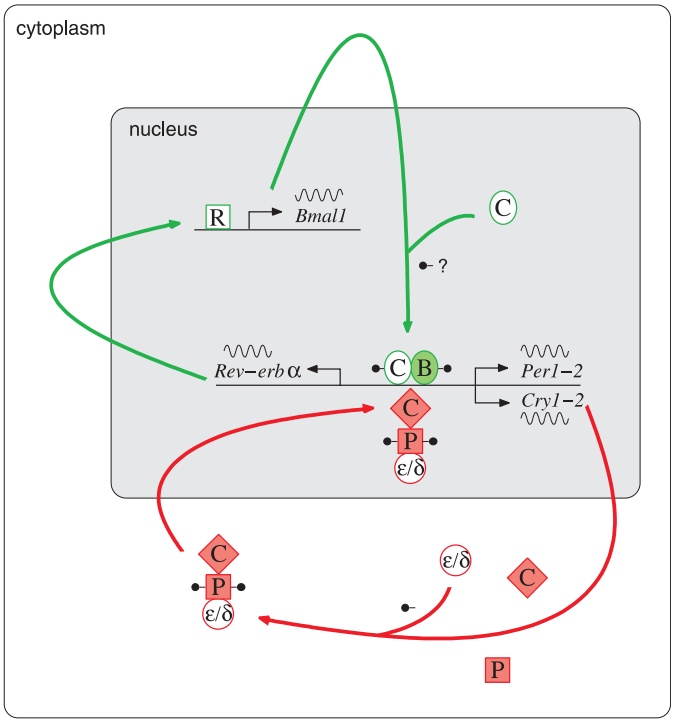

Figure 1.6: Schematic view of the mammalian circadian core oscillator (modified from [100]). The clock mechanism comprises interlocked positive (green) and negative (red) feedback loops. The heterodimer BMAL1/CLOCK (C, B, green ovals) activates transcription of Per, Cry and Rev-erbα genes. PER proteins (P, red square) are phosphorylated (•) and form a complex with CRY proteins (C, red diamond) and CKIϵ, δ (ϵ, δ, red circle). In the nucleus this complex inhibits the transactivational activity of BMAL1/CLOCK, thus forming the negative feedback loop. In the positive feedback loop, Bmal1 transcription is activated (de-repressed) by PER/CRY/CKIϵ, δ, since this complex also inhibits REV-ERBα synthesis (R, green square), which on its part represses Bmal1 transcription. The action of kinases (?) other than CKIϵ and CKIδ is likely (Sanada et al., 2002).

dynamics, e.g. by high Hill coefficients that simulate cooperativity in chemical reactions [38] or Michaelis Menten kinetics that describe saturated reaction rates [69] (see chapter 2).

The period of an oscillator depends on the time constants of the processes involved. In mathematical models, the parameters are determined by those time constants. Unfortunately, most of the time constants for circadian processes are not known today, and therefore information about the parameters of a model is very limited. As a substitute, the time constants of processes such as transcription, transport and degradation for mRNA and proteins not involved in the clock can be taken from the literature [47, 141]. These can be used to make reasonable estimates of parameters for the models. Most

recent models are therefore semi-quantitative and will be so, until more kinetic data is available.
A qualitative investigation of the period of the oscillator can be done by simulating circadian mutants: They show an altered period or a loss of oscillations. The comparison of such period changes in the model with the corresponding experimental outcomes is a good quality control for the model [69]. In a next step, a model should be able to also reproduce counterintuitive period changes and predict the outcome of future experiments.
In this thesis, we investigate the effect of different kinetics for the occurrence of oscillations. In two new models of the circadian oscillator mutants are reproduced and predictions for a further mutant is made.

Synchronization

Two different aspects of synchronization are interesting: the synchronization between the clock and the external Zeitgeber, e.g. the day/night rhythm, and the synchronization between different clocks in the body, like between cells or between the SCN and other tissues.
In the detailed molecular models, biological knowledge of the signal that synchronizes the clock is taken into account. In models of the clock in *Drosophila* therefore synchronization with the day/night rhythm is realized by degradation of the protein TIM, the analog of the mammalian CRY protein in *Drosophila* [68]. In a model investigating synchronization between cells in the SCN, the release of neurotransmitter and a signaling cascade that acts on neurotransmitter release are taken into account [12].
For mammals, modeling synchronization with the day/night rhythm is a bit more difficult: Reasonable phase-response curves are not easily modeled (see chapter 5, [69]). PRCs indicate in which phase relation the oscillator synchronize to the day/night rhythm. The reason might be, that here the synchronizing event seems to be an increase of *Per1* and/or *Per2* mRNA rather than degradation as in *Drosophila*. Modeling synchronization in mammals could therefore reveal characteristics of the circadian oscillator that are so far not understood.
In this thesis synchronization of the mammalian oscillator with the day/night rhythm is investigated.

Temperature compensation/Robustness of the circadian clock

How can the clock be robust towards disturbances, but sensitive towards signals? Period and phase changes are usually not desired, but the clock has to be able to react on stimuli under according conditions.
Investigation of the sensitivity of mathematical models towards parameter changes not only sheds light on the 'weak spots' of the oscillator (e.g. which biological reactions have to be stabilized in the cell, which might be used for regulation), but also tells us where refinement of the model might be useful.
The stability of the circadian oscillator can be investigated using sensitivity analysis:

Parameters of the mathematical models are varied to certain degrees and the effect on the period or other criteria like phase are investigated [69, 115, 119, 7]. These parameter variations indicate how sensitive the model is towards perturbations, where the weak spots of the circadian oscillator could be that have to be stabilized and that can be used for regulation. It also shows which processes are sensitive towards temperature changes. Temperature compensation in modeling means that a variation of all parameters reflecting a change of temperature does not lead to a change of the period. This has been investigated e.g. by [67, 105, 131].
In this thesis, the influence of a positive feedback and of the structural design of the oscillator on the robustness are investigated in the newly constructed model of the circadian oscillator and in several models of biological oscillators, respectively.

1.4 Description of this work

Mathematical models have to i. be compatible with experiments and ii. possess the right complexity to answer specific questions. In this thesis I use models with varying kinetics, complexity and underlying mechanism to examine fundamental features of the circadian clock. The focus is on the meaning of the feedback design on the circadian characteristics.
Using a relatively simple model with only one feedback with three components, I investigate how different kinetics influence the occurrence of circadian oscillations. I find that Michaelis Menten kinetics in a degradation term, but not in a production term supports oscillations.
Two models of the circadian core oscillator in mice are introduced: One includes a negative and a positive feedback and consists of seven components. The other model includes an additional negative feedback and consists of eight components. They are detailed enough to investigate the effect of biological mutations but are minimized with respect to the number of components and the kinetic complexity.
With the two models I reproduce not only the circadian period of about 24h in wildtype mice, but the models also describe well the phases and amplitude of components and the phenotype of several circadian mutants. The interplay of the different feedback loops lead to complex dynamic behavior in both models.
Further investigation of the first model shows how period changes due to parameter variation in one feedback loop can be compensated for by variation of a parameter in the other loop. The observed pattern of period changes and compensation is in agreement with the non-intuitive rescue of oscillations in the $Per2^{Brdm}$/ $Cry2^{-/-}$ double mutant. With the same model, I was also able to predict the phenotype of the $Per2^{Brdm1}$/ $Rev\text{-}erb\alpha^{-/-}$ double mutant: I expect a rhythmic phenotype. The verification of this result would be a strong hint for the suitability of the model.
Together with Florian Geier, I investigated the synchronization of the circadian clock with the day/night rhythm using the two feedback model. By varying the period of the oscillator and the phase response curve, the conditions for a stable phase of synchronization to either light onset or offset with varying daylengths are examined. We find

that the combination of the period and the shape of the PRC determines which phase is conserved and how well it is conserved.
The sensitivity of different biological feedback systems towards disturbances is investigated and compared in a work with Jana Wolf. The two feedback model was used along with other models of the circadian clock, the glycolysis, and the cell cycle. The circadian models tend to be more robust than the others. In addition, the robustness of more general models including a single positive or a single negative feedback with varying chain length was compared. The models including the negative feedback are more robust. The results indicate a correlation between the robustness of the system and temperature compensation.

1.5 Outline

In chapter 2, a variation of the Goodwin model is used to examine the role of saturating kinetics for the development of oscillations analytically. In chapters 3 and 4 new models of the circadian core oscillator are described. A model with a negative and a positive feedback is used in chapter 3 to explain the behavior of clock mutants, make predictions for future experiments. In chapter 4, this model is extended by another negative feedback loop and adjusted to circadian data. In chapter 5, the two feedback model is used to investigate entrainment to the day/night rhythm. The robustness of the period in several circadian models is compared with the robustness in other biological oscillators in chapter 6. In chapter 7, the results are discussed, and in chapter 7.2, an outlook into the future of the work is given.

2 Michaelis-Menten kinetics in the Goodwin model

The Goodwin model (see 1, [38, 108]) is a simple and widely used model for molecular oscillations (and especially circadian). It consists of three differential equations with only one non-linear term containing a Hill-coefficient. It has been shown by Griffith [40], that oscillations can only occur in the Goodwin model with three states, if the Hill coefficient is larger than 8. The Goodwin model itself cannot be solved analytically, but the conditions for oscillations can be obtained by linearization of the system around the steady state and usage of the Hurwitz's criterion.
In this chapter, the necessary conditions for oscillations of the Goodwin model are examined, assuming Michaelis-Menten kinetics for various terms in the model. In particular, I analyze, how the introduction of Michaelis Menten kinetics affects the minimum Hill-coefficient that is necessary for oscillations.
Michaelis-Menten kinetics describes the saturation of a reaction velocity. It is used, if a reaction rate is limited to some maximum rate. This could, for example, occur if the reaction rate does not only depend on a single component that is included in the model, but also on another factor that is not explicitly described in the model. In the circadian system, transport proteins or components of the protein production or degradation machinery could be such a factor, if they are not included into the model.
The Hill-coefficient is an exponent of a concentration, whose introduction is motivated by the cooperativity of several molecules in an inhibition or activation process. In circadian models it is often used to describe the inhibition of transcription by PER and CRY proteins. In those models, it most likely does not represent a cooperative effect in the classical sense, but rather simulates a switch-like response of the transcription on small changes of inhibitor concentration. This switch most likely results from a complex change of chromatin structure and protein complex formation, that regulates gene transcription and is not modeled explicitly [11].
Both Michaelis-Menten kinetics and the Hill-term are kinetic descriptions that can increase the parameter space in which a model is oscillating and therefore can promote oscillations. Due to that, they are often found in simple models of the circadian oscillator [33, 108].
In this chapter, I introduce Michaelis-Menten kinetics into different terms of the Goodwin model and investigate how they affect the minimum Hill-coefficient that is necessary for oscillations. It turns out, that Michaelis-Menten kinetics in certain but not all terms reduces the necessary Hill-coefficient. The analysis also demonstrates that the occurrence of oscillations does not depend on the cooperativity described by the Hill-coefficient, but only on a high value of the first derivative of the amplifying term.

2.1 Michaelis Menten kinetics in a production term

For the calculations, a normalized Goodwin model [40] is used. The model describes a negative feedback loop. The production of the the protein x_2 is proportional to the amount of mRNA x_1, the production of inhibitor x_3 is to the amount of x_2. x_3 down-regulates the transcription of x_1 (see Appendix 1). In this chapter, the linear kinetics of the production of x_2 is replaced by Michaelis Menten kinetics, i.e. the production is saturating (Eq. 2.2). The differential equations are given by

$$\frac{dx_1}{dt} = \frac{1}{1+(\frac{x_3}{K_I})^p} - \kappa_1 x_1\,, \tag{2.1}$$

$$\frac{dx_2}{dt} = \frac{Vx_1}{K+x_1} - \kappa_2 x_2\,, \tag{2.2}$$

$$\frac{dx_3}{dt} = x_2 - \kappa_3 x_3\,. \tag{2.3}$$

V is the maximal production rate of x_2, K is the Michaelis constant, that equals the concentration of x_1 with half-maximal production rate of x_2. If $V = K \gg x_1$, the term is equivalent to the original linear term.

The linearized system has the form $dx/dt = \mathbf{J}x$ with

$$\mathbf{J} = \begin{pmatrix} -\kappa_1 & 0 & \frac{-p(\frac{x_3}{K_I})^{p-1}}{K_I(1+(\frac{x_3}{K_I})^p)^2} \\ \frac{VK}{(K+x_1)^2} & -\kappa_2 & 0 \\ 0 & 1 & -\kappa_3 \end{pmatrix} \tag{2.4}$$

being the Jacobian matrix.
The characteristic equation for finding the eigenvalue is

$$(\lambda+\kappa_1)(\lambda+\kappa_2)(\lambda+\kappa_3) + \frac{VK}{(K+x_1)^2}\frac{p(\frac{x_3}{K_I})^{p-1}}{K_I(1+(\frac{x_3}{K_I})^p)^2} = 0\,. \tag{2.5}$$

In a system of three differential equations with the characteristic equation

$$\lambda^3 + \alpha\lambda^2 + \beta\lambda + \gamma = 0 \tag{2.6}$$

the steady state is stable if and only if the coefficients of the characteristic equation α,β and γ are positive (First of Hurwitz's criteria) and the determinants

$$H_1 = \alpha > 0 \qquad \text{and} \qquad H_2 = Det\begin{pmatrix} \alpha & \gamma \\ 1 & \beta \end{pmatrix} = \alpha\beta - \gamma > 0 \tag{2.7}$$

(Second of Hurwitz's criteria). In this particular system

$$\alpha = \kappa_1 + \kappa_2 + \kappa_3 > 0\,, \tag{2.8}$$

$$\beta = \kappa_1\kappa_2 + \kappa_2\kappa_3 + \kappa_1\kappa_3 > 0\,, \tag{2.9}$$

$$\gamma = \kappa_1\kappa_2\kappa_3 + \frac{VK}{(K+x_1)^2}\frac{p(\frac{x_3}{K_I})^{p-1}}{K_I(1+(\frac{x_3}{K_I})^p)^2} > 0\,. \tag{2.10}$$

The first of Hurwitz's criteria is fulfilled as all $\kappa_{1-3} > 0$. In order to check whether the remaining condition of the second of Hurwitz's criteria is fulfilled, γ is evaluated using the solutions of the differential equations at the steady state: In Eqs. 2.1-2.3, we insert $\dot{x_1} = \dot{x_2} = \dot{x_3} = 0$ and obtain

$$x_2^* = \kappa_3 x_3^*\,, \tag{2.11}$$

$$x_1^* = \frac{K\kappa_2\kappa_3 x_3^*}{V - \kappa_2\kappa_3 x_3^*}\,, \tag{2.12}$$

$$\frac{1}{1+x_3^{*p}} = \kappa_1\kappa_2\kappa_3 x_3^*\frac{K}{V-\kappa_2\kappa_3 x_3^*}\,. \tag{2.13}$$

By inserting Eq. 2.13 into Eq. 2.10 we obtain

$$\gamma = \phi + \frac{VK}{(K+x_1^*)^2}p\phi^2 x_3^*\frac{x_3^*}{K_I}(\frac{x_3^*}{K_I})^{p-1}\frac{K^2}{(V-\kappa_2\kappa_3 x_3^*)^2} \tag{2.14}$$

at the steady state. We have abbreviated $\phi = \alpha\beta\gamma$. Rearrangement of eqs. 2.12 and 2.13 leads to

$$\frac{VK}{(K+x_1^*)^2} = \frac{(V-\kappa_2\kappa_3 x_3^*)^2}{VK} \tag{2.15}$$

and

$$(\frac{x_3^*}{K_I})^p = \frac{V-\kappa_2\kappa_3 x_3^*}{\phi x_3^* K} - 1\,. \tag{2.16}$$

Insertion of Eqs. 2.15 and 2.16 into Eq. 2.14 and simplification leads to

$$\gamma = \phi + \frac{(V-\kappa_2\kappa_3 x_3^*)^2}{VK}p\phi^2 x_3^*(\frac{V-\kappa_2\kappa_3 x_3^*}{\phi x_3^* K} - 1)\frac{K^2}{(V-\kappa_2\kappa_3 x_3^*)^2} \tag{2.17}$$

$$= \phi + p\phi^2 x_3^*\frac{K}{V}(\frac{V-\kappa_2\kappa_3 x_3^*}{\phi x_3^* K} - 1) \tag{2.18}$$

$$= \phi + p\phi - p\phi^2 x_3^*(\frac{1}{\kappa_1 V} + \frac{K}{V}) \tag{2.19}$$

and so the remaining condition of the second of Hurwitz's criteria for a stable system

reads

$$\alpha\beta - \phi - p\phi + p\phi^2 x_3^*(\frac{1}{\kappa_1 V} + \frac{K}{V}) > 0\,. \tag{2.20}$$

We now use the inequality

$$\frac{1}{3}\alpha \geq (\frac{1}{3}\beta)^{\frac{1}{2}} \geq \phi^{\frac{1}{3}} \tag{2.21}$$

with $\alpha = \kappa_1 + \kappa_2 + \kappa_3$, $\beta = \kappa_1\kappa_2 + \kappa_2\kappa_3 + \kappa_1\kappa_3$ and $\phi = \kappa_1\kappa_2\kappa_3$ [46]. By multiplication with 3β we obtain

$$\alpha\beta \geq \sqrt{3}\beta^{\frac{3}{2}} \geq 3\beta\phi^{\frac{1}{3}} \tag{2.22}$$

$$\geq 3 \cdot 3\phi^{\frac{2}{3}}\phi^{\frac{1}{3}} \tag{2.23}$$

$$\geq 9\phi\,. \tag{2.24}$$

and therefore

$$\phi(8-p) + p\phi^2 x_3^*(\frac{1}{\kappa_1 V} + \frac{K}{V}) \geq 0\,. \tag{2.25}$$

This needs to be fulfilled for the system to be stable. As without Michaelis Menten term, oscillations can be obtained if $p > 8$. Michaelis-Menten kinetics in a synthesis term therefore does not reduce the Hill-coefficient necessary for oscillations in the model. Simulation of the model with $\kappa_1 = \kappa_2 = \kappa_3 = 0.5$ shows, that indeed oscillations do not occur with $p < 8$. The larger V and the smaller K are, the smaller p has to be in order to obtain oscillations (fig. 2.1).

2.2 Michaelis Menten kinetics in a degradation term

In a second modification of the Goodwin model one of the linear degradation terms instead of a production term is replaced by a Michaelis-Menten term. This model is described by the differential equations:

$$\frac{dx_1}{dt} = \frac{1}{1+x_3^p} - \kappa_1 x_1\,, \tag{2.26}$$

$$\frac{dx_2}{dt} = x_1 - \frac{V\kappa_2 x_2}{K + x_2}\,, \tag{2.27}$$

$$\frac{dx_3}{dt} = x_2 - \kappa_3 x_3\,. \tag{2.28}$$

In this case the Jacobian matrix is

$$\mathbf{J} = \begin{pmatrix} -\kappa_1 & 0 & \frac{-p(\frac{x_3}{K_I})^{p-1}}{K_I(1+(\frac{x_3}{K_I})^p)^2} \\ 1 & -\frac{VK\kappa_2}{(K+x_2)^2} & 0 \\ 0 & 1 & -\kappa_3 \end{pmatrix}. \tag{2.29}$$

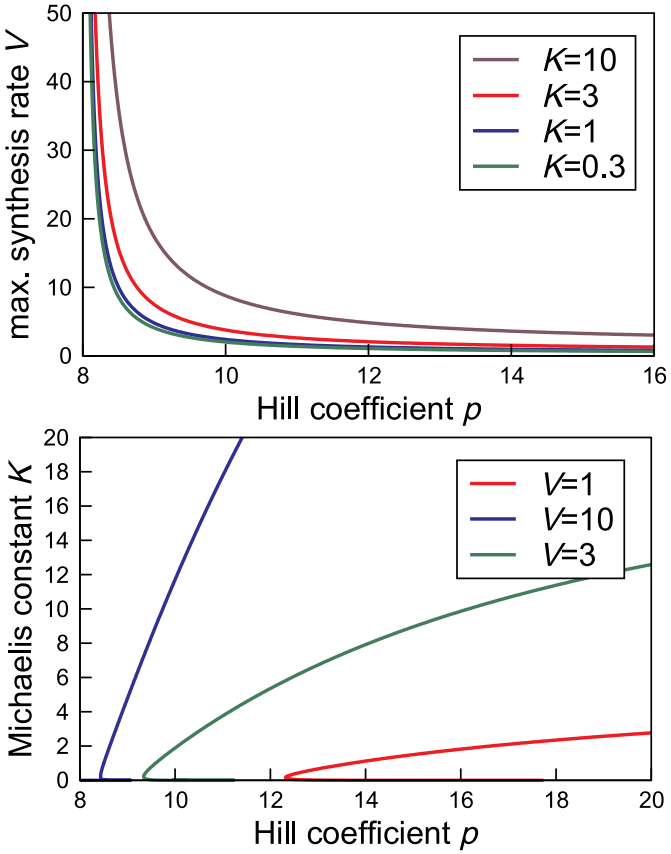

Figure 2.1: Introduction of Michaelis-Menten kinetics into the production term of Eq. 2.2 in the Goodwin model does not promote oscillations. A: Bifurcation diagram of the model with varying p and V with different values of K. The lines mark the boundary between parameter sets leading to oscillations (above lines) and stable steady states (below lines). For larger V and smaller K the oscillatory region increases, but the Hill-coefficient necessary for oscillations never goes below 8. The same can be seen in B: Bifurcation diagram of the model with varying p and K with different values of V. Oscillations occur below, steady states above the lines.

and the characteristic equation is

$$(\lambda+\kappa_1)(\lambda+\frac{VK\kappa_2}{(K+x_2)^2})(\lambda+\kappa_3)+\frac{p(\frac{x_3}{K_I})^{p-1}}{K_I(1+(\frac{x_3}{K_I})^p)^2}=0\,. \tag{2.30}$$

The coefficients of the characteristic equation

$$\lambda^3+\alpha\lambda^2+\beta\lambda+\gamma=0 \tag{2.31}$$

therefore are

$$\alpha = \kappa_1 + \frac{VK\kappa_2}{(K+x_2)^2} + \kappa_3 > 0\,, \tag{2.32}$$

$$\beta = \kappa_1\kappa_2 + (\kappa_1+\kappa_3)\frac{VK\kappa_2}{(K+x_2)^2} > 0\,, \tag{2.33}$$

$$\gamma = \frac{VK\kappa_1\kappa_2\kappa_3}{(K+x_2)^2} + \frac{p(\frac{x_3}{K_I})^{p-1}}{K_I(1+(\frac{x_3}{K_I})^p)^2} > 0\,. \tag{2.34}$$

To find out whether $\alpha\beta - \gamma > 0$ (Second of Hurwitz's criteria) is fulfilled we simplify γ using the solutions of the differential equations at the steady state:

$$x_2^* = \kappa_3 x_3^*\,, \tag{2.35}$$

$$x_1^* = \frac{V\kappa_2\kappa_3 x_3^*}{K+\kappa_3 x_3^*}\,, \tag{2.36}$$

$$\frac{1}{1+x_3^{*p}} = \kappa_1\kappa_2\kappa_3 x_3^* \frac{V}{K+\kappa_3 x_3^*}\,. \tag{2.37}$$

Inserting Eqs. 2.36 and 2.37 in Eq. 2.34 and simplifying, we obtain ($\phi = \kappa_1\kappa_2\kappa_3$)

$$\gamma = \frac{VK\phi}{(K+\kappa_3 x_3^*)^2} + p\phi^2 x_3^* \frac{x_3^*}{K_I}\frac{x_3^*}{K_I}^{p-1}(\frac{V}{K+\kappa_3 x_3^*})^2 \tag{2.38}$$

$$= \frac{VK\phi}{(K+\kappa_3 x_3^*)^2} + p\phi^2 x_3^*(\frac{1}{\phi x_3^*}\frac{K+\kappa_3 x_3^*}{V} - 1)(\frac{V}{K+\kappa_3 x_3^*})^2 \tag{2.39}$$

$$= \frac{VK\phi}{(K+\kappa_3 x_3^*)^2} - p\phi(\phi x_3^*\frac{V}{K+\kappa_3 x_3^*} - 1)\frac{V}{K+\kappa_3 x_3^*}\,. \tag{2.40}$$

With α and β from Eqs.2.32 and 2.33 we can formulate the inequality

$$\alpha\beta \geq 9\tilde{\phi} \qquad \text{with} \qquad \tilde{\phi} = \frac{VK}{(K+\kappa_3 x_3^*)^2}\phi \tag{2.41}$$

in analogy to Eq. 2.24. The second of Hurwitz's criteria for a stable system can therefore be written as

$$0 \leq 8\tilde{\phi} - p\tilde{\phi}(1-\tilde{\phi}x_3^*\frac{K+\kappa_3 x_3^*}{K})\frac{K+\kappa_3 x_3^*}{K} \tag{2.42}$$

$$= \tilde{\phi}(8 - p\frac{K+\kappa_3 x_3^*}{K}) + p\tilde{\phi}^2 x_3^*(\frac{K+\kappa_3 x_3^*}{K})^2\,. \tag{2.43}$$

Therefore, oscillations can only occur if $p > \frac{8K}{K+\kappa_3 x_3^*}$. In this case oscillations are possible even for $p < 8$. Using Michaelis-Menten kinetics for a degradation term is therefore leads to oscillations even with a reduced Hill-coefficient.

Simulation of the model with $\kappa_1 = \kappa_2 = \kappa_3 = 0.5$ shows that oscillations can occur with $p < 8$ (Fig. 2.2), if K is small, i.e. the system operates in the saturating range of the Michaelis-Menten term. There is an optimal value of V for each K in order to obtain oscillations with a low value of p.

2.3 Discussion

This analytic investigation of the effect of Michaelis-Menten kinetics in different positions of the Goodwin model on the range of oscillations shows that saturation in degradation processes favors oscillations, while for saturation in production terms this is not the case. This is in agreement with results obtained with computational approaches, where saturation in degradation terms reduced the necessary Hill-coefficient [33], and obtained in similar calculations by Palsson and Groshans [89] and Kurosawa et al. [64].
The result has certain implications for the cellular conditions that favor oscillations. Saturation of the degradation processes supports oscillations and therefore reduces the need for a high cooperativity in the transcription process. The second of Hurwitz's criteria shows that the exact form of the term describing the inhibition of transcription ($\partial(dx_1/dt)/\partial dx_3$) is not relevant. Only the value of the first derivative at the steady state decides whether or not the system is oscillating. The Hill-function could well be replaced by another function with a large first derivative. Therefore, non-linear switch-like processes like the chromatin-remodeling or complex formation that coincide with the start and stop of transcription, can well explain the oscillations without saturation, even though the Hill-function does not reflect those exact molecular processes.
It is obvious that the kinetic description that is used in a model has a major influence on its dynamic behavior. Therefore, in order to find out how exactly oscillations are generated in the cell, knowing the involved components and interactions is not enough, but a close look at the kinetics is important. Only when that data is available, we will be able to really understand how the circadian oscillations arise in the cell.

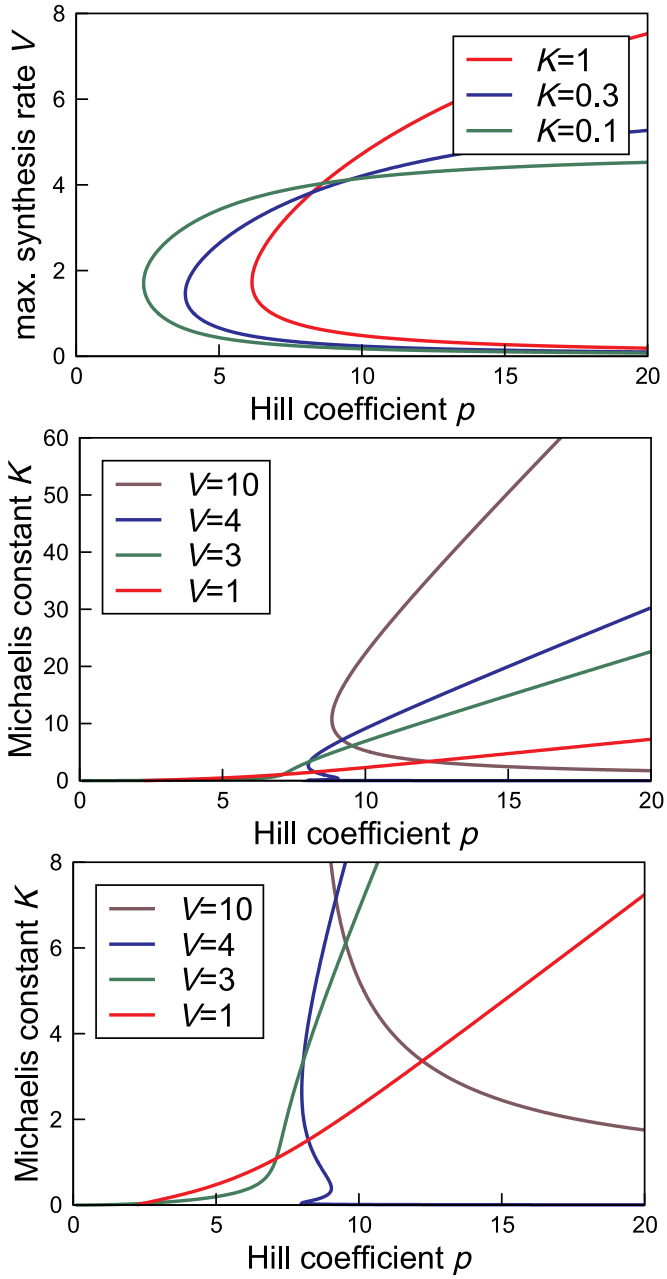

Figure 2.2: Introduction of Michaelis Menten kinetics into a degradation term can lower the value of the Hill-coefficient that is necessary for oscillations. A: Bifurcation diagram of the model with varying p and V with different values of K. Oscillations (right side of lines) are observed for Hill-coefficients as low as 2 (for K=0.1). The same can be seen in B: Bifurcation diagram of the model with varying p and K with different values of V. Oscillations occur with a Hill-coefficient lower than 8, if K is small.

3 Positive and negative feedback in the circadian oscillator

The basic element of the circadian oscillator that can be found throughout species is a delayed negative feedback loop: PERs and CRYs indirectly downregulate their own transcription by inhibiting the transcriptional activator BMAL1 (in mice). Another functional unit, that seems to be present in many circadian clocks is an additional positive feedback loop. In mice, BMAL1 activates it's own transcription via up-regulation of PER which then indirectly activates *Bmal1* transcription (for details see chapter 1). Experiments in the circadian systems of Neurospora, Drosophila and mammals as well as theoretical studies, show the importance of the delayed negative feedback for the generation of oscillations [32]. The function of the positive feedback in the circadian clock, however, is much less understood. Interlocked feedback loops potentially allow for multiple inputs and outputs at different phases [3]. A contribution of the positive feedback to the robustness of the clock has been demonstrated in a study with *Rev-erbα*$^{-/-}$ mutant mice. They essentially lack the positive feedback [95].
In two models [115, 116] the role of the positive feedback in the Drosophila clock has been discussed. Also, models of the circadian oscillator describing the molecular processes in great detail were published [26, 69]. However, they do not focus on the specific function of the positive feedback.
Here, we describe a model for the mammalian circadian oscillator that was designed for investigating the interdependence of the positive and negative feedback. A reduced but essential set of variables is used to analyze the impact of these feedback loops on the dynamics of the oscillator. The model shows sustained oscillations with a period and phases between the components that are in agreement with experimental observations. With and without positive feedback the period, phase and amplitudes of the oscillations show a similar robustness in response to varying single parameters. The simultaneous regulation of the two interlocked feedback loops contributes to the maintenance of oscillations and the stability of the period. Using this model, we propose an explanation for the unexpected phenotype of the *Per2*^{Brdm1}/*Cry2*$^{-/-}$ double mutant mice [87]. In addition, we predict the yet unknown phenotype of the *Per2*^{Brdm1}/*Rev-erbα*$^{-/-}$ double mutant mice to be rhythmic.
The results presented in this chapter were also published in [9].

3.1 Construction of the model

We use a system of ordinary differential equations for the description of the mammalian circadian core oscillator. The variables of the system represent the concentrations of

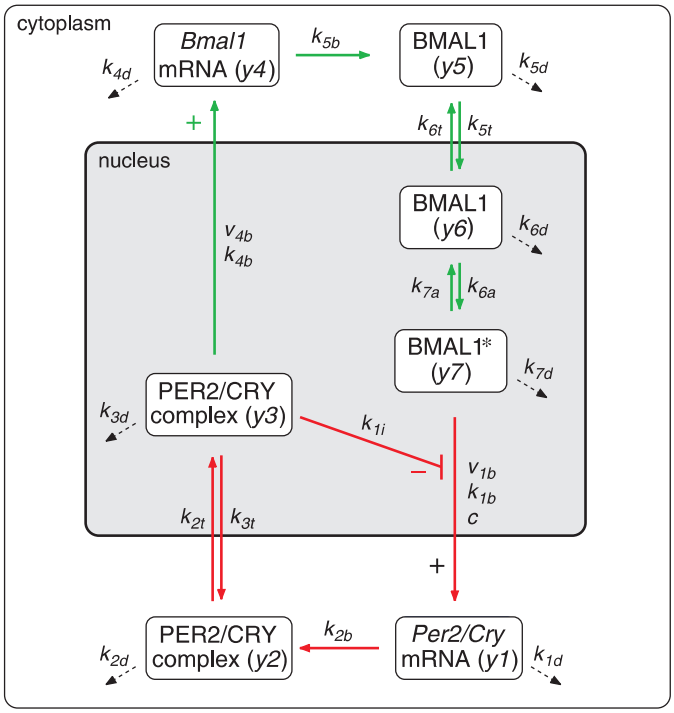

Figure 3.1: Model of the mammalian circadian core oscillator. An activated form of BMAL1 (BMAL1*) activates the transcription of *Per2* and *Cry* genes resulting in an increase of *Per2/Cry* mRNA (y_1). As the levels of PER2 and CRY proteins increase, they form a complex (y_2), which is transported to the nucleus. The nuclear PER2/CRY complex (y_3) inhibits *Per2/Cry* transcription and activates *Bmal1* transcription. As a result, *Bmal1* mRNA (y_4) and protein (y_5) increase. Nuclear BMAL1 (y_6) in its active form (BMAL1*, y_7) restarts transcription of *Per2* and *Cry* genes. Dashed arrows represent degradation of mRNAs and proteins. Reference parameters of the reaction kinetics are given in Table 3.1

clock genes' mRNAs and proteins (Fig. 3.1). We focus specifically on the essential structure of the molecular network in order to characterize the role of the positive and negative feedback loops.

The delay, which is necessary for oscillations in negative feedback loops [27, 32], is caused by processes including post-translational modification, degradation, complex formation as well as nuclear import and export [100]. The transcription factors CLOCK and BMAL1 form a heterodimer and as such activate the transcription of *Per*, *Cry* and *Rev-erbα* genes. For our model, we only consider the activation by BMAL1, since CLOCK is expressed at a constant level [75] and thus can be represented by a fixed parameter. The proteins PER and CRY downregulate their own synthesis by inhibiting the transactivation activity of BMAL1/CLOCK. The *Cry* genes are essential components of the clock network, since null-mutations in these genes have been shown experimentally to disrupt oscillations (in $Cry1^{-/-}$/ $Cry2^{-/-}$ double mutant mice) or alter their

period (in *Cry1*$^{-/-}$ or *Cry2*$^{-/-}$ single mutant mice) [134, 137]. Little is known about the differential functions of the CRY proteins. Therefore, we represent them by a combined variable in the model. In the case of *Per* genes we only include *Per2*, since a null-mutation in the *Per2* gene causes arrhythmicity [153], whereas different phenotypes have been reported for three *Per1*-/- mutant mouse strains [6, 15, 153]. However, in principle, *Per1* could be included into the model (see 3.7). Besides being an inhibitor of BMAL1/CLOCK, PER2 is thought to act positively on the transcription of *Bmal1* [113]. *Per2* and *Cry* mRNAs and proteins are represented by the same variables, respectively, for the following reasons:

- Their expression is co-regulated by BMAL1/CLOCK.
- They form a complex that is necessary for nuclear accumulation [62].
- They are both targets of casein kinase Iδ/ϵ (CKIδ/ϵ) [127, 23].
- The phase of their nuclear accumulation is similar [100].
- They both act negatively on BMAL1/CLOCK transactivational activity in vitro [54, 113].
- Details about the exact differential function of *Cry* and *Per* genes in the core oscillator are not known.

CKIϵ is considered implicitly by assuming fast phosphorylation of PER2 and CRY. This assumption together with the one of a rapid degradation of the monomeric proteins [1, 113] lead to a quasi-steady state of the monomeric PER2 and CRY proteins. Here, we assume similar kinetics for PER2 and CRY, as no data exist about the stability of monomeric CRY. As a consequence, it can be shown that it is not necessary to consider the monomeric proteins as a separate variable in the model (see section 3.2). The PER2/CRY complex in the nucleus inhibits BMAL1/CLOCK activation of *Per*, *Cry* and *Rev-erb*α genes. REV-ERBα has been described to repress *Bmal1* transcription [95, 132]. The double inhibition — PER2/CRY inhibits transcription of *Rev-erb*α, REV-ERBα inhibits transcription of *Bmal1* — constitutes a positive feedback loop.
In our model, REV-ERBα is implicitly taken into account by assuming a positive action of the PER2/CRY complex on *Bmal1* transcription. The model is depicted in Fig. 3.1. The variable y_1 represents the concentration of *Per2* or *Cry* mRNA, which are considered to be identical. The variables y_2 and y_3 represent the concentrations of the PER2/CRY complex in the cytoplasm and the PER2/CRY complex in the nucleus, respectively. The variable y_4 represents the concentration of *Bmal1* mRNA, y_5 the one of cytoplasmatic BMAL1 protein and y_6 the one of BMAL1 protein in the nucleus. The variable y_7 describes the concentration of a transcriptionally active form BMAL1*, which can be understood as a complex with CLOCK [31] and/or as a phosphorylated form of BMAL1 [23].
The dynamics of these variables is described by the following system of differential equations:

$$\frac{dy_1}{dt} = f_{trans(Per2/Cry)} - k_{1d}y_1 \tag{3.1}$$
$$\frac{dy_2}{dt} = k_{2b}y_1^q - k_{2d}y_2 - k_{2t}y_2 + k_{3t}y_3 \tag{3.2}$$
$$\frac{dy_3}{dt} = k_{2t}y_2 - k_{3t}y_3 - k_{3d}y_3 \tag{3.3}$$
$$\frac{dy_4}{dt} = f_{trans(Bmal1)} - k_{4d}y_4 \tag{3.4}$$
$$\frac{dy_5}{dt} = k_{5b}y_4 - k_{5d}y_5 - k_{5t}y_5 + k_{6t}y_6 \tag{3.5}$$
$$\frac{dy_6}{dt} = k_{5t}y_5 - k_{6t}y_6 - k_{6d}y_6 + k_{7p}y_7 - k_{6p}y_6 \tag{3.6}$$
$$\frac{dy_7}{dt} = k_{6p}y_6 - k_{7p}y_7 - k_{7d}y_7 \tag{3.7}$$

Both transcription rates, $f_{trans(Per2/Cry)}$ and $f_{trans(Bmal1)}$, are described by Hill functions implying switch-like behavior of the transcriptional effectors [151] and saturation of transcriptional activity.
The rate of the *Per2/ Cry* transcription

$$f_{trans(Per2/Cry)} = \frac{v_{1b}(y_7 + c)}{k_{1b}(1 + \frac{y_3^p}{k_{1i}^p}) + (y_7 + c)} \tag{3.8}$$

increases with rising BMAL1* concentration y_7 and with decreasing nuclear PER2/CRY concentration y_3. Moreover, a constitutive transcriptional activator of *Per2/Cry* transcription is included in the transcription term by the parameter c. This term is a phenomenological representation of the switch-like behavior of this transcriptional regulation rather than a precise description of molecular processes (see chapter 2).
The transcription rate of *Bmal1* is given by:

$$f_{trans(Bmal1)} = \frac{v_{4b}y_3^r}{k_{4b} + y_3^r}\,. \tag{3.9}$$

It increases with rising PER2/CRY concentration y_3.
We use linear and bilinear kinetics for the description of translation, degradation, complex formation, transport across the nuclear membrane and post-translational modification, as the molecular details of these processes are not fully characterized. A description of the corresponding parameters is given in Table 3.1.

High Hill coefficients, an explicit delay or Michaelis Menten kinetics in negative feedback loops, can reduce the number of reaction steps that are needed in order to obtain oscillations (see chapter 2). For the purpose of this model, we chose to use a small system based on linear kinetics and with a high Hill coefficient, as this keeps the number

Table 3.1: Parameters of the model including one negative and one positive feedback

Parameter	Value	Description
v_{1b}	9 $\mathrm{nMh^{-1}}$	Maximal rate of *Per2/Cry* transcription
k_{1b}	1 nM	Michaelis constant of *Per2/Cry* transcription
k_{1i}	0.56 nM	Inhibition constant of *Per2/Cry* transcription
c	0.01 nM	Concentration of constitutive activator
p	8	Hill coefficient of inhibition of *Per2/Cry* transcription
k_{1d}	0.12 $\mathrm{h^{-1}}$	Degradation rate of *Per2/Cry* mRNA
k_{2b}	0.3 $\mathrm{nM^{-1}h^{-1}}$	Complex formation rate of PER2/CRY
q	2	Number of PER2/CRY complex forming subunits
k_{2d}	0.05 $\mathrm{h^{-1}}$	Degradation rate of the cytoplasmatic PER2/CRY
k_{2t}	0.24 $\mathrm{h^{-1}}$	Nuclear import rate of the PER2/CRY complex
k_{3t}	0.02 $\mathrm{h^{-1}}$	Nuclear export rate of the PER2/CRY complex
k_{3d}	0.12 $\mathrm{h^{-1}}$	Degradation rate of the nuclear PER2/CRY complex
v_{4b}	3.6 $\mathrm{nMh^{-1}}$	Maximal rate of *Bmal1* transcription
k_{4b}	2.16 nM	Michaelis constant of *Bmal1* transcription
r	3	Hill coefficient of activation of *Bmal1* transcription
k_{4d}	0.75 $\mathrm{h^{-1}}$	Degradation rate of *Bmal1* mRNA
k_{5b}	0.24 $\mathrm{h^{-1}}$	Translation rate of BMAL1
k_{5d}	0.06 $\mathrm{h^{-1}}$	Degradation rate of cytoplasmatic BMAL1
k_{5t}	0.45 $\mathrm{h^{-1}}$	Nuclear import rate of BMAL1
k_{6t}	0.06 $\mathrm{h^{-1}}$	Nuclear export rate of BMAL1
k_{6d}	0.12 $\mathrm{h^{-1}}$	Degradation rate of nuclear BMAL1
k_{6a}	0.09 $\mathrm{h^{-1}}$	Activation rate of nuclear BMAL1
k_{7a}	0.003 $\mathrm{h^{-1}}$	Deactivation rate of nuclear BMAL1*
k_{7d}	0.09 $\mathrm{h^{-1}}$	Degradation rate of nuclear BMAL1*

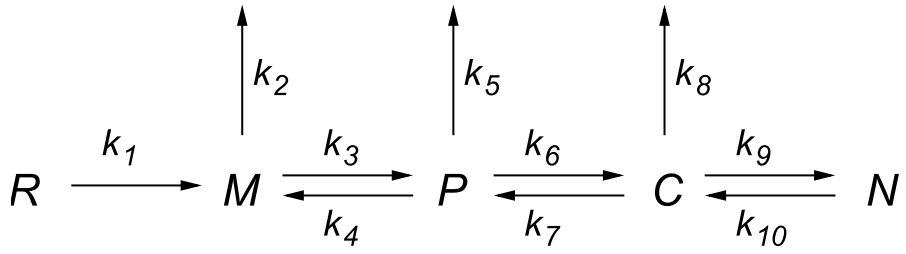

Figure 3.2: Detailed scheme of the steps of PER and CRY production and accumulation.R: *Per2* or *Cry* mRNA; M: PER2 or CRY monomer; P: phosphorylated PER2 or CRY monomer; C: PER2/CRY cytoplasmatic complex; N: nuclear PER2/CRY complex; k_2, k_5, k_8: degradation rates; k_1: translation rate; k_3, k_4: phosphorylation/dephosphorylation rate; k_6, k_7: complex formation/dissociation rate; k_9, k_{10}: nuclear import/export rate

of parameters in the system low. This implies a strong non-linearity of the regulation of *Per2*/*Cry* transcription. Indeed, Etchegaray et al. [24] have recently found that the regulation of CLOCK/BMAL1 activity by CRY proteins is likely to be modulated by histone acetylation and chromatin remodeling in the promoter regions of circadian genes. Multiple histone acetylation events, or other chromatin modifications could contribute to the kinetic non-linearity, which we modeled by using high Hill coefficients in Eqs. (3.8) and (3.9).
The system of differential equations was solved numerically by using a Runge-Kutta algorithm. For the comparison with experimental data and the analysis of robustness the model was implemented in MATLAB (The MathWorks Inc., Natick, Massachusetts), the bifurcation analysis was performed with XPP/AUTO (G. Bard Ermentrout, http://www.pitt.edu/ phase/).

3.2 Simplification of the model

Here we explain in detail the simplification steps done in order to reduce the model. Using the same variables for *Per2* and *Cry* and assuming that PER2 and CRY only enter the nucleus as a phosphorylated complex, the processes of translation, phosphorylation, complex formation and nuclear entry of *Per2*/*Cry* gene products can be described by the following reaction scheme:

The dynamics of M,P and C (Fig. 3.2) can be described as a system of three differ-

ential equations:

$$\frac{dM}{dt} = k_1R - k_2M - k_3M + k_4P \tag{3.10}$$

$$\frac{dP}{dt} = k_3M - k_4P - k_5P - k_6P^2 + k_7C \tag{3.11}$$

$$\frac{dC}{dt} = k_6P^2 - k_7C - k_8C - k_9C + k_{10}N \tag{3.12}$$

The following assumptions are used for the simplification:

1. Phosphorylation and dephosphorylation are considered to be fast processes compared to others (i.e. k_3 and k_4 have a very large value).

2. The monomers are rapidly degraded (large values for k_5 and/or k_2; [113]).

3. Complex dissociation (k_7) is slow and therefore neglected.

Because of (1.) we can assume a rapid equilibrium between M and P. Forward and backward reaction are nearly equally fast, which can be expressed as:

$$k_3M = k_4P \tag{3.13}$$

In this case M can be replaced by P in equation (1). Taking into account (3.), summation of equation (1) and (2) and some transformation steps lead to:

$$\frac{dP}{dt} = \frac{k_3}{k_4 + k_3}(k_1R - \frac{k_2k_4}{k_3}P - k_5P - k_6P^2) \tag{3.14}$$

With the assumption of fast degradation of the monomers (2.) variable P is in a quasi-steady state. In this case the system can be further reduced [49], since

$$\frac{dP}{dt} = 0 \tag{3.15}$$

converts Eq. (3.11) into a quadratic equation for P. Solving it gives the concentration of P as a function of R:

$$P_\pm = -\frac{k_3k_5 + k_2k_4}{2k_3k_6} \pm \sqrt{\frac{(k_3k_5 + k_2k_4)^2}{4k_3^2k_6^2} + \frac{k_1R}{k_6}} \tag{3.16}$$

Of the two solutions only P_+ is biologically relevant, as $P_- < 0$. Inserting P_+ in equation

(3.12) results in:

$$\frac{dC}{dt} = k_6 \frac{(k_3k_5 + k_2k_4)^2}{4k_3^2k_6^2} \left(-1 + \sqrt{1 + \frac{4k_3^2k_6k_1R}{(k_3k_5 + k_2k_4)^2}} \right)^2 - k_8C - k_9C + k_{10}N \tag{3.17}$$

Due to (1.) and (2.)

$$\frac{4k_3^2k_6k_1R}{(k_3k_5 + k_2k_4)^2} \ll 1 \tag{3.18}$$

and therefore we can approximate

$$\sqrt{1 + \frac{4k_3^2k_6k_1R}{(k_3k_5 + k_2k_4)^2}} \approx 1 + \frac{1}{2}\frac{4k_3^2k_6k_1R}{(k_3k_5 + k_2k_4)^2} \tag{3.19}$$

and obtain from equation (3.17):

$$\frac{dC}{dt} = k_6 \frac{(k_3k_5 + k_2k_4)^2}{4k_3^2k_6^2} \left(\frac{4k_3^2k_6k_1R}{2(k_3k_5 + k_2k_4)^2} \right)^2 - k_8C - k_9C + k_{10}N$$

After some algebra this results in:

$$\frac{dC}{dt} = k_6 \frac{k_3^2k_1^2R^2}{(k_3k_5 + k_2k_4)^2} - k_8C - k_9C + k_{10}N \tag{3.20}$$

Defining now $k_{2b} = \frac{k_6k_3^2k_1^2}{(k_3k_5+k_2k_4)^2}$, $k_{2d} = k_8$, $k_{2t} = k_9$ and $k_{3t} = k_{10}$ and with $R = y_1$, $C = y_2$ and $N = y_3$, equation (3.20) can be rewritten as:

$$\frac{dy_2}{dt} = k_{2b}y_1^2 - k_{2d}y_2 - k_{2t}y_2 + k_{3t}y_3 \tag{3.21}$$

which is identical to Eq. 3.2.

3.3 Phases and amplitudes of the oscillations

Using Eqs. 3.1 to 3.7 with parameters within a biologically plausible range [47, 141] we were able to reproduce experimentally observed circadian oscillations. Due to their relatively small number the parameters could be optimized by trial and error. Criteria for parameter estimations in the order of their importance were:

- the existence of oscillations with a period close to 24 hours,

- correct phases between various oscillator components and
- reasonable peak-to-trough ratios (i.e. the ratio of the maximum concentration to the minimum concentration during the oscillation) of the mRNA and protein concentrations.

The values of the parameters are listed in Table 3.1.

With the given set of parameters, the clock components oscillate with a period of 23.8 h, which is a typical period for mice (Fig. 3.3 A; [91]). In the model, the peak-to-trough ratios for *Per2*/*Cry* and *Bmal1* mRNA are 5.8 and 7.0, respectively. For nuclear PER2/CRY and BMAL1 protein we observe peak-to-trough ratios of 2.4 and 1.7. Experimentally observed peak-to-trough ratios of mRNA and protein vary in a wide range from 1.5 to 20, depending on the tissue and the detection method used [14, 86, 95, 112, 126, 153] . Most of our values are consistent with these experimental findings. Higher peak-to-trough ratios as observed for PER2 protein in liver tissue [65] are not reproduced in the model; they might be due to additional non-linear processes or higher non-linearities in the circadian oscillator. For example, complex formation with a higher number of PER2 and CRY proteins (e.g. for $q = 4$) substantially increases the peak-to-trough ratio. In the model, the peak concentration of BMAL1 is about the same as the peak concentration of the sum of all (nuclear and cytoplasmatic) PER2/CRY concentrations (not shown). Again, this has been found experimentally [65].

Fig. 3.3 B shows a comparison of the peak phases of clock components observed in experiments [99, 126] and in the model. All phases in the model are in agreement with experimental data. In particular, the delay of approximately three to eight hours between *Per2*/*Cry* mRNA and nuclear PER2/CRY protein is reproduced by the model. In the model, this delay is due to the small degradation rates of *Per2*/ *Cry* mRNA and cytoplasmatic and nuclear PER2/CRY as well as to a slow transport to the nucleus. Moreover, the almost antiphasic phase relation between BMAL1 and *Per2*/*Cry* mRNA that is observed experimentally is reproduced in our model. This delay at first glance does not fit to the idea of BMAL1 being the activator of *Per2*/*Cry* transcription. In our model, the large delay only occurs if an activated form of BMAL1 exists. Activation may be achieved by various processes, such as complex formation with CLOCK [31] or post-translational modification [23].

The delay between *Per2*/*Cry* mRNA and nuclear PER2/CRY protein is fundamental and cannot be changed considerably without abolishing oscillations in our model. Extreme delays are achieved by variation of k_{1d} ($k_{1d} = 0.492\text{h}^{-1}$: delay 8.8 circadian hours), which is the degradation rate of *Per2*/*Cry* mRNA and k_{2t} ($k_{2t} = 0.6\text{h}^{-1}$: delay 7.2 circadian hours), which is the transport rate of PER2/CRY into the nucleus. In the negative feedback loop, oscillations occur if firstly the sum of the delays (*Per2*/*Cry* mRNA — cytoplasmic PER2/CRY complex— nuclear PER2/CRY complex) is above a quarter of the period [32, 76] and secondly if the amplitude of the inhibitor (nuclear PER2/CRY) is large enough. With a delay smaller than the observed 7.2 circadian hours (*Per2*/*Cry* mRNA vs. nuclear PER2/CRY complex) not enough *Per*/*Cry* mRNA accumulates before the increasing inhibitor concentration prevents transcription, and the oscillations dampen. On the other hand, a large delay ($>$ 8.8 hours) between *Per2*/*Cry* mRNA and

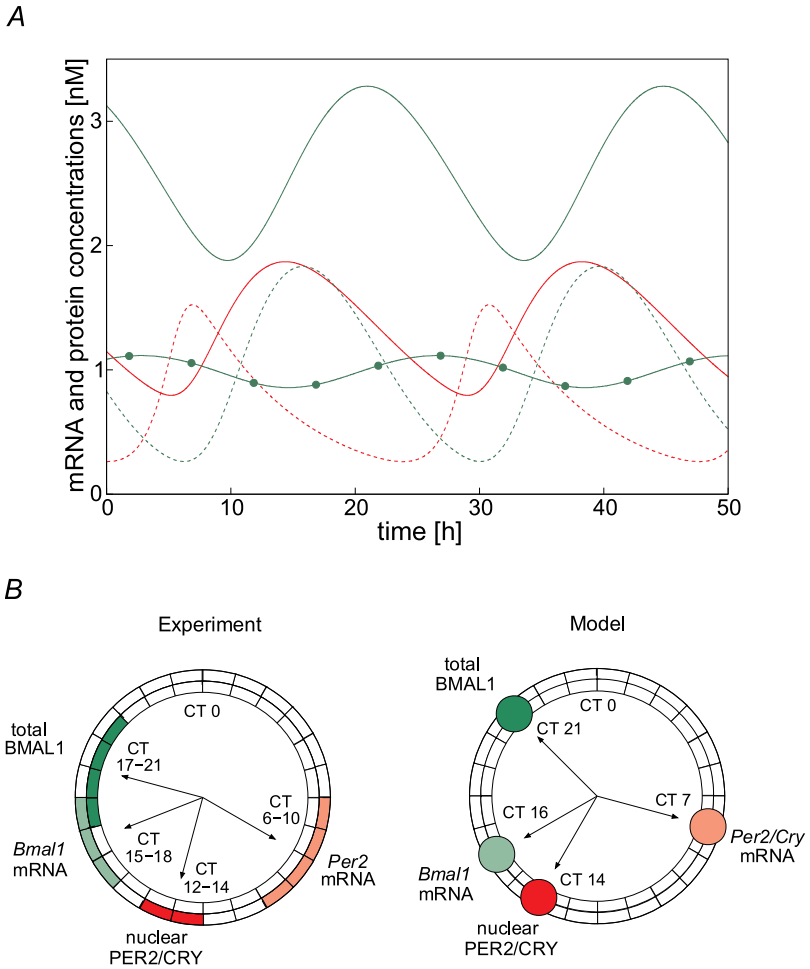

Figure 3.3: The model shows sustained circadian oscillations with correct phase relations. (A) Oscillations of clock gene mRNAs and proteins generated by the model (Fig. 3.1) with parameters as given in Table 3.1. *Per2/Cry* mRNA (y_1, red, dashed line), nuclear PER2/CRY protein (y_3, red, solid line), *Bmal1* mRNA (y_4, green, dashed line), activated BMAL1* (y_7, green, solid line, filled circles) and total BMAL1 protein ($y_5+y_6+y_7$, green, solid line) oscillate with a period of 23.8 hours. BMAL1 protein oscillates antiphasic to *Per2/Cry* mRNA. Nuclear PER2/CRY protein oscillates with a phase delay of 7.4 hours compared to *Per2/Cry* mRNA. (B) The phases between the clock components obtained by the model are in good agreement with experimental data. Experiment: The circadian times of the maximum concentrations of *Per2* mRNA (light red), nuclear PER2/CRY protein (dark red), *Bmal1* mRNA (light green) and total BMAL1 protein (dark green) are shown, given as the interval in which the highest concentrations were measured [99, 126]. Model: The phases between the maximum concentrations of the corresponding components are determined and translated into circadian times with the *Per2/Cry* mRNA peaking at CT7.

nuclear PER2/CRY protein correlates with lower amplitudes of the inhibitor and thus oscillations are lost as well.
The delay between BMAL1 protein and *Per2/Cry* mRNA as well as the delay between *Bmal1* mRNA and BMAL1 protein are less crucial for the system. They can vary from 3 to 12 circadian hours or from 3 to 6 circadian hours, respectively, without loss of oscillations. This wide range of possible delays is observed, e.g., if all rate parameters in the positive feedback are multiplied by the same factor. An increase of these rate parameters reduces the delay between *Bmal1* mRNA and BMAL1 protein and simultaneously increases the delay between BMAL1 and *Per2/Cry* mRNA and vice versa. The range of possible delays is limited because (1) with very high rates in the positive feedback BMAL1 is rapidly degraded, which leads to a complete loss of oscillations and (2) with decreasing rates the peak-to-trough ratios in the positive feedback become small and finally oscillations disappear in the positive feedback.

3.4 Rhythmic versus constant activation of *Per2/Cry* transcription

To test whether the positive feedback is essential for the occurrence of oscillations, we compared the dynamics of the model with and without positive feedback for a given strength of the negative feedback. This was done by varying the parameters v_{4b} and c, which reflect the maximal transcription rate of *Bmal1* and a constant activator concentration for *Per2/Cry* transcription, respectively. By varying these parameters, the relative amount of positive feedback dependent and independent activation of *Per2/Cry* transcription can be controlled. First, the dynamics of the system was investigated by varying positive feedback strength for a low fixed activator concentration $c = 0.01$nM (Fig. 3.4 A). For v_{4b} below a threshold of 0.35nMh^{-1} the system reaches a steady state indicated by a stable *Per2/Cry* mRNA concentration, above this threshold the system oscillates. Thus, a positive feedback of a certain strength is necessary for oscillations in the case of low activator concentration. To compare, the concentration of the constitutive activator c was varied in a system without positive feedback (v_{4b} =0nMh^{-1}) (Fig. 3.4 B). With a low concentration of c (<0.02nM) no oscillations of *Per2/Cry* mRNA occur, whereas a high value of c leads to oscillations. Thus, the positive feedback can be replaced by a constantly expressed activator to generate oscillations.
In both cases the period is close to 24 hours for a wide range of v_{4b} and c respectively (Fig. 3.4 C,D). Only close to the Hopf bifurcation point, beyond which oscillations cease to exist, the period shortens with a constant activator and with the positive feedback. Therefore, according to our studies a low maximal transcription rate of *Bmal1* (e.g. due to mutation) as well as a constant low expression of activator should decrease the period.
These dynamical changes are consistent with experimental data from gene knock-out studies. The lack of oscillations for low *Bmal1* transcription and low constant activation in the model might reflect the molecular and behavioral arrhythmicity of $Bmal1^{-/-}$

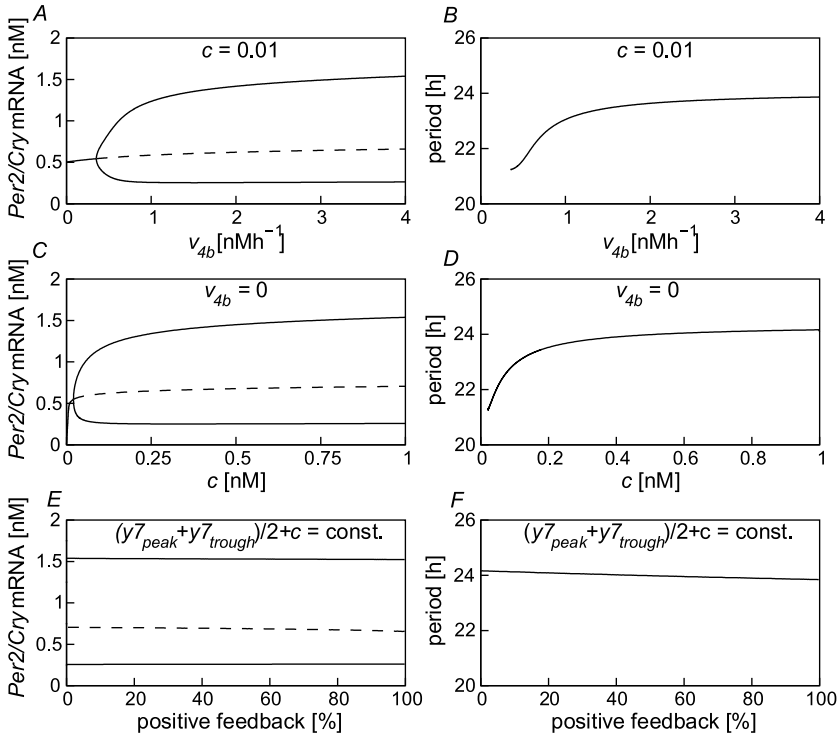

Figure 3.4: Positive feedback and constant activation can both lead to oscillations. (A) *Per2/Cry* mRNA concentration with varying transcription rate of *Bmal1* (v_{4b}). For a low transcription rate of *Bmal1*, the *Per2/Cry* concentration reaches a steady state. In the Hopf bifurcation point at v_{4b} =0.35nMh^{-1} the steady state becomes unstable, for higher values of v_{4b} the *Per2/Cry* mRNA concentration oscillates. Thick lines represent maximum and minimum of the oscillation. For instance, with the default parameter value v_{4b} =3.6nMh^{-1} the *Per2/Cry* mRNA concentration oscillates between 0.3 and 1.5 nM (see Fig. 3.3A). The dashed line marks the unstable steady state. (B) *Per2/Cry* mRNA concentration with varying amount of constantly expressed activator c. With low levels of activator the *Per2/Cry* mRNA concentration reaches a steady state. An activator concentration above the Hopf bifurcation point at c =0.02nM results in *Per2/Cry* mRNA oscillations. (C,D) Oscillation periods as a function of *Bmal1* transcription rate v_{4b} and constantly expressed activator c, respectively. In both cases the period is stable for a broad parameter range and shows a stronger parameter dependence close to the Hopf bifurcation point. (E,F) The positive feedback is gradually replaced by constant activation. Here, the average amount of total activator $(y_7(peak) + y_7(trough))/2 + c$ is kept constant. 0% positive feedback corresponds to v_{4b} =0nMh^{-1} and c = 1nM, 100% to v_{4b} =3.6nMh^{-1} and c =0.01nM. Oscillations of *Per2/Cry* mRNA occur in all cases (E), the period remains stable (F).

mutant mice, which lack a functional transcriptional activator complex BMAL1/CLOCK [14]. The maintenance of oscillations without positive feedback but with high concentra-

tion of constitutive activator may correspond to the dynamics observed in *Rev-erbα*$^{-/-}$ mutant mice. These mice are behaviorally rhythmic, and *Per2* and *Cry* mRNAs and proteins are rhythmically expressed, although *Bmal1* mRNA and protein are expressed at a constant high level [95].
In order to determine how positive feedback and constant activation act together, they were varied simultaneously, while keeping the average concentration of activator ($y_7 + c$) constant. Varying the ratio of positive feedback strength v_{4b} to constant activation c hardly affects the dynamics in the negative feedback: The maximum and minimum concentrations of *Per2*/*Cry* mRNA remain the same (Fig. 3.4 E) and the period of the oscillations changes only slightly (Fig. 3.4 F). However, for other values of the parameters of v_{4b} and c the dynamics may change (Fig. 3.5): While a strong positive feedback as well as a high activator concentration result in oscillations (white area) for a low concentration of constant activator c attractors coexist: Oscillations coexist with a stable steady state for low c and high v_{4b} (light gray area). Here, the dynamics of the system depends on the initial conditions (inlets; see figure legend).

3.5 Robustness of the system with and without positive feedback

In several studies, an increase of robustness of the circadian oscillator has been proposed as a possible function of the positive feedback [16, 95]. Here, we compared the robustness of the system with and without positive feedback towards parameter changes. All parameters were varied for a given positive feedback strength or, alternatively, with a given amount of constantly expressed activator. For the system with the positive feedback we use the default parameters (v_{4b} =3.6nMh^{-1} and c =0.01nM). In the system without positive feedback we assume v_{4b} =0nMh−1 and c =1nM (corresponding to the average amount of BMAL1* with v_{4b} =3.6nMh^{-1}). In both cases, each parameter was increased or decreased by a factor of two.

The robustness of the systems was investigated with respect to the existence of oscillations, the period of oscillations and the phases and amplitudes of the oscillator components. Oscillations persist in all cases when we change parameters by a factor of 2. The period and phases (Fig. 3.6 A-C) tend to be more robust with respect to parameter variations than the peak concentrations (selected parameters: Fig. 3.6 D,E, all parameters: Tables 3.2 and 3.3). The largest changes of the period are caused by the variation of degradation and transport rates in Eqs.3.1-3.3, which form the negative feedback loop (Fig. 3.6 A: k_{1d}). The inhibitory constant k_{1i} has a pronounced influence on the peak concentrations.

The sensitivity of the period, the phases and the peak concentrations in the negative loop towards parameter variation differ only slightly with and without positive feedback (Fig. 3.6 A,B,D), i.e. the positive feedback has only a minor effect on the negative loop of the oscillator. The phases and peak concentrations in the positive feedback loop (Fig. 3.6 C,E) are somewhat more sensitive towards parameter variations.

Table 3.2: Effect of single parameter variations on the period of the oscillations and the phases and amplitudes of selected components in the model with positive feedback

Parameter	Period	Amplitudes				Phase differences			
		y_1	y_3	y_4	$y_5+y_6+y_7$	y_1-y_3	y_3-y_4	y_4-$(y_5+y_6+y_7)$	$(y_5+y_6+y_7)$-y_1
1/2 fold					fold change				
v_{1b}	0.98	0.90	0.83	0.69	0.68	1.00	1.03	0.94	1.02
k_{1b}	1.01	1.07	1.13	1.24	1.27	1.02	0.98	0.97	1.01
k_{1i}	0.95	0.52	0.31	0.05	0.05	1.02	0.91	0.93	1.04
k_{1d}	1.11	0.72	0.79	0.62	0.68	1.02	0.81	0.92	1.06
k_{2b}	0.99	1.35	0.92	0.85	0.84	1.01	0.97	0.97	1.01
k_{2d}	1.04	0.98	1.04	1.07	1.07	1.00	0.90	1.01	1.01
k_{3d}	1.09	0.55	0.67	0.43	0.48	1.03	0.81	0.93	1.04
k_{2t}	1.24	1.29	1.17	1.31	1.35	1.02	0.77	0.93	1.06
k_{3t}	1.02	1.03	1.05	1.09	1.09	1.01	0.91	0.97	1.02
v_{4b}	0.99	0.92	0.86	0.37	0.36	1.01	1.01	0.95	1.02
k_{4b}	1.01	1.10	1.18	2.33	2.89	0.99	1.15	1.19	0.88
k_{4d}	1.01	1.09	1.16	2.41	2.56	0.99	1.94	0.94	0.89
k_{5b}	0.99	0.92	0.86	0.74	0.36	1.00	0.93	0.98	1.02
k_{5d}	1.00	1.01	1.02	1.03	1.11	1.00	1.01	1.01	0.99
k_{6d}	1.01	1.05	1.08	1.14	1.45	1.00	0.93	1.11	0.95
k_{5t}	1.01	1.00	1.00	1.00	1.05	1.01	0.88	1.03	1.00
k_{6t}	1.00	1.00	1.00	1.01	1.00	1.02	0.89	1.00	1.00
k_{6a}	1.00	0.96	0.92	0.85	0.82	1.00	0.95	0.96	1.03
k_{7a}	1.00	1.00	1.00	1.01	1.01	1.02	0.89	1.00	1.01
k_{7d}	1.01	1.08	1.14	1.26	1.66	0.99	0.96	1.04	0.99
c	1.00	1.00	1.00	1.00	1.00	1.00	1.00	1.00	1.00

Parameter	Period	Amplitudes				Phase differences			
		y_1	y_3	y_4	$y_5+y_6+y_7$	y_1-y_3	y_3-y_4	y_4-$(y_5+y_6+y_7)$	$(y_5+y_6+y_7)$-y_1
2 fold		fold change							
v_{1b}	1.01 1.08	1.15	1.27	1.30	1.01	0.98	1.01	0.99	
k_{1b}	0.99	0.92	0.86	0.74	0.72	1.00	0.94	0.98	1.02
k_{1i}	1.01	1.50	2.23	2.28	2.79	1.01	1.02	1.18	0.89
k_{1d}	0.78	0.99	0.77	0.57	0.56	1.03	1.19	1.01	0.95
k_{2b}	1.01	0.74	1.08	1.14	1.15	1.00	0.94	1.02	1.00
k_{2d}	0.92	1.02	0.92	0.85	0.84	1.00	0.99	1.03	0.99
k_{3d}	0.82	1.40	1.12	1.20	1.15	1.00	1.21	1.03	0.96
k_{2t}	0.73	0.64	0.65	0.37	0.40	0.99	1.19	1.06	0.95
k_{3t}	0.97	0.95	0.91	0.84	0.84	1.01	0.99	0.99	1.00
v_{4b}	1.01	1.07	1.13	2.47	2.53	1.01	0.97	1.01	0.99
k_{4b}	0.90	0.52	0.42	0.02	0.02	0.99	1.05	0.91	1.05
k_{4d}	0.98	0.91	0.84	0.36	0.35	1.01	0.49	0.97	1.09
k_{5b}	1.01	1.07	1.13	1.24	2.53	1.01	0.97	1.01	0.99
k_{5d}	0.99	0.98	0.97	0.94	0.82	1.01	0.99	0.95	1.02
k_{6d}	0.98	0.93	0.88	0.79	0.59	1.02	0.96	0.81	1.09
k_{5t}	0.99	0.99	0.99	0.98	0.95	1.02	0.90	0.96	1.02
k_{6t}	1.00	1.00	0.99	0.99	1.00	1.01	0.89	0.99	1.01
k_{6a}	0.99	1.02	1.04	1.08	1.12	1.00	1.05	1.00	0.99
k_{7a}	1.00	1.00	1.00	0.99	0.99	1.02	0.89	1.00	1.00
k_{7d}	0.97	0.89	0.82	0.67	0.56	1.02	0.94	0.95	1.02
c	1.00	1.00	1.00	1.00	1.00	1.02	0.89	1.00	1.00

Table 3.3: Effect of single parameter variations on the period of the oscillations and the phases and amplitudes of selected components in the model without positive feedback

Parameter	Period	Amplitudes		Phase differences	
		y_1	y_3	y_1-y_3	y_3-y_1
1/2 fold			fold change		
v_{1b}	0.98	0.92	0.88	0.99	1.01
k_{1b}	1.00	1.05	1.10	1.01	0.99
k_{1i}	1.01	0.73	0.53	1.01	0.99
k_{1d}	1.13	0.74	0.83	1.02	0.99
k_{2b}	0.99	1.36	0.94	1.01	1.00
k_{2d}	1.04	0.98	1.03	1.02	0.99
k_{3d}	1.10	0.58	0.73	1.03	0.99
k_{2t}	1.25	1.29	1.17	1.01	1.00
k_{3t}	1.01	1.02	1.04	1.00	1.00
c	0.99	0.94	0.90	1.01	1.00
2 fold			fold change		
v_{1b}	1.01	1.06	1.11	1.01	0.99
k_{1b}	0.99	0.94	0.90	1.01	0.99
k_{1i}	0.99	1.36	1.88	1.02	0.99
k_{1d}	0.78	1.01	0.82	1.01	1.00
k_{2b}	1.01	0.73	1.06	1.01	0.99
k_{2d}	0.92	1.02	0.93	1.01	1.00
k_{3d}	0.81	1.36	1.07	1.02	0.99
k_{2t}	0.71	0.65	0.69	1.01	0.99
k_{3t}	0.97	0.96	0.93	1.02	0.99
c	1.00	1.05	1.10	1.00	1.00

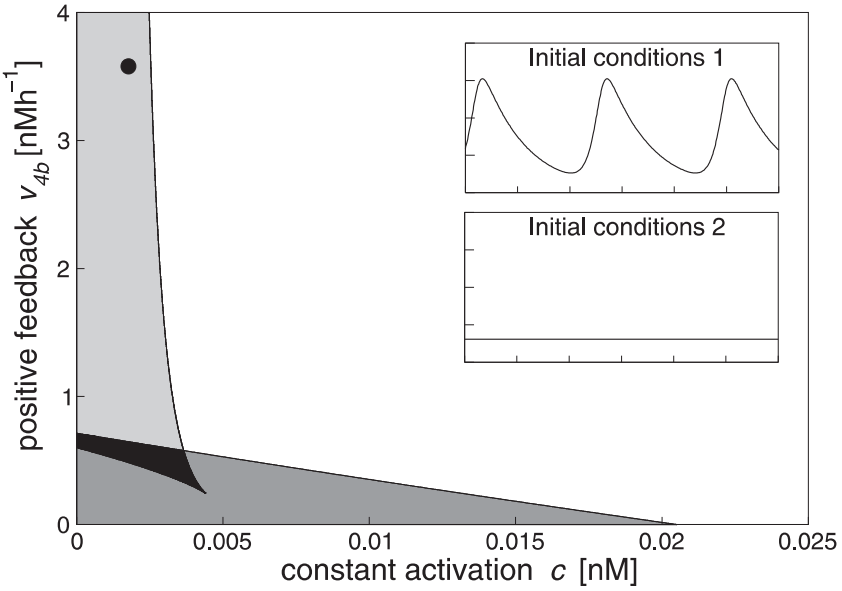

Figure 3.5: The positive feedback allows coexisting states in the system. The transcription rate of *Bmal1*, v_{4b}, and the concentration of the constitutively expressed transcriptional activator, c, are varied simultaneously. The color of the parameter regions encode different types of dynamical behavior. In the white area the system shows oscillations, for parameters of the dark gray area a stable steady state is reached. Complex dynamics are observed for low values of c. In that case, oscillations may coexist with a stable steady state (light gray area). An example of coexisting states is shown for v_{4b} =3.6nMh^{-1}, c =0.002nM (black circle, inserts): The same system (shown: y_1) either oscillates or is in a stable steady state depending on the initial conditions (initial conditions 1: all variables initialized at 1; initial conditions 2: all variables initialized at 0). For lower v_{4b}, the coexistence of two steady states (black area) is observed.

To summarize, the negative feedback loop turns out to be a robust mechanism, while the positive feedback itself is more sensitive towards parameter variations. This raises the idea that the negative feedback provides undisturbed circadian oscillations, while the easily achieved modulation of the components of the positive feedback provides the possibility to change the phase and level of clock-dependent gene transcription.

3.6 Reproduction and prediction of non-intuitive mutants

As described in the previous section, the strength of the negative feedback represented by the inhibitory constant k_{1i} particularly influences the peak concentration of the oscillations. Since the nuclear PER2 and CRYs both regulate the positive and the negative feedback, it is interesting to study the interdependence of both feedbacks with respect to the dynamics of the system. To this end, the strength of the positive and the negative

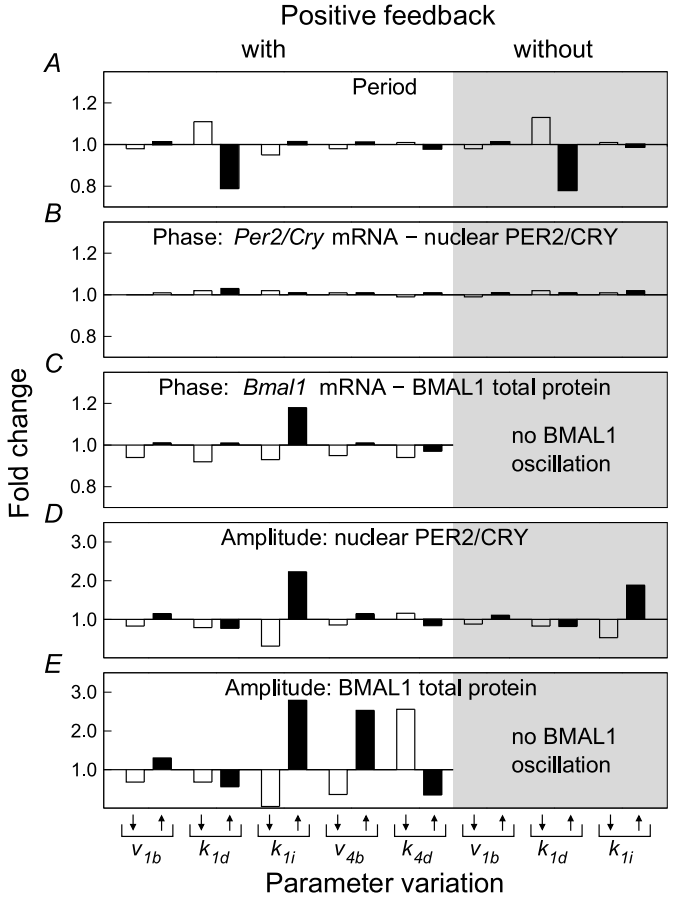

Figure 3.6: Circadian oscillations are robust towards parameter variations with respect to period, phases and amplitudes with and without positive feedback. Single parameters are varied systematically (↓: divided by 2, white bars, ↑: multiplied with 2, black bars) in the system with (left) and without (right) positive feedback. As representatives for all parameters (see tables 3.2 and 3.3) the variation of v_{1b} (synthesis rate in the negative loop), k_{1d} (degradation rate in the negative loop), k_{1i} (inhibitory constant), v_{4b} (synthesis rate in the positive loop) and k_{4d} (degradation rate in the positive loop) is shown. The relative changes of the period (A), phase differences (B,C) and peak concentrations (D,E) of the oscillations are determined: B: phase difference between y_1 and y_3, C: phase difference between y_4 and $y_5 + y_6 + y_7$, D: peak concentration of y_3, E: peak concentration of $y_5 + y_6 + y_7$. With and without positive feedback the period only changes significantly when k_{1d} is varied. The relative changes of phase and amplitude are smaller in the negative loop (B,D) than in the positive loop (C,E).

feedback was changed simultaneously by varying the *Bmal1* transcription rate v_{4b} and the inhibitory constant k_{1i} for various fixed concentrations of activator c (Fig. 3.7). Note, that the strength of the negative feedback falls with rising k_{1i}.

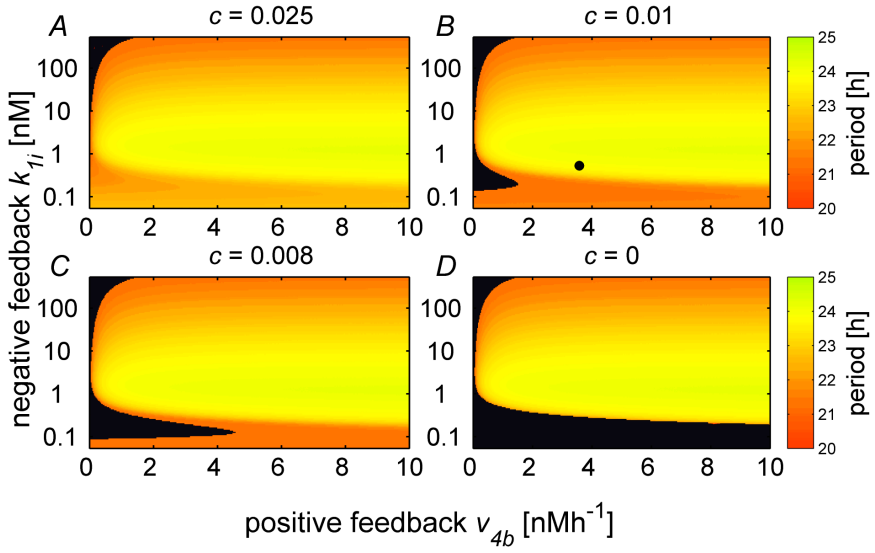

Figure 3.7: The state of the system depends on the positive and the negative feedback as well as on the constant activator concentration c. The dynamics of the system is analyzed for varying strength of the positive (v_{4b}) and negative (k_{1i}) feedback with various concentrations of constantly expressed transcriptional activator c ((A) c =0.025nM, (B) c =0.01nM, (C) c =0.008nM and (D) c =0nM; colored area: oscillations, black area: steady state). Very weak and very strong negative feedback lead to a loss of oscillations. Stronger positive feedback increases the range of oscillations. High values of the activator c support oscillations. The color indicates the period of the oscillations in hours for the reference parameter set and v_{4b} and k_{1i} given in each point (•: reference values of v_{4b} and k_{1i} as given in Table 3.1). With rising v_{4b} the period increases, with rising k_{1i} it either decreases or increases depending on the position. Note: The strength of the negative feedback falls with rising k_{1i}.

For large values of c (e.g. c =0.025nM, see Fig. 3.7, A), an increasing negative feedback strength as well as an increasing positive feedback strength supports oscillations. For smaller values of c, the positive feedback is still supporting oscillations. Regarding the negative feedback, however, there exists a limited range of oscillations. Here, oscillations only occur if the negative feedback does not exceed an upper and a lower limit. Thus, for small values of c where the positive feedback is the dominant source of activation there exists a complex interplay of positive and negative feedback. Changes in both the positive and the negative feedback strength are accompanied by a change of the period: The period is smaller near the bifurcation line which separates the oscillatory from the non-oscillatory parameter range. The default parameter values, which lead to the best consistency of the model with the experimentally observed oscillatory behavior, are marked by a filled circle (Fig. 3.7 B, Fig. 3.8, Point 1). For these parameters, a loss of oscillations due to a decrease in the positive feedback can be prevented by decreasing negative feedback, i.e. an increase of k_{1i} (Fig. 3.8, see below).

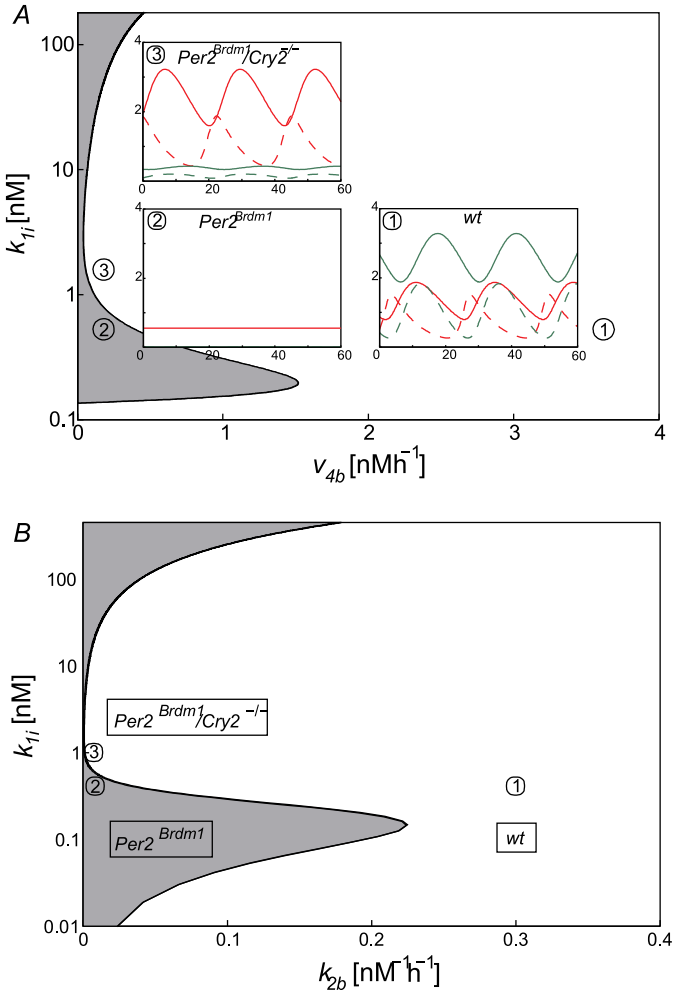

Figure 3.8: Variations of the strength of positive and the negative feedback lead to dynamical changes observed experimentally in mouse mutants. (A) Loss-of-function mutations of *Per2* and *Cry* are simulated using the assumption that PER2 is mainly activating *Bmal1* transcription and CRY is predominantly inhibiting BMAL1/CLOCK transcriptional activity. Compared to the wild-type (wt) mice (1) in the $Per2^{Brdm1}$ mutant mice v_{4b} is decreased which leads to a loss of oscillations (2). The additional mutation of *Cry2* is simulated by an increase of k_{1i} (3), i.e. a decrease of the strength of the negative feedback. This leads to a rescue of oscillations, as seen in the $Per2^{Brdm1}/Cry2^{-/-}$ double mutant [87]. (B) The $Per2^{Brdm1}$ mutant is modeled by a decrease of the complex formation instead of a decrease of the positive feedback strength v_{4b}. Despite the additional effect on the negative feedback, the loss of oscillations in the $Per2^{Brdm1}$ mutant and the rescue of oscillations in the $Per2^{Brdm1}/Cry2^{-/-}$ double mutant double mutant are reproduced.

We can relate this observation to well-characterized mouse mutants. Reppert and colleagues proposed that PER2 positively regulates *Bmal1* transcription as an element of the positive feedback [113]. Assuming that PER2 predominantly activates *Bmal1* transcription and CRYs inhibit *Per2*/*Cry* transcription, our model can explain the non-intuitive rhythmic phenotype of the $Per2^{Brdm1}$/ $Cry2^{-/-}$ double mutant mice (Fig. 3.8). The $Per2^{Brdm1}$ mutation (functional null-mutation) leads to a decrease of the *Bmal1* transcription rate, resulting in a loss of oscillations (Fig. 3.8, Point 2). For simulation of the $Per2^{Brdm1}$ mutation, we assume that PER1 and/or PER3 have some ability to substitute for PER2 in the PER/CRY complex, so that the affected parameter values remain greater than zero. The second mutation $Cry2^{-/-}$ is associated with a decrease of the negative feedback, leading to a rescue of oscillations (Fig. 3.8, Point 3). The phases of the oscillations are influenced little by this 'double mutation', whereas the amplitudes are not maintained. Interestingly, the period is preserved, when the positive and negative feedback are decreased simultaneously (Fig. 3.7 B). While a decrease in the positive feedback is accompanied by a shortening of the period, the decrease of the negative feedback lengthens the period. Similar results have been obtained in corresponding mutation experiments: While $Per2^{Brdm1}$ mutant mice have a shortened period before they get arrhythmic [152], the $Cry2^{-/-}$ mutant mice have a longer period than wildtype mice [134, 137]. The period of $Per2^{Brdm1}$/ $Cry2^{-/-}$ double mutant mice is approximately the same compared to that of wildtype mice [87].
The role of PER2 is probably far more complex than only being an activator of *Bmal1* transcription. E.g. mutation of the *Per2* gene might also affect complex formation with CRY proteins, thereby influencing both negative and positive feedback. Considering this dual role of PER2, the $Per2^{Brdm1}$ mutant has been simulated by reducing the rate of formation of the PER2/CRY complex (k_{2b}). The results of these simulations are qualitatively similar to those described above where we only changed the positive feedback for the $Per2^{Brdm1}$ mutation: Oscillations disappear in the $Per2^{Brdm1}$ mutant and reappear in the $Per2^{Brdm1}$/ $Cry2^{-/-}$ double mutant (Fig. 3.8 B). The rescue of oscillations in the $Per2^{Brdm1}$/ $Cry2^{-/-}$ double mutant is also observed, if, in addition to its function in the positive feedback, PER2 inhibits *Per2*/*Cry* transcription to a low extent (i.e. v_{4b} is decreased and k_{1i} is increased in the $Per2^{Brdm1}$ mutation, e.g. shift of point 2 in Fig. 8 A to k_{1i} =0.7nM). In the case of PER2 being a stronger inhibitor of *Per2*/*Cry* transcription, the negative feedback would be largely decreased in the $Per2^{Brdm1}$ mutation, and the loss of oscillations (e.g. v_{4b} =0.2nMh^{-1}, k_{1i} =80nM) could not be rescued by a further decrease of the negative feedback. Therefore our simulations only account for the oscillations in the $Per2^{Brdm1}$/ $Cry2^{-/-}$ double mutant if we assume the inhibition of *Per2*/*Cry* transcription by PER2 to be weak. Experiments indeed suggest, that PER2 is a rather weak inhibitor compared to CRY1 and CRY2 [39].
The period of the $Cry1^{-/-}$ mutant mice is shorter than that of wildtype mice [134, 137] and this mutation cannot rescue the oscillations in the $Per2^{Brdm1}$ mice [87]. The functional difference between the homologs is not known, however, a difference in the inhibitory strength is discussed, CRY1 being the stronger inhibitor [39]. Under this assumption, the negative feedback in the $Cry1^{-/-}$ mutant is weaker than in the $Cry2^{-/-}$ mutant. In our model, the period changes for varying negative feedback strength are

indeed non-trivial (Fig. 3.7 B): Depending on how much the strength of the negative feedback is reduced, the period can either become longer or shorter than under default conditions. Close to the default conditions the period increases with decreasing negative feedback (i.e. rising k_{1i}, corresponding to the *Cry2*$^{-/-}$ mutation). A further decrease of the negative feedback leads to a shortening of the period (k_{1i} >1.5nM). A decrease under a certain threshold (k_{1i} >60nM) fails to rescue the oscillations in the case of a weak positive feedback (v_{4b} =0.2nMh^{-1}). This parameter setting (k_{1i} >60) might reflect the state observed in the *Cry1*$^{-/-}$ mutant: This mutation leads to a short period in a wildtype background (v_{4b} =3.6nMh^{-1}), and it fails to rescue oscillations in *Per2*^{Brdm1} mice (v_{4b} =0.2nMh^{-1}). Thus, the persisting arrhythmicity of *Per2*^{Brdm1}/*Cry1*$^{-/-}$ mutant mice [87] can be reproduced by the model. For a very weak negative feedback (k_{1i} >756.8nM) the oscillations disappear (not depicted in the figure) even for a positive feedback strength corresponding to wildtype (v_{4b} =3.6nMh^{-1}). This is consistent with the loss of rhythmicity in the *Cry1*$^{-/-}$/*Cry2*$^{-/-}$ double mutant [134].
Taking these considerations together this leads us to a testable prediction. In our model, a loss of oscillations due to a decrease of the positive feedback can be rescued by an increase of the constant activator concentration c (e.g. Fig. 3.7 A: c =0.025nM). A high activator concentration c also supports oscillations if k_{2b} instead of v_{4b} is decreased (c >0.073nM for k_{2b} =0.005nM^{-1}h^{-1}, k_{1i} =0.56nM, v_{4b} =3.6nMh^{-1} as in Fig. 8 B, not shown). In *Rev-erbα*$^{-/-}$ mutant mice the BMAL1 concentration is constantly high, which may be reflected by a high value of c in the model. Therefore, independent of the model representation of the *Per2*^{Brdm1} mutation, our model predicts that the simultaneous mutation of the *Rev-erbα* gene should prevent the loss of oscillations in *Per2*^{Brdm1} mutant mice.

3.7 Biological interpretation

With the quickly expanding knowledge about the circadian oscillator our view of the clock is getting more and more complex. The model presented here is designed to describe the basic structure of the oscillator, focusing on positive and negative feedback loops. While a more detailed model is useful for examining elementary molecular processes of the mammalian clock [26, 69], for the investigation of the positive feedback a reduced model as presented here is more appropriate. In a simple model that includes only a low number of components which are necessary to construct the feedback loops, manipulating and understanding the dynamics of the system is much easier than with a complicated model. The dynamics of the resulting model is in accordance with experimental data regarding period, phase relations and peak-to-trough ratios of the oscillating components.
A motivation for this study was to explore possible functions of the positive feedback within the circadian core oscillator. It turned out that the negative feedback is sufficient for the occurrence of oscillations, i.e., the positive feedback can be replaced by a constantly expressed activator. Similar results have been found in a model for the

Drosophila oscillator which is based on delay differential equations [115]. This finding suggests that the loss of oscillations in *Bmal1*$^{-/-}$ mutant mice is due to a lack of transcriptional activator rather than a lack of the positive feedback. This idea is supported by the phenotype of *Rev-erbα*$^{-/-}$ mutant mice, in which the activator BMAL1 is expressed at a constant high level. These mice are behaviorally rhythmic although they lack a functional positive feedback. The *Rev-erbα*$^{-/-}$ mice provide an optimal tool to test whether the regulation of output processes (other than locomotor activity) is a function of the positive feedback. If this is the case, at least some circadianly regulated processes should lose their rhythmicity in the *Rev-erbα*$^{-/-}$ mice, as those mice lack oscillations of BMAL1. A loss of oscillations for an increased *Bmal1* transcription rate as described in a detailed model by Leloup and Goldbeter [69] has not been observed in our model.

Does the positive feedback influence the robustness of the circadian oscillator? It turned out that with and without positive feedback the oscillations of components in the negative feedback loop are quite robust. In contrast, components of the positive feedback loop itself are more sensitive towards parameter variations. This is interesting in the context of the positive feedback and the resulting BMAL1 oscillations, which might be used to regulate output processes: The higher variability of phases and peak concentrations in the positive feedback principally allows to modulate output pathways without disturbing circadian oscillations. Variations of parameters such as synthesis rates in the positive feedback loop will hardly affect the basic core oscillation, but change the phase and strength of gene expression regulated by components of the positive feedback loop. The period of the oscillations is little affected by changes in the positive feedback.

Positive and negative feedback are not independent from each other. The inhibition of BMAL1/CLOCK by PER and CRY proteins affects both the positive and the negative feedback, since BMAL1/CLOCK activates transcription of *Per*, *Cry* and *Rev-erbα* genes via binding to E-box elements in their promoters (Fig. 1; [31]. Any change of the conditions in the cell that influences the inhibitory strength of PER and CRY proteins on BMAL1/CLOCK therefore leads to simultaneous changes in the positive and the negative feedback. In the model, this corresponds to a coordinated change of v_{4b} and k_{1i} in opposite directions. Compared to a single parameter variation of v_{4b} or k_{1i} the oscillations are maintained for a wider range of v_{4b} and k_{1i} if the parameters are varied simultaneously (Fig. 7 B). The co-regulation of positive and negative feedback by PER and CRY proteins therefore increases the stability of oscillations towards environmental changes, such as redox potential, nutrient conditions or metabolic state of the cell [110].

While a role of PERs and CRYs in the circadian core oscillator is generally accepted, the exact molecular function of these proteins is not fully understood. In the arrhythmic *Cry1*$^{-/-}$/ *Cry2*$^{-/-}$ double mutant mice *Per2* mRNA is expressed at a rather high constant level, supporting a role of CRY proteins in the negative feedback [86]. In contrast, in *Per2*^{Brdm1} mutant mice (loss-of-function mutation), the mRNA concentrations of *Bmal1* and *Cry1* are severely blunted. This lead to the proposal that PER2 positively acts on *Bmal1* transcription and is therefore a player in the positive feedback loop [113]. Although PER2 and CRY proteins are represented by a lumped variable in our model, these considerations allow us to simulate the effect of mutations in those clock genes

using parameter variations. The mutations are modeled by changing the features of the lumped variable. The mutation of *Per2* is reflected by a decrease of the activating strength of the complex, whereas the mutation of *Cry1* or *Cry2* is modeled by a decrease of the inhibitory strength to different extents.
Interestingly, in the arrhythmic $Per2^{Brdm1}$ mutant mice, molecular and behavioral oscillations can be rescued with an additional loss-of-function mutation for *Cry2* [87]. This can be explained by our model (see Fig. 8): A decrease of the positive feedback ($Per2^{Brdm1}$) leads to a loss of oscillations. This is compensated by a simultaneous decrease of the negative feedback ($Cry2^{-/-}$) resulting in the preservation of oscillations. By knocking out *Cry1* rather than *Cry2* in a $Per2^{Brdm1}$ background, oscillations are not rescued (Oster et al., 2002). While a moderate increase of k_{1i} representing a *Cry2* mutation lengthens the period, a shorter period is observed with a strong increase of k_{1i} representing the *Cry1* mutation. A difference in the inhibitory strength of the two homologs therefore can explain the experimentally observed opposite effect of the mutations on the period.
The function of PER2 is probably more complex than exclusively activating *Bmal1* transcription. It forms a complex with CRY proteins [65] and thus might play a role in the inhibition of BMAL1/CLOCK [62]. In our model, however, this role does not seem to be responsible for the loss of oscillations in the $Per2^{Brdm1}$ mutant, as a moderate decrease of the negative feedback strength rather supports oscillations than prevents them (Fig. 3.7, Fig. 3.8). The loss of oscillations in the $Per2^{Brdm1}$ mutant therefore seems to be due to the changes in the positive feedback strength.
For PER2 being a player in the positive feedback loop we can make the following prediction: Oscillations in the arrhythmic $Per2^{Brdm1}$ mutant mice should be rescued by an additional loss-of-function mutation for *Rev-erbα*. This can be tested by crossing *Rev-erbα*$^{-/-}$ and $Per2^{Brdm1}$ mutant mice. In the resulting double mutant mice a constant high expression of BMAL1 due to the mutation of *Rev-erbα* should replace the positive feedback. In the model, the *Rev-erbα*$^{-/-}$ mutant is described by a high concentration of constitutive activator c , that replaces the positive feedback dependent *Bmal1* transcription rate ($v_{4b} = 0$). Therefore the additional mutation of *Per2*, that is simulated by a decrease of v_{4b}, has no further effect and the oscillations are maintained. Consequently, we predict a rhythmic behavior of those double mutant mice.
Another important clock gene, *Per1*, is not explicitly included in the model, since its specific role within the positive or negative feedback loop (in contrast to its function in response to light) is not well understood. As soon as more data accumulate, the role of *Per1* can in principle be investigated by varying parameters of the model, as it has been done for differentiating the functions of *Cry1*, *Cry2* and *Per2* (Fig. 3.8).
A characteristic feature of the circadian oscillator is temperature compensation, which provides for a remarkably stable circadian period over a wide temperature range [154]. Temperature compensation of circadian oscillators has been addressed in models, assuming either a varying [104] or the same sensitivity [71] of all parameters towards temperature changes (for temperature compensation and sensitivity, see chapter 6). The crucial condition for the first method is the existence of parameters which being changed have the opposite effect on the period. As this condition is fulfilled in our model (Fig. 3.6

A), temperature compensation can be achieved with the method of Ruoff and Rensing [104].
In our study, we focus on oscillations generated in a single cell. While the circadian oscillation in the SCN is generated at the level of individual neurons [143], under natural conditions the cells interact and thereby form whole networks of coupled oscillators. Additional dynamic phenomena can be expected from this more complex system. A molecular model as presented here is a good tool to approach questions of coupling and synchronization, as has been done before for ultradian cellular rhythms [51, 146] and for a non-molecular model of the circadian clock [63].
In summary, our model describes well the molecular rhythms observed in the neurons of the suprachiasmatic nucleus and their associated behavioral rhythms. Focusing on modules such as negative or positive feedback loops within the transcriptional/translational regulatory network helped to dissect their differential roles in this system. The specific design of the model - taking into account only essential processes - should make it a valuable tool for various additional studies including:

- the entrainment of the oscillator to light-dark cycles (appropriate phase response curves are obtained when ‘gating‘ is included; see chapter 5);
- the incorporation of putative novel components or mechanisms;
- stochastic simulations for investigating the influence of molecular noise on circadian oscillations;
- output processes for the expression of different phases;
- the coupling of oscillators for the simulation of synchronization events within the suprachiasmatic nuclei as well as between the clock in the brain and in peripheral tissues;
- temperature compensation.

4 A model including two interlocked negative feedback loops

In this chapter, we extend the previous mathematical model of the circadian oscillator (chapter 3). The previous model already describes the negative feedback of PER2 and CRY and the positive feedback of PER2 on its own transcription: Here, we include explicitly REV-ERBα into the model. The transcription of *Rev-erbα* is activated by BMAL1-CLOCK, the encoded protein REV-ERBα is an inhibitor of *Bmal1* transcription. Therefore, by adding *Rev-erbα*, another negative feedback loop is added. Without functional *Per2* the amount of *Bmal1* transcript is decreased, therefore PER2 is assumed to support *Bmal1* transcription [113]. The positive feedback of the previous model is realized by an inhibitory effect of PER2 on the transcription of *Rev-erbα*. Thus, the positive feedback loop is, in fact, a negative-negative one. (see Fig. 4.1)

With an appropriate set of parameters, we obtain oscillations with the correct period and reasonable phases between the concentration peaks of several clock components. Parameter variations are used to simulate clock-gene mutations in the model.
We find that parameter changes which correspond to the arrhythmic $Per2^{Brdm1}$ mice and the $Bmal1^{-/-}$ mice, destroy oscillations. With a parameter variation that reflects the $Rev\text{-}erb\alpha^{-/-}$ mutation, the oscillations are sustained.
Additionally, assuming a different inhibitory strength of *Cry1* and *Cry2*, the model can account for the decrease and increase of the period in the corresponding knock-out mutants. The agreement with the experimental data and the simple structure of the model make it a valuable tool to elucidate further the function of the different feedback loops.
The results of this chapter were also published in [10].

4.1 Construction of the model

We extend the model of seven differential equations described in chapter 3 by adding an additional loop in which REV-ERBα inhibits *Bmal1* transcription. In the previous model, *Rev-erbα* is not considered explicitly and the negative feedback of BMAL1 on its own expression via REV-ERBα is not accounted for.
Here, we include an additional variable for the REV-ERBα protein. Only one additional variable is needed if we consider the turnover of REV-ERBα to be comparatively large and the translation rate to be proportional to the mRNA concentration. The possibility of direct activation of PER2 on *Bmal1* transcription cannot be eliminated, but an indirect action via inhibiting *Rev-erbα* transcription is very likely: In that case, PER2

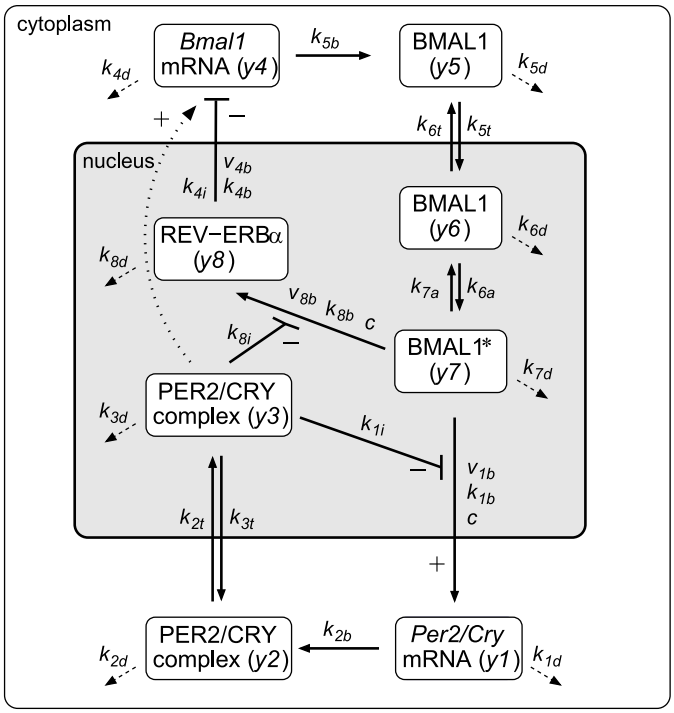

Figure 4.1: Model of the mammalian circadian oscillator: BMAL1* activates the transcription of *Per2* and *Cry* genes and the synthesis of REV-ERBα resulting in an increase of *Per2*/*Cry* mRNA (y_1) and REV-ERBα (y_8). As the levels of PER2 and CRY increase, they form a complex (y_2), which is transported to the nucleus. The nuclear PER2/CRY complex (y_3) inhibits *Per2*/*Cry* transcription and REV-ERBα synthesis. As REV-ERBα represses the *Bmal1* transcription, its decrease leads to an increase of *Bmal1* mRNA (y_4) and protein (y_5). Nuclear BMAL1 (y_6) in its active form (BMAL1*, y_7) restarts transcription of *Per2* and *Cry* genes. Dashed arrows represent degradation of mRNAs and proteins. The activation of *Bmal1* transcription via PER2/CRY as assumed in a previous model without REV-ERBα [9] is indicated by a dotted arrow. Parameters of the reaction kinetics are given in Table 4.1.

could act on the *Rev-erb*α transcription in a similar way as it does on its own transcription: by binding to the transcriptional activator BMAL1. In this case, the synthesis of REV-ERBα increases with a rising amount of BMAL1 and decreases with an increase of PER2/CRY concentration. The transcription of *Bmal1* is decreased by REV-ERBα. The model shown in Fig. 4.1 is described by the following set of differential equations:

$$\frac{dy_1}{dt} = \frac{v_{1b}(y_7^s + c)}{k_{1b}^s(1 + (y_3^p/k_{1i}^p)) + (y_7^s + c)} - k_{1d}y_1 \tag{4.1}$$

$$\frac{dy_2}{dt} = k_{2b}y_1^q - k_{2t}y_2 + k_{3t}y_3 - k_{2d}y_2 \tag{4.2}$$

$$\frac{dy_3}{dt} = k_{2t}y_2 - k_{3t}y_3 - k_{3d}y_3 \tag{4.3}$$

$$\frac{dy_4}{dt} = \frac{v_{4b}}{k_{4b} + (y_8^u/k_{4i}^u)} - k_{4d}y_4 \tag{4.4}$$

$$\frac{dy_5}{dt} = k_{5b}y_4 - k_{5t}y_5 + k_{6t}y_6 - k_{5d}y_5 \tag{4.5}$$

$$\frac{dy_6}{dt} = k_{5t}y_5 - k_{6t}y_6 - k_{6a}y_6 + k_{7a}y_7 - k_{6d}y_6 \tag{4.6}$$

$$\frac{dy_7}{dt} = k_{6a}y_6 - k_{7a}y_7 - k_{7d}y_7 \tag{4.7}$$

$$\frac{dy_8}{dt} = \frac{v_{8b}(y_7^r + c)}{k_{8b}^r(1 + (y_3^v/k_{8i}^v)) + (y_7^r + c)} - k_{8d}y_8 \tag{4.8}$$

Here, y_1 represents the concentrations of *Per2* and *Cry* mRNA, y_2 and y_3 describe the ones of the PER2/CRY complex in the cytoplasm and the PER2/CRY complex in the nucleus, respectively. The variable y_4 represents the concentration of *Bmal1* mRNA, y_5 the one of cytoplasmatic BMAL1 protein, and y_6 of BMAL1 protein in the nucleus. The variable y_7 describes the concentration of a transcriptionally active form BMAL1*, which can be understood as a complex with CLOCK and/or as phosphorylated BMAL1. The added component, REV-ERBα, is represented by y_8 (Eq. 4.8. The production of REV-ERBα is activated by transcriptionally active BMAL1 and inhibited by the nuclear PER2/CRY complex. Furthermore, the transcription of *Bmal1* (Eq. 4.4) which was activated by the nuclear PER2/CRY complex in the previous model, is now inhibited by REV-ERBα.
To keep the model as simple as possible, most reactions are modeled by linear kinetics. Nonlinearities appear in the terms that control transcription of y_1, y_4 and y_8 and due to complex formation (Eq. 4.2).

4.2 Circadian phases

As mentioned in chapter 3, not much is known about the rate constants of the molecular processes in the circadian oscillator, and we used the oscillations themselves to fit the model to the experiment. Criteria were the existence of oscillations with a period of about 24 hours, the phase relation of the oscillator components and the response of the system towards parameter variations. Table 4.1 shows the reference set of parameters used for all further simulations if nothing else is mentioned.

Table 4.1: Parameter values

Parameter	Value	Description
v_{1b}	18 nMh^{-1}	Maximal rate of *Per2*/*Cry* transcription
k_{1b}	1 nM	Michaelis constant of *Per2*/*Cry* transcription
k_{1i}	0.65 nM	Inhibition constant of *Per2*/*Cry* transcription
c	0.001 nM	Concentration of constitutive BMAL1*
p	8	Hill coefficient of inhibition of *Per2*/*Cry* transcription
s	5	Hill coefficient of activation of *Per2*/*Cry* transcription
k_{1d}	0.12 h^{-1}	Degradation rate of *Per2*/*Cry* mRNA
k_{2b}	0.3 nM^{-1}h^{-1}	Complex formation rate of PER2/CRY
q	2	Number of PER2/CRY complex forming subunits
k_{2d}	0.07 h^{-1}	Degradation rate of the cytoplasmatic PER2/CRY
k_{2t}	0.24 h^{-1}	Nuclear import rate of the PER2/CRY complex
k_{3t}	0.02 h^{-1}	Nuclear export rate of the PER2/CRY complex
k_{3d}	0.12 h^{-1}	Degradation rate of the nuclear PER2/CRY complex
v_{4b}	3.0 nMh^{-1}	Maximal rate of *Bmal1* transcription
k_{4b}	1 nM	Michaelis constant of *Bmal1* transcription
k_{4i}	0.9 nM	Inhibition constant of *Bmal1* transcription
u	3	Hill coefficient of inhibition of *Bmal1* transcription
k_{4d}	1.8 h^{-1}	Degradation rate of *Bmal1* transcription
k_{5b}	0.14 h^{-1}	Translation rate of BMAL1
k_{5d}	0.03 h^{-1}	Degradation rate of cytoplasmatic BMAL1
k_{5t}	0.15 h^{-1}	Nuclear import rate of BMAL1
k_{6t}	0.06 h^{-1}	Nuclear export rate of BMAL1
k_{6d}	0.03 h^{-1}	Degradation rate of nuclear BMAL1
k_{6a}	0.03 h^{-1}	Activation rate of nuclear BMAL1
k_{7a}	0.003 h^{-1}	Deactivation rate of nuclear BMAL1
k_{7d}	0.02 h^{-1}	Degradation rate of activated nuclear BMAL1
v_{8b}	10.6 nMh^{-1}	Maximal rate of REV-ERBα synthesis
k_{8b}	1 nM	Michaelis constant of REV-ERBα synthesis
k_{8i}	1.1 nM	Inhibition constant of REV-ERBα synthesis
r	1	Hill coefficient of activation of REV-ERBα synthesis
v	2	Hill coefficient of inhibition of REV-ERBα synthesis
k_{8d}	1.5 h^{-1}	Degradation rate of REV-ERBα

Using these reference parameters, the concentration of all components are oscillating. The period of the oscillations is 23.4 hours and therefore lies within the circadian range (Fig. 4.2A). In table 4.2, the phases of maximum concentration are given for various clock components in circadian time (1 period = 24 circadian hours). As a reference phase we use *Per2*/*Cry* mRNA that by definition peaks at circadian time 7 (CT7), all other phases are determined with respect to this reference.

Table 4.2: Peaking time of various clock components.

Phase	Model	Experiment	Reference
Per2/*Cry* mRNA	CT7	CT6-10	[100]
PER2/CRY nuclear complex	CT14.4	CT12-14	[100]
Bmal1 mRNA	CT15.8	CT15-18	[100]
BMAL1 protein	CT21.7	CT17-21	[126]
REV-ERBα	CT5.8	CT6-10	[95]

All calculated phases are in reasonable agreement with measured phases. A delay of 7.4 circadian hours is observed between the maximum concentration of *Per2*/*Cry* mRNA and the peak concentration of nuclear PER2/CRY. Like in experiments, the BMAL1 concentration peak appears long before the *Per2*/*Cry* mRNA concentration peak. The REV-ERBα concentration oscillates antiphasic with the nuclear PER2/CRY.
In order to function properly, a reliable circadian oscillator should be robust against small variations in the reaction rates. We examined the robustness of the system towards parameter changes with respect to the circadian period. The parameters were increased or decreased systematically by 10%. The oscillations persisted in all cases and the period was quite stable: The largest change of the period (about 10%) was found by decreasing the Michaelis constant of *Per2*/*Cry* transcription, k_{1b} (data not shown). This implies that slight perturbations of the clock components will not destroy the clock function.

4.3 Clock-gene mutants

Most mutations of clock-genes have a more or less severe effect on the circadian phenotype, either resulting in a loss of circadian rhythmicity or in a change of the circadian period under constant environmental conditions. These mutations are investigated in order to validate and improve the model. The *in silico* homolog of a clock-gene mutation is a change of a certain parameter. We investigated the effect of several parameter changes that correspond to experimental clock-gene mutants:
In experiment, the mutation of *Bmal1* leads to a loss of circadian rhythmicity: The behavior of mutated mice is arrhythmic, and the oscillations of clock-gene mRNA and protein concentrations disappear [14]. In the model we simulate this knock-out mutation by a removal of *Bmal1* transcription, i.e. $v_{4b} = 0$. Indeed, we observe a loss of oscillations under these conditions (Fig. 4.2B): The system reaches a stable steady state with low levels of *Per2*/*Cry* mRNA and protein. Low constant levels of *Per2* have also been found in experiments [14].
Only slight changes of the circadian phenotype are observed, if *Rev-erb*α is mutated [95], unlike for the *Bmal1*$^{-/-}$ mutant. The *Rev-erb*α mutation is modeled by setting its

transcription rate v_{8b} to 0, as done for the *Bmal1* mutant. With the resulting parameter set, the oscillations of *Per2*/*Cry* mRNA and protein remain stable with a period slightly shorter than in the wildtype mice. At the same time, *Bmal1* mRNA and protein are not oscillating, but are expressed at constant high levels (Fig. 4.2C). This corresponds to the nearly constant, high expression levels of *Bmal1* mRNA, that have been found experimentally in *Rev-erbα*$^{-/-}$ mice [95].
In this model, *Per2*, *Cry1*, and *Cry2* are represented by the same variable. Therefore, a mutation of either of those genes cannot be simulated by a loss of transcription as done for *Bmal1* and *Rev-erbα*. Instead, we change the activities of the nuclear PER2/CRY complex in order to consider the specific effect of either mutation on the different activities.
The level of *Bmal1* mRNA in mice that lack PER2 is rather low; this lead to the idea of PER2 being an activator of *Bmal1* transcription [113]. As PER2 is a much weaker inhibitor of *Per2*/*Cry* transcription than the CRYs [62], we assume that the main function of PER2 is activation of *Bmal1* transcription. Most probably, this activation is via inhibition of *Rev-erbα* transcription. Therefore, to simulate the *Per2* mutation, we decrease the inhibitory strength of PER2/CRY on the synthesis of REV-ERBα (i.e. we increase k_{8i}). As a result, the oscillations disappear in the system and the levels of *Bmal1* mRNA are low (Fig. 4.2D). These results are in agreement with the arrhythmicity observed in *Per2*^{Brdm1} mice that lack functional PER2. They show an arrhythmic activity pattern under constant conditions [152] and blunted circadian oscillations of mRNA [113].
As both *Cry*s are inhibitors of *Per* and *Cry* transcription, we simulate their mutation by decreasing the inhibitory strength of PER2/CRY on their own transcription (i.e., an increase of k_{1i}). Not much is known about the differential function of the two homologs *Cry1* and *Cry2*.
However, surprisingly, we find that the null-mutation of either gene has the opposite effect on the period: While in the *Cry1*$^{-/-}$ mutant mice the circadian period is shorter than in wildtype mice, the period is increased in the *Cry2*$^{-/-}$ mutant mice [134, 137]. Griffin et al. discuss different inhibitory strength of the two homologs as an explanation of this phenomenon [39]. *Cry2* is the weaker inhibitor. The difference in the inhibitory strengths is either due to different concentrations of CRY1 and CRY2 or due to their different effect on BMAL1/CLOCK. As the concentrations of CRY1 and CRY2 in liver differ not much [65], the second alternative is more likely. In our model, both alternatives correspond to a stronger decrease of the inhibitory strength for simulation of the *Cry1*$^{-/-}$ mutation and a weaker decrease of the inhibitory strength in case of the *Cry2*$^{-/-}$ mutation. In Fig. 4.3 the period is shown for varying inhibitory strength (variation of k_{1i}), the black dot indicating the reference parameter. A decrease of the inhibitory strength first increases the period and then decreases the period. This reflects the period changes observed in the *Cry2*$^{-/-}$ and *Cry1*$^{-/-}$ mutant mice, respectively. If the inhibitory strength is decreased even further in the model, the oscillations cease to exist. This corresponds to the loss of rhythmicity in *Cry1*$^{-/-}$/ *Cry2*$^{-/-}$ double mutant mice. Our results indicate, that a difference in the inhibitory strength can account for the different phenotype without assuming a different mechanism of the two homologs.
In summary, the phenotype of all investigated mutations can be reproduced in our model

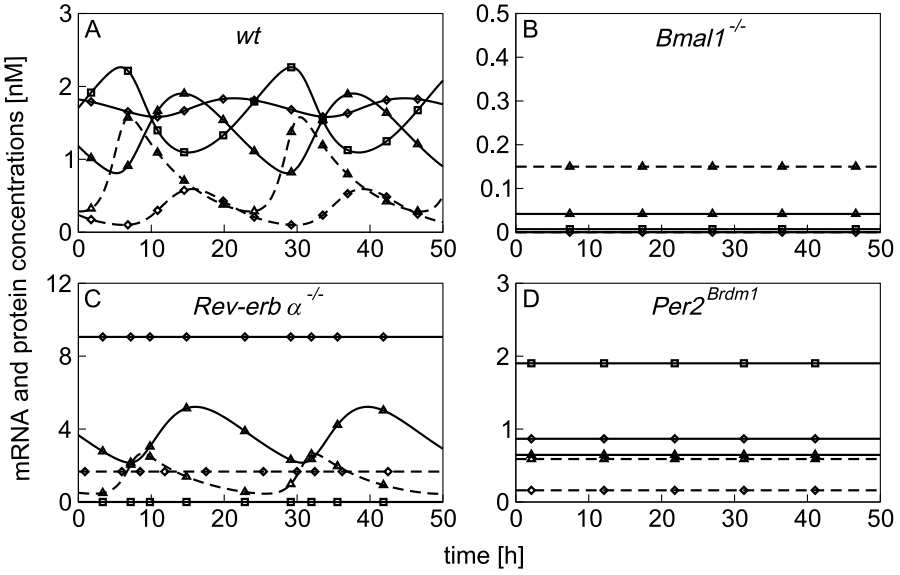

Figure 4.2: The model shows the correct dynamic behavior in simulations corresponding to wildtype and circadian mutants. *Per2/ Cry* mRNA: dashed line, triangle; nuclear PER2/CRY: solid line, triangle; *Bmal1* mRNA: dashed line, diamond; BMAL1 total protein: solid line, diamond; REV-ERBα: solid line, square. A: Circadian oscillations obtained with the reference parameters given in Table 4.1. The period of the oscillations is 23.4 hours. Similar oscillations of clock-gene mRNA and protein concentrations have been found in wildtype mice. B: Without transcription of *Bmal1* ($v_{4b} = 0\text{nMh}^{-1}$) the system reaches a stable steady state. This corresponds to the arrhythmicity observed in *Bmal1*$^{-/-}$ mutant mice. C: The oscillations persist without synthesis of REV-ERBα ($v_{8b} = 0\text{nMh}^{-1}$). In experiments, *Rev-erb*$\alpha^{-/-}$ mice have been shown to have a rhythmic phenotype. D: The *Per2*^{Brdm1} mutation is modeled by a decreased inhibitory strength of PER2/CRY on REV-ERBα synthesis ($k_{8i} = 11\text{nM}$). This leads to a loss of oscillations as found experimentally.

by appropriate parameter variations.

4.4 Constant activation of the transcription of *Bmal1*

The examination of the circadian period under different conditions is a fundamental tool to improve our understanding of the circadian oscillator. One experimental method is the overexpression of certain clock-genes. The level of expression can be varied by using different promoters and amounts of vector. Overexpression experiments have been done for *white collar* (*wc*) — the counterpart of *Bmal1* in *Neurospora*. Here, the period decreases with a rising amount of both WC homologs [16]. In a rescue experiment in mice, rising concentrations of the transcriptional activator CLOCK (i.e. the partner of

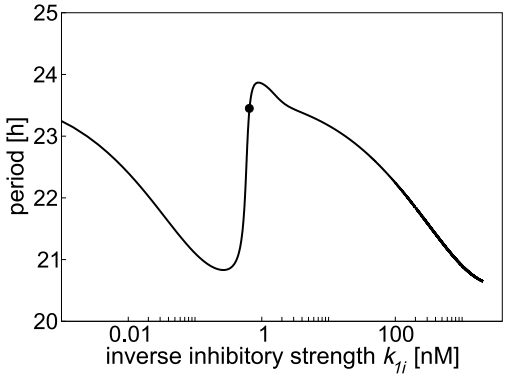

Figure 4.3: The opposite effect of *Cry1*$^{-/-}$ and *Cry2*$^{-/-}$ mutation on the period is reproduced in the model. The black circle marks the reference conditions corresponding to the wildtype. The *Cry1*$^{-/-}$ and *Cry2*$^{-/-}$ mutations are modeled by a decrease of the inhibitory strength of PER2/CRY on its own transcription (i.e. an increase of k_{1i}). With a slight decrease the period becomes longer, as has been shown for the *Cry2*$^{-/-}$ mutant mice. A strong decrease leads to a shorter circadian period as observed for the *Cry1*$^{-/-}$ mutant mice. With a further decrease of the inhibitory strength the oscillations disappear. The corresponding *Cry1*$^{-/-}$/ *Cry2*$^{-/-}$ double mutant mice become arrhythmic.

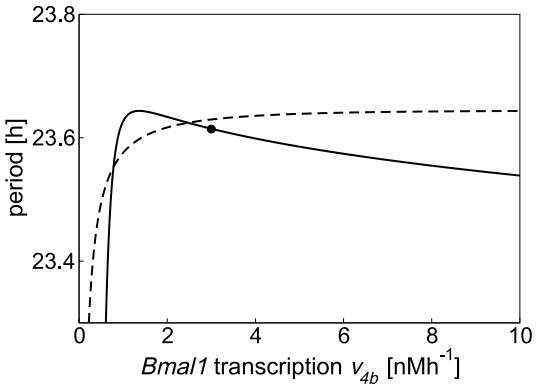

Figure 4.4: The period changes that occur with variation of the amount of BMAL1 depend on the Hill-coefficient s. We modeled the REV-ERBα independent overexpression of *Bmal1* ($k_{4i} = 1000$nM) and varied the amount of *Bmal1* mRNA and protein by changing v_{4b}. Around the reference point $v_{4b} = 3\text{nMh}^{-1}$ (black circle) the period decreases with rising *Bmal1* transcription for $s = 5$ (solid line) and increases for $s = 1$ (dashed line). As the Hill-coefficient indicates the impact of BMAL1 on *Per2*/*Cry* transcription, the period changes occurring in overexpression experiments give hints on this impact.

BMAL1 for transcriptional activation) lead to a shortening of the period [4]. To our knowledge, *Bmal1* has not been overexpressed with different concentrations, as this

is rather difficult to achieve in mammals. As an alternative one could use an *in vitro* system to investigate the effect of different BMAL1 concentrations.
Here, we simulate the overexpression of *Bmal1* by reducing the inhibitory strength of REV-ERBα to almost zero ($k_{4i} = 1000$nM). The amount of *Bmal1* mRNA is varied by variation of v_{4b}. The system is not oscillating below a threshold of v_{4b} ($v_{4b} < 0.31\text{nMh}^{-1}$), above this threshold we observe first an increasing, than a decreasing period with rising *Bmal1* expression (Fig. 4.4, solid line). The decrease of the period near the reference point is related to the high Hill-coefficient $s = 5$ in Eq.1, that quantifies the impact of BMAL1 concentration on the *Per2/Cry* transcription. With a lower Hill-coefficient ($s = 1$, dashed line) the period increases with rising v_{4b} near the reference point.
These results indicate that by investigating the effect of different BMAL1 concentrations on the period one may find out how the *Per2/Cry* transcription is regulated by BMAL1. The comparison of simulations with forthcoming experiments might reveal possible explanations of period changes.

4.5 Biological interpretation of the results

The discussed model of the circadian oscillator represents an extended version of a previous model with the additional clock-gene *Rev-erbα* (chapter3, [9]). With this additional component, the model represents better the biological mechanisms underlying the clock. It also accounts for phase delays between the nuclear PER2/CRY accumulation and the activation of *Bmal1* transcription. The model shows sustained oscillations with a circadian period and reasonable phases of the mRNA and protein concentrations. Furthermore, with this model, we can reproduce the phenotype of several clock-gene mutations. Comparable results for the oscillations as well as for the mutations have been obtained using the model without *Rev-erbα* [9]. Thus, essential features of the model are robust with respect to the incorporation of additional components.
A widely discussed question is why the circadian system consists of more than one feedback loops given that a single delayed negative feedback loop would be sufficient to obtain oscillations [32]. With the previous model (chapter 3), we were able to show that with the additional positive feedback we can account for the counterintuitive phenotype of the $Per2^{Brdm1}/Cry2^{-/-}$ double mutant [9].
Here, we included an additional negative feedback in order to investigate its impact on the dynamics: BMAL1 is inhibiting its own expression via activation of *Rev-erbα* transcription, which is an inhibitor of *Bmal1* transcription. First studies indicate that the robustness of the system towards parameter variations with respect to period and phases does not depend critically on this feedback. Other possible functions of the additional feedback are temperature compensation of the circadian oscillations and the regulation of input and output phases. In a recent work Leloup and Goldbeter show that due to this negative feedback, oscillations with a different period can occur even if *Per2* is mutated [69]. Indeed, rhythms with a period of several hours (ultradian rhythms) are observed in mice if the circadian control of activity is disturbed [60]. The molecular basis is not

known. In our model, we have not yet observed oscillations in the *Per2* mutant.
In our studies we found that the behavior of the system depends on the Hill-coefficients (Fig. 4.4). A model of the circadian oscillator by Ueda et al. [133] can be simplified in a way, that it has the same topology as our model. However, it uses different kinetics and more variables. Therefore, a comparison of both models is well suited to examine the impact of those features on the dynamic behavior of the system. A comparison of several independent models will help to distinguish between characteristics of the specific model and the generic properties of the oscillator.
With this model we have a valuable tool to decipher the functions of yet another negative feedback loop in the circadian oscillator. Due to the relatively simple structure of the model and the small number of variables the model is very well suited for this task.

5 Entrainment of the circadian clock

In chapters 3 and 4 I describe in detail, how models of the molecular circadian clock generate oscillations with a circadian period and how their dynamics change if the clock is disturbed, e.g. by a mutation of a clock-gene. As the corresponding experiments were done in a constant environment, external constant conditions were assumed for those investigations (i.e. there were no synchronizing stimuli, that could e.g. alter the circadian period). However, under natural conditions the circadian clock is exposed to an environment with daily fluctuations of light, temperature and other stimuli. The circadian clock is synchronized (entrained) by those stimuli. Only if the phase between the circadian clock and the environment in the synchronized state (phase of entrainment) is correct, the organism is optimally adapted to external conditions. The organism has to be able to maintain the phase of entrainment even though the duration of the daily light phase can vary.
Here, we investigate the entrainment of a mathematical model for the circadian core oscillator in mammals under different photoperiods. We show that a phase-dependent sensitivity toward light input (i.e., gating) and a deviation of the free-running period τ from 24h are the critical features of the model oscillator that determine its phase of entrainment under different photoperiods. Our study indicates that gating is an important process in adapting the circadian oscillator in mammals to seasonally varying photoperiods.
This work was done in collaboration with Florian Geier and is published in [30].

5.1 Phase-response curves, photoperiod and entrainment

Biological processes that are regulated by the circadian oscillator are temporally organized. In a periodic environment such as the day/night cycle, the circadian oscillator is synchronized to this environment. The phase between the circadian oscillator and the environment in the synchronized state (phase of entrainment) has to be regulated tightly: Only with the right phase, the organism is optimally adapted to its environment at all times, and periodic events like sunrise or sunset can be anticipated [21].
During the course of the year, the phase of entrainment has to be adjusted permanently because of seasonally changing day lengths (photoperiods). Pittendrigh and Daan [93] found that the phase relation between activity onset and dusk is conserved under a wide range of different photoperiods in nocturnal rodents. Using computer simulation and experimentally recorded phase-response curves (PRCs), they hypothesized that two properties of the circadian clock are necessary to determine the phase of entrainment [93]: Those are the free-running period and the PRC of an organism. It depends on

the free-running period, whether the circadian clock has to speed up (free-running period smaller than 24h) or to slow down (free-running period larger than 24h) in order to synchronize with the 24h day/night cycle. Free-running periods of many nocturnal mammals are shorter than 24 h, while free-running periods of many diurnal mammals exceed 24h [18, 5]. The PRC describes the phase shift of the circadian clock in response to a perturbation by a short light pulse given at a certain phase of the circadian cycle [92]. The phase-shift can be a delay or an advance. In the synchronized state, a balance between delay and advance has to compensate for the difference between 24h and the free-running period. The necessity to achieve this balance determines the phase of entrainment. The range of photoperiods that leads to a constant phase of entrainment, depends on the shape of the PRC, especially the delay-to-advance ratio.
On the molecular level, it is assumed that the phase of entrainment under different photoperiods is represented in the mRNA and protein oscillations of clock genes [79, 80, 84, 123, 124, 128]. How the phase of entrainment is controlled on a molecular and physiological level is unknown.
In mammals, a short light pulse administered during subjective night leads to a rapid induction of *Per1* and *Per2* gene transcription on the level of SCN neurons [2]. In contrast, there is only a weak effect of light on the induction of *Per1* and *Per2* transcription during subjective day [114, 81]. Activation of *Per1* transcription by light is suppressed between CT 4 and CT 12, and induction *Per2* is only light sensitive during early subjective night, CT 16 [81]. The low sensitivity of the oscillator towards light during the day is considered to be the result of "gating" of the light-input [78]. In the PRC, gating is reflected by very small phase shifts administered during the phases corresponding to the subjective day. It is still unknown whether the biological mechanism responsible for gating is an immanent feature of the core oscillator (e.g., due to a saturation of the CLOCK/BMAL1 driven *Per1* and *Per2* transcription rate during subjective day) or an external mechanism (e.g., a clock-controlled regulation of the light input pathway).
So far, a mathematical model studying the entrainment of a molecular circadian oscillator in mammals under different photoperiods has not been developed. With such a model, we might be able to identify critical features involved in the phase control of the mammalian core oscillator.
Here, we investigate the entrainment of a mathematical model for the circadian core oscillator in mammals under different photoperiods. We show that a phase-dependent sensitivity toward light input (i.e., gating) and a deviation of the free-running period τ from 24h are the critical features of the model oscillator that determine its phase of entrainment under different photoperiods. Our study indicates that gating is an important process in adapting the circadian oscillator in mammals to seasonally varying photoperiods.

5.2 Modeling light-input

For a description of the circadian core oscillator in mammals, we use the mathematical model described in chapter 3 with the given parameter set.
In mammals, the exposure to light leads to the induction of *Per1* and *Per2* transcription in the SCN of mammals. This induction is independent of the CLOCK/BMAL1 driven transcription [129]. Therefore, we model light input by including an additional term in equation 3.1 of chapter 3 that describes the transcriptional activation of *Per*/*Cry* mRNA:

$$\frac{dy_1}{dt} = f_{trans(Per2/Cry)} - k_{1d} \cdot y_1 + lightinput \tag{5.1}$$

(see Appendix 1 for the complete system of differential equations and the kinetic parameters). *Per* and *Cry* genes are modeled as 1 variable (for a detailed discussion on the model derivation, see chapter 3). To keep our model as simple as possible,we do not take the experimentally observed differences in *Per1* and *Per2* light induction into account [2]. The scheme of the model oscillator including light input is shown in Figure 5.1.
LD cycles are simulated by a rectangular alteration of the light input $li(t)$ between 0 and a constant value denoted as light input strength lis. We want to investigate the meaning of the PRC for entrainment. In order to be able to modulate the shape of the PRC, we include the gating of light-input: Gating modifies the responsiveness towards light at different phases of the oscillation. Since the biological mechanisms behind gating are unknown, we include gating into the model oscillator by using a heuristic approach: Light input is modulated by a filter function (gating function) that is constructed with a combination of clock variables. Two different gating functions are created to increase the flexibility in shaping the PRC:

$$lightinput = li(t) \cdot \left(\frac{y_3}{y_{3max}} \right)^{10} \tag{5.2}$$

$$lightinput = li(t) \cdot \left(\frac{\frac{y_4}{2} + y_5}{y_4 y_{5max}} \right)^{6} \tag{5.3}$$

Both functions reflect the experimentally observed light insensitivity of *Per* induction by light during subjective day. They are based on the dynamical model variables y_3, y_4, and y_5, where y_{3max} is the maximum of y_3 oscillation and $y_4 y_{5max}$ is the maximum of the $\frac{y_4}{2} + y_5$ oscillation (see the appendix).
The free-running period τ of the original model oscillator is $\tau = 23.8$ h ($lis = 0$). To investigate the influence of the period τ on the phase of entrainment, the model is rescaled by multiplying all rate constants with a constant f. The alternative periods used are $\tau = 23.3$h ($f = 1.0233$) and $\tau = 24.4$h ($f = 0.9772$). These alterations of the freerunning period τ are used to simulate nocturnal and diurnal mammals with shorter and longer period τ [18, 5].
The phase of the circadian oscillator is defined by the circadian time (CT): The oscillation under free-running conditions is divided into 24 circadian hours, so that the phases

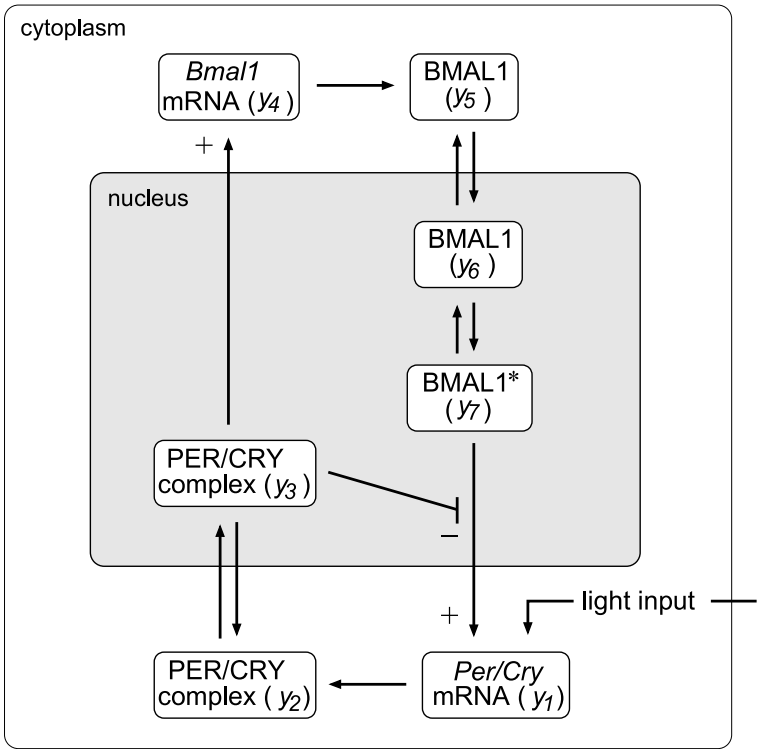

Figure 5.1: Scheme of the mammalian circadian model oscillator including light input [9]. The activated nuclear BMAL1 (y_7) promotes transcription of the *Period* and *Cryptochrome* genes, which are treated as 1 variable. The *Per*/*Cry* mRNA (y_1) is translated (cytoplasmic PER/CRY complex, y_2), and the PER/CRY complex is translocated into the nucleus (nuclear PER/CRY complex, y_3). The nuclear PER/CRY complex inhibits its own production by repressing *Per*/*Cry* gene transcription (negative feedback loop). The nuclear PER/CRY complex also activates transcription of the *Bmal1* gene, leading to production of cytoplasmic *Bmal1* mRNA (y_4). *Bmal1* mRNA is translated to cytoplasmic BMAL1 (y_5), which is translocated into the nucleus (nuclear BMAL1, y_6). Nuclear BMAL1 is activated (e.g., phosphorylated) and drives *Per*/*Cry* transcription (positive feedback loop). See the appendix for model equations and parameters.

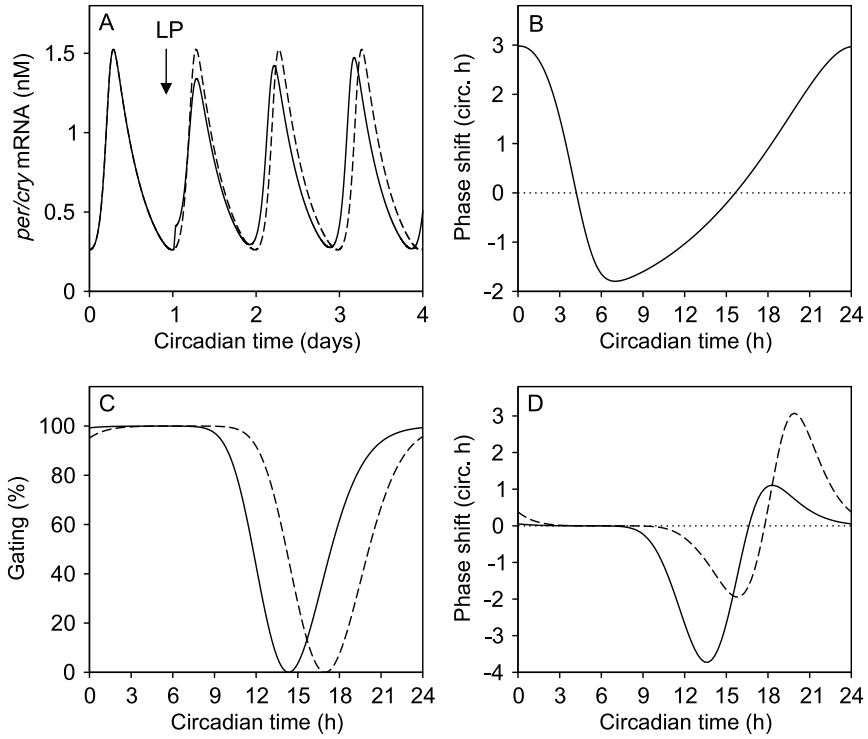

Figure 5.2: The PRCs of the mammalian circadian model oscillator. (A) A 30-min light pulse (LP; light input strength $lis = 0.28$) given at CT 0 advances the phase of the Per/Cry mRNA oscillations about 3h (measured after 10 days). The dashed line indicates unperturbed Per/Cry mRNA oscillation; the solid line indicates perturbed Per/Cry mRNA oscillation. (B) The PRC (solid line) of the model oscillator without a phase-dependent sensitivity toward light input (i.e., gating). In contrast to many experimentally recorded light pulse PRCs of mammals, the computed model PRC shows no dead zone during subjective day: $lis = 0.28$; pulse length = 30min. The dotted line indicates no light input. (C) Phase-dependent gating of light input: gating function 1 (solid curve) and gating function 2 (dashed curve). The 100% gating corresponds to zero sensitivity toward light input. (D) Corresponding PRCs of the model oscillator including gating. A larger delay-to-advance ratio within the model PRC, as observed in experimentally recorded light pulse PRCs of nocturnal mammals [17], is modeled with gating function 1 (solid curve). Smaller delay-to-advance ratios, as observed in many light pulse PRCs of diurnal mammals, are modeled with gating function 2 (dashed curve): $lis = 1$; light pulse length = 30 min. The dotted line indicates no light input.

range from CT 0 to CT 24. The maximum of Per/Cry mRNA is defined as CT 7.
The PRCs of the model oscillator are determined by calculating the phase shift in Per/Cry oscillation after 10 cycles. The accuracy of the phase shift after 10 cycles is about 1min. The light pulse is simulated by an abrupt change of the light input strength lis from 0 to a constant value for 30min.
Under the LD condition, we consider the model oscillator to be entrained if the period of the Per/Cry oscillation equals 24h and the phase relation between an internal phase marker of the model oscillator and the external LD cycle is constant. We use the Per/Cry mRNA maximum as an internal phase marker. This is an arbitrary choice, and other phase markers, for example, Per/Cry mRNA minimum or nuclear BMAL1 maximum, lead to qualitatively similar results (data not shown). For each simulated LD cycle, the phase differences between light onset and Per/Cry mRNA maximum, denoted as $\Psi_{morning}$, and between light offset and Per/Cry mRNA maximum, denoted as $\Psi_{evening}$, are calculated.
All models and programs are implemented in the programming language Python. The Numerical Python and Scipy modules are used for fast numerical computation and ODE integration (www.scipy.org). Visualization is done with Gnuplot (www.gnuplot. info) and Grace (http://plasma-gate.weizmann.ac.il/ Grace).

5.3 Biological assumptions

Our investigation rests on 2 main assumptions:

- The photoperiod of the external LD cycle is transmitted onto the single-cell level in the SCN: Many experimental studies indicate an influence of the photoperiod onto the oscillations of single clock components. However, the molecular phase of entrainment of a single cell (as defined above) is difficult to derive experimentally, and therefore data are rare (for data based on population sampling, see [84, 123, 118, 128]; for observations of phase groups in the SCN, see [96, 148]. Our assumption enables us to both investigate and suggest molecular mechanisms that might have an impact on the behavior of single SCN neurons in the context of changing photoperiods.

- Light responsiveness and sustained oscillations are confined to a single-model oscillator: Hamada et al. [44] showed that gated light induction of *Per* and rhythmic expression of *Per* are located in distinct compartments of the SCN. However, light information is transmitted to the rhythmic part of the SCN and entrains these neurons by a yet unknown mechanism [57]. To circumvent this lack of knowledge, we simplify our model by treating both features, light induction of *Per* and *Per* rhythmicity, within a single-model oscillator.

For assumptions specific to modeling the core oscillator, we refer to chapter 3 and Becker-Weimann et al.[9, 10].

5.4 Results

5.4.1 Phase Response Curves

We analyze the phase-dependent influence of light input on the oscillator by computing PRCs using 30-min light pulses ($lis = 0.28$). The effect of a single light-pulse given at CT 0 on the circadian oscillation is shown in Figure 5.2. The perturbed oscillations show a phase advance of about 3h compared to the unperturbed oscillations after a transient of 10 cycles.
If no gating is assumed ($lightinput = lis$), the model oscillator responds strongly to light during most of its circadian cycle as seen in the PRC in Figure 5.2B: Between CT 16 and CT 4.5, a light pulse advances the model oscillator, while a light pulse given between CT 4.5 to CT 16 delays the model oscillator. This is in contrast to many experimental PRCs obtained from behavioral studies. They show phases of little or no response toward light pulses("dead zone") during subjective day [93, 55].
In order to obtain reasonable PRCs, gating is included into the model. Both gating functions (Eqs. 5.2 and 5.3) lead to a suppression of light input during subjective day. They differ in their phase of lowest and highest sensitivity: Gating function 1 leads to the highest sensitivity towards light at CT 14 and to low sensitivity between CT 0 and CT 9. With gating function 2 the maximal sensitivity is reached at CT 17 (Figure 5.2C), the lowest sensitivity lies between CT 3 and CT 10. PRCs obtained by including those gating functions, both show the dead zone during subjective day, that is found in experimental PRCs (Fig. 5.2D): During the dead zone, no phase-shift occurs in response to a light pulse. The PRCs differ in their shape: Gating function 1 leads to a PRC with a large delay-to-advance ratio, which is similar to many PRCs of nocturnal animals. With gating function 2, the model PRC shows a small delay-to-advance ratio, which is similar to many PRCs of diurnal animals [93, 55].

5.4.2 Phase of Entrainment

In analogy to Pittendrigh and Daan [93], we investigate entrainment under different photoperiods in the molecular circadian oscillator. In particular, we study the influence of the free-running period and the PRC on the phase of entrainment (Figure 5.3). The phase of entrainment between the circadian clock and the day/night cycle can depend on the photoperiod in different ways. Either a constant phase between light onset and the clock is maintained with different photoperiods, or the phase between the clock and light offset is constant. In a third possibility, none of those phases is maintained.
We measure the phases between the clock and light onset which we call $\Psi_{morning}$, and between the clock and light offset, which we call $\Psi_{evening}$. Phase-marker for the clock is the phase of maximal Per/Cry mRNA concentration. The phases are measured for all combinations of free-running periods (23.3 h and 24.4 h) and of PRCs (no gating, gating function 1 and gating function 2).

Without gating, oscillators with longer or shorter free-running period than 24 h are not able to conserve $\Psi_{morning}$ or $\Psi_{evening}$ under different photoperiods (5.3, first and second row). Similarly, a model oscillator including gating but with a free-running period of

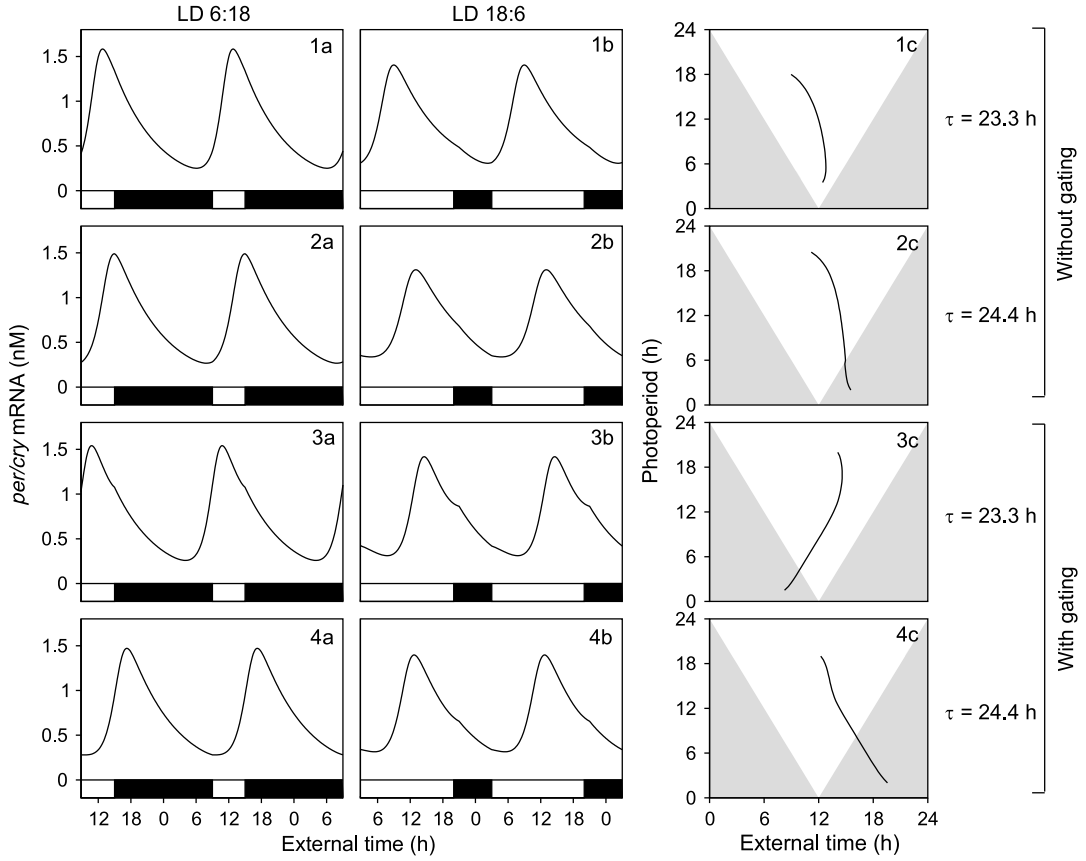

Figure 5.3: The influence of gating and free-running period on the molecular phase of entrainment under different photoperiods. Two model oscillators with different free-running periods ($\tau = 23.3$h and 24.4h) are simulated without gating (upper 2 rows) and including gating (lower 2 rows). The first 2 columns (a and b) show the Per/Cry mRNA oscillation after 30 days in 2 different LD conditions: LD 6:18 and LD 18:6. The 3rd column (c) shows the peak time of Per/Cry mRNA during the whole range of different photoperiods. The curve indicates the range of stable entrainment after 30 LD cycles. Only the 2 model oscillators including gating (rows 3 and 4) show constant molecular phases of entrainment over a wide range of different photoperiods. The model oscillator with $\tau = 23.3$h and gating function 1 conserves $\Psi_{evening}$ under photoperiods ranging from 2h to 13h (panel 3c). The model oscillator with $\tau = 24.4$h and gating function 2 conserves $\Psi_{morning}$ under photoperiods ranging from 2h to 14h (panel 4c). For the 1st and 2nd rows, light input strength $lis = 0.02$. To achieve entrainment of the model oscillator with gating, a stronger light input strength was chosen, that is, $lis = 0.2$ (3rd and 4th rows).

exactly 24h does not conserve the phase relation between *Per*/*Cry* mRNA maximum and dusk or dawn under different photoperiods (data not shown).
However, a combination of free-running periods deviating from 24h and gating conserves $\Psi_{morning}$ or $\Psi_{evening}$ under a wide range of different photoperiods (Fig. 5.3 third and forth row). The free-running period τ determines which of the 2 defined molecular phases of entrainment are conserved: $\Psi_{evening}$ is conserved if τ <24 h, $\Psi_{morning}$ is conserved if τ >24 h.

5.4.3 Role of Delay-to-Advance Ratio of the PRC

Based on studies of animal behavior, Pittendrigh and Daan [93] hypothesized that the shape of a PRC determines the range of photoperiods under which a constant phase difference between activity onset and dusk can be observed. This range is better conserved if the PRC shows a large delay-to-advance ratio. Following their line of argumentation, a small delay-to-advance ratio of the PRC should be favorable to conserve the phase difference between activity onset and dawn. We test both hypotheses using the molecular model oscillator in analogy to the studies based on animal behavior. Thus, we compare the conservation of $\Psi_{morning}$ and $\Psi_{evening}$ with the 4 combinations of τ = 23.3h and τ = 24.4h and gating functions 1 and 2. The model oscillator with a period τ = 24.4h shows a wider range of stable entrainment if gating function 2 is used. This gating function leads to a small delay-to-advance ratio in the model PRC (see Fig. 5.2D, dashed curve). The model oscillator with a period τ = 23.3h conserves $\Psi_{evening}$ under different photoperiods only with gating function 1. This gating function corresponds to a large delay-to-advance ratio in the model PRC (see Fig. 5.2D, solid curve). If the model oscillator is scaled to a freerunning period τ = 23.6h (i.e., closer to 24h), it conserves $\Psi_{evening}$ under different photoperiods with gating function 2 but only for a very small range of photoperiods (data not shown). We conclude that for the conservation of $\Psi_{evening}$, a model PRC with a large delay-to-advance ratio is preferred, while conservation of $\Psi_{morning}$ is favored if the model PRC has a small delay-to-advance ratio. Thus, our results are in agreement with the hypothesis stated above.

5.5 Discussion

Understanding how the phase of the circadian clock is controlled is central to the understanding of its function as a temporal coordinator of physiology and behavior. The clinical relevance of this question is emphasized by genetic diseases leading to an altered phase of entrainment, such as the advanced and delayed sleep phase syndromes [56, 102]. Different features of the circadian clock might be involved in phase control. Among them are the free-running period of animal behavior [5], the shape of PRCs [93], the coupling strength of the circadian clock to the external LD cycle, as well as mutual coupling between SCN neurons [148] or between the SCN and peripheral oscillators [149]. Within our model of the mammalian circadian oscillator, we are able to investigate the importance of two of these features: the shape of the PRC that is controlled by gating,

and the free-running period τ.

5.5.1 PRCs and Gating

In our study, we include a model-intrinsic phase-dependent sensitivity of the circadian oscillator towards light-input ('gating') in order to reproduce the experimentally observed insensitivity of *Per1* and *Per2* induction by light during subjective day [114, 81]. Why is the model oscillator without gating strongly light sensitive during subjective day? The *Per*/*Cry* mRNA production rate peaks around CT 6, that is, when the nuclear PER/CRY repressor reaches its lowest concentration. While the *Per*/*Cry* mRNA production rate is increasing, the additional light-input leads to an advance of the oscillator. When the *Per*/*Cry* mRNA production rate is decreasing, the light-input delays the oscillator. In the model, the *Per*/*Cry* mRNA production rate is at all times sensitive towards light-input. Consequently, the model oscillator shows a PRC without a dead zone during subjective day.
A mechanism that like gating leads to a dead zone of the phase response curve in the model is the induction of *Per*/*Cry* transcription in response to light via BMAL1. The saturation of the BMAL1-driven *Per*/ *Cry* transcription rate would in this case be responsible for the dead zone. However, in experiments an independence of light-induced *Per1* and *Per2* gene transcription from CLOCK/BMAL1 controlled transcription was observed [129]. This suggests that the gating mechanism is outside of the core oscillator .
The molecular mechanisms behind gating are unknown, and several have been discussed. Among them are a phase-dependent phosphorylation of CREB, PACAP signaling, and circadian expression of glutamate receptors [45, 140, 41, 29]. Our heuristic approach allowed us to include gating without specifying a mechanism. The dynamical variables used to model gating might be in phase with gating processes such as the expression of glutamate receptors.
Based on our results, we suggest a behavioral screen of mutants for altered entrainment phases under different photoperiods to identify molecular mechanisms involved in gating.

5.5.2 Phase of Entrainment

Gating is not only important in explaining experimentally recorded PRCs of rodents. The phase relation between the circadian clock and light onset or offset under different photoperiods (i.e., the phase of entrainment) is only conserved if gating is included into the oscillator model. However, gating alone is not sufficient to conserve the molecular phase of entrainment under different photoperiods: The free-running period τ is also important. This deviation of the free-running period from 24 h determines whether the oscillator conserves $\Psi_{evening}$ (if $\tau < 24$h) or $\Psi_{morning}$ (if $\tau > 24$h) under different photoperiods. These findings are in accordance with earlier suggestions by Pittendrigh and Daan [93].

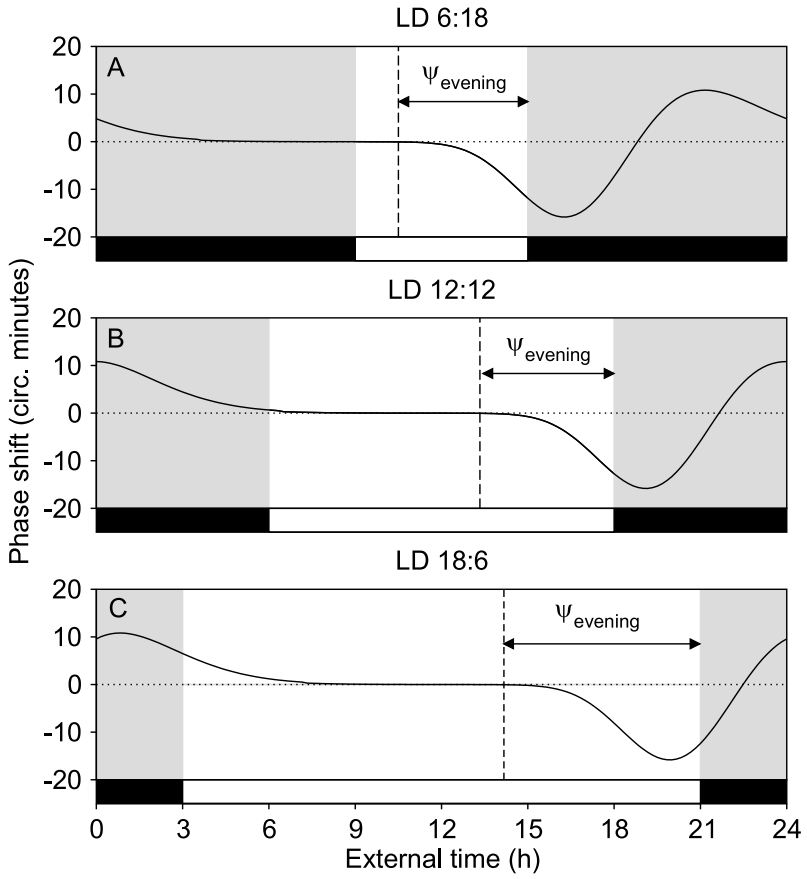

Figure 5.4: The conservation of the molecular phase of entrainment under different photoperiods can be understood with the help of PRCs. Three exemplary LD conditions ($lis = 0.2$) are shown. The dashed vertical line in each graph indicates the peaking time of Per/Cry mRNA. The model PRC (solid curve) based on gating function 1 and $lis = 0.2$ is superimposed with CT7 (i.e., time of Per/Cry mRNA peak in DD) onto the peaking time in LD. The molecular phase of entrainment $\Psi_{evening}$ is indicated by the horizontal arrow. In the synchronized state, the PRC portion in the light phase (hatched area) of the LD cycle compensates for the difference between $\tau = 23.3$h and 24h. Because of the dead zone,$\Psi_{evening}$ is almost independent of the length of photoperiod. Thus,$\Psi_{evening}$ is conserved under LD 6:18 (panel A) and LD 12:12 (panel B) conditions. Photoperiods above 13h cause the model oscillator to exhibit a larger delay part into the light phase (e.g., $\Psi_{evening}$ increases) to compensate for the phase advance during the morning phases (LD 18:6 in panel C).

How can the interplay between gating, PRC shape, and conservation of the phase of entrainment be understood? PRCs can be used to explain the constant phase relation between the circadian clock and light offset under LD cycles with different photoperiods (Fig. 5.4). The shaded area under the PRC represents the delay that is needed to compensate for the deviation of the free-running period $\tau = 23.3$h from 24h. The dead zone that is introduced with the gating implies that a prolonged day length up to 13h conserves $\Psi_{evening}$ under different photoperiods: For a wide range of photoperiods, the phase of the oscillator can be locked to light offset without exposing the advance part of the PRC to light.

Because of the simplification of our model, light-input always acts on the whole model in the same way. Experimental observations indicate, however, that the phase of entrainment of different clock components is influenced in opposite ways by a varying photoperiod; for example, the phase relations between *Per* and *Cry* mRNA [72, 125] or between *Per1*/*Cry1* and *Per2*/*Cry2* mRNA [19] increase with longer photoperiods. These observations have been discussed in the context of a morning/evening oscillator pair that is possibly involved in annual timekeeping. Similar to our model, this view implies that the oscillation of each component is locked to distinct daily events, for example, light onset or light offset under different photoperiods. Thus, our model can be considered a first approach of investigating a molecular mechanisms that can control the phasing of a single oscillator in a possible network of oscillators.

In contrast to the mammalian clock, the circadian clock of *Drosophila* responds with a rapid degradation of the TIM protein to light [83]. Low levels of TIM protein concentration during subjective day are an intrinsic mechanism of the model oscillator that leads to a dead zone in the PRC. Therefore, explicit gating is dispensable in this model oscillator. And indeed, reasonable PRCs with dead zones have been modeled for the *Drosophila* oscillator without including explicit gating [68]. A PRC without explicit gating is also described for the model of the mammalian circadian oscillator [70]. In this model, intrinsic gating by additional components might be responsible for the dead zone.

Our results suggest that the flexibility of the mammalian circadian oscillator to adapt to changing photoperiods is obtained by gating. What might be the benefits of gating for the mammalian circadian system? The core mechanism responsible for the 24-h oscillations is based on a highly conserved feature: a negative feedback of gene products [20]. It is temperature compensated and robust with respect to molecular noise [37, 53]. The flexibility to adapt to changing photoperiods by means of gating can be achieved by external mechanisms that are relatively easy to optimize on evolutionary time scales without changing the robust core oscillator.

So far, a conservation of the phase of entrainment under different photoperiods has not been observed on the molecular level. Many experiments indicate a prolonged elevation time in mRNA and protein concentration under long photoperiods compared with short photoperiods, such as PER1 protein [84, 123] and *Per1* and *Per2* mRNA [118, 128]. Since most experimental data are based on population sampling, the peaking phases of mRNA and protein oscillations are also pooled. Phase groups within the SCN make it difficult to draw any conclusions about the molecular phase of entrainment based on

pooled data [96, 148]. Single SCN cell recordings of mRNA and protein oscillations under different photoperiods could strongly advance our understanding of the phase of entrainment on the molecular level.
In summary, our results show that gating might play a central role for the phase of entrainment of the mammalian circadian clock. In addition, our results support the idea that the deviation of the free-running period τ from 24h is not a mere imprecision of the circadian clock but has a functional role since it can determine the phase of entrainment under different photoperiods.

6 The influence of the feedback mechanism on the robustness

The robustness of the circadian system, in particular towards temperature fluctuations, is one of its key features. In the following chapter, we investigate how the robustness of the circadian oscillator and of other biological feedback systems towards perturbations correlates with their specific feedback design. It is a work done in collaboration with Jana Wolf and is published in [147]. I was involved in planning the analysis, creating the general models and interpreting the results. Also, I did the sensitivity analysis for some of the models.

The circadian clock is very robust with respect to environmental influences, e.g. nutritional conditions or pH [90, 101, 106]. In particular, its ability for temperature compensation, that is, the ability to keep the oscillatory period nearly constant with changing temperature, is striking [103, 130, 145]. The high robustness of the circadian period towards environmental disturbances might be required for a precise time keeping. The robustness of the mathematical model described in chapter 3 has been analyzed extensively.

In contrast, the period of calcium oscillations which are discussed to play a role in intra- and intercellular signalling in a frequency encoded manner should be strongly dependent on certain regulatory signals. The examples show that the balance between robustness and sensitivity might be different for various rhythms.

It is discussed that robustness and sensitivity properties are determined by underlying design principles (see e.g. [8]). However, their interrelation is not well understood (see [120] for an overview about the concept of robustness and applications to cellular systems). Mathematical models of circadian rhythms have been used to investigate their sensitivity to noise [37, 135] and to changes in their kinetic parameters [67, 115, 69, 9, 119]. These studies show that circadian models are very robust and/or analyze the impact of certain clock parts that are added or removed in different model versions, respectively. However, by focussing on the impact of model parts, the contribution of the overall model design to robustness and sensitivity characteristics cannot be clarified. A more comprehensive picture of the relation between design principles and robustness can be elucidated by a comparison of different cellular oscillators.

Here we analyze and compare the robustness of oscillations in calcium signalling, glycolysis and the circadian system. We address the question whether these cellular rhythms show a specific sensitivity of their period towards parameter perturbations. In order to reveal the characteristics of the underlying network rather than the specific model description, we analyze models of different complexity for each of the rhythms. The comparison shows that the rhythms differ significantly in their robustness properties. In

order to understand the impact of overall design principles we analyze the period sensitivity in a more general approach. For that purpose, a specifically designed system is used that allows a direct comparison of the sensitivity of positive and negative feedback for different reaction chain lengths under regulation. We demonstrate that the type of feedback has a significant effect on the period sensitivity of the oscillator.

6.1 The biological oscillators

In this study, we concentrate on oscillations in calcium signalling, glycolysis and the circadian system which are briefly introduced. For each of these rhythms at least three mathematical models are included which differ in the amount of detail and extent of their descriptions.
Calcium oscillations arise in various cell types either spontaneously or after stimulation by hormones or neurotransmitter and have a period in the range of seconds or minutes. A central process in the generation of these oscillations is the release of the ions from intracellular Ca^{2+}-stores. The initiating event usually is the binding of ligands to membrane receptors leading to the activation of phospholipase C which in turn synthesizes inositol-1,4,5 triphosphate (IP_3). IP_3 binds to specific receptors at the internal Ca^{2+}-stores which release Ca^{2+} in the cytosol. This release is self-amplifying since cytoplasmic Ca^{2+} triggers further release of Ca^{2+} from internal stores; the process is known as calcium-induced-calcium-release (CICR). For the description of the oscillations a variety of models were developed. Core models are based on the CICR mechanism. More extended models take additional regulations into account, like IP_3-calcium cross-coupling, Ca^{2+} sequestration by mitochondria or the detailed kinetics of the IP_3 receptor (for a review see [111]. Here, three models are analyzed. Those of Somogyi and Stucki [117] and Goldbeter *et al.* [36] are core models, accounting for one or two intracellular Ca^{2+} pools, respectively. In the more extended model of Marhl et al. [74] mitochondria are additionally taken into account.
Glycolytic oscillations are characterized by a period in the range of minutes and occur in a broad spectrum of cells, e.g. yeast, muscle, heart and pancreatic β-cells. The generation of oscillations was found to be strongly dependent on the complex regulation of the glycolytic enzyme phosphofructokinase. Goldbeter and Lefever [35] developed a core model based on the kinetic properties of that enzyme. The model of Bier *et al.* [13] describes the pathway qualitatively by a 2-variable model. The model by Wolf and Heinrich [146] is more detailed and includes the main processes of anaerobic glycolysis, the production of ethanol and glycerol, as well as the transmembrane diffusion and extracellular degradation of acetaldehyde.
As for the circadian oscillator, besides the model described in chapter 3 of this work, three additional models are taken into account. The first is the 3-variable model developed originally by Goodwin [38], which describes a transcriptional negative feedback in general and was recently applied to the *Neurospora* system (Ruoff *et al.* [108]). Additionally, we consider the *Drosophila* model by Goldbeter [33] describing the negative

feedback of PER protein on the transcription of the *per* gene by a 5-variable model. Finally, we take the 16- variable model of Leloup and Goldbeter [69] into account, which also includes the negative feedback loop via *Rev-erbα*.
Each model is used with its reference parameters given in the original papers as these parameter sets have been optimized for a most accurate description of the rhythms with the corresponding model. The differential equation systems and reference parameters of all models are given in Appendix 7.2. Full details can be found in the original papers.

6.2 Measures of robustness

All models considered in this study describe the time dependent changes in the concentrations S_i of cellular substances by a system of coupled differential equations

$$\frac{\mathrm{d}S_i}{\mathrm{d}t} = \sum_j n_{ij}\nu_j \,, \tag{6.1}$$

where n_{ij} and v_j denote the stoichiometric coefficients of the given system and the reaction rates, respectively. The reaction rates v_j are functions of the kinetic parameters and the intermediate concentrations. All models under discussion show limit cycle oscillations for certain parameter sets. The sensitivity of an oscillatory period to changes in enzyme kinetic parameters p can be quantified by sensitivity coefficients

$$C_p^{per} = \frac{\Delta period/period}{\Delta p/p} \,. \tag{6.2}$$

In the following, we confine our consideration on parameters p_j which affect specifically a reaction j and which enter the kinetic description of that reaction in a linear way, such as enzyme concentrations, turnover numbers or maximal activities of enzyme catalyzed reactions. This allows a comparison of the sensitivities of models based on different kinetic descriptions. In the framework of metabolic control analysis the effects of infinitesimal parameter changes are considered and the resulting sensitivity coefficients represent control coefficients which fulfil general rules such as the summation relationship

$$\sum_{j=1}^{r} C_j^{per} = -1 \tag{6.3}$$

with r denoting the total number of reactions of the given system (see [50, 25, 98]. It should be noted that Eq. 6.3 is valid for all models for infinitesimal changes in the parameters. It does not hold necessarily for stronger parameter variations which, however, might be of greater biological significance. In our numerical studies we evaluate responses of oscillatory periods resulting from finite changes in the enzymatic parameters. In all models studied parameter changes of 10% around their reference value will not destroy the oscillatory behavior of the system. For these changes the summation theorem (Eq. 6.3) holds approximately true for all models ($-1.07 \leq \sum_{j=1}^{r} C_j^{per} \leq -0.97$) except

that of Leloup and Goldbeter [69] ($\sum_{j=1}^{r} C_j^{per} = -0.61$).
When the absolute value of a control coefficient is high, the corresponding parameter has a strong effect on the period, meaning that a high C_j^{per} value indicates a low robustness with respect to a specific parameter p_j. For a quantification of the overall sensitivity of the model period against changes in the activity of all reactions we use the measure

$$\sigma = \sqrt{\frac{1}{r}\sum_{j=1}^{r}(C_j^{per})^2} \tag{6.4}$$

introduced recently for a kinetic characterization of signal transduction pathways [66, 61]. In general, σ characterizes the average response of the oscillatory period to random parameter changes $\Delta p_j/p_j$ around reference values p_j^{ref} . High values of σ indicate a high sensitivity (low robustness) of the oscillatory period towards parameter changes, whereas low σ-values reflect a low sensitivity (high robustness). The definition of the overall sensitivity includes a normalization with respect to the total number r of reactions allowing to compare the robustness of systems of different size.

6.3 Period sensitivities of different oscillators

For all models the control coefficients are calculated numerically. They are shown for the models of calcium oscillations and glycolytic oscillations in 6.1, and for the models describing circadian systems in 6.2. Clearly, each model is characterized by a set of control coefficients that would be worth being discussed on its own. However, we focus here on the following questions: Do models of the same rhythm have similarities in their sensitivities? Are there characteristic differences in the period sensitivity of the different rhythms? Consequently we start with a comparison of control coefficients of models describing the same rhythm before comparing those of different rhythms.
In all three models for calcium oscillations we find a very strong negative period control by some parameters, i.e. by those characterizing the degree of stimulation ($v_1 \cdot \beta$ in Goldbeter *et al.* [36]; $k_{ER,ch}$ in Marhl *et al.* [74]), the calcium influx into the cell (γ in Somogyi and Stucki, [117]) and the release of the ions from protein-calcium-complexes ($k\_$ in Marhl *et al.* [74]), which result in control coefficients in the range of -1.5 to 3.0. On the other hand, a strong positive control is exerted by processes reducing the free calcium concentration in the cytosol by either pumping Ca^{2+} into intracellular stores (k_s in Somogyi and Stucki [117]; $k_{ER,pump}$ in Marhl *et al.* [74]), binding it to proteins (k_+ in Marhl et al. [74]) or by calcium fluxes out of the cell (k in Goldbeter et al. [36]; β in Somogyi and Stucki [117]). The corresponding control coefficients have values between 1.0 and 3.0.
The coefficients in the models describing glycolytic oscillations are generally characterized by smaller absolute values. The process of highest impact is the injection rate of substrate in the model of Goldbeter and Lefever [35] ($C_{\sigma_1}^{per} = -0.53$), the enzyme activity of phosphofructokinase ($C_{k_1}^{per} = -1.12$) in Bier *et al.* [13] and the rate constant of the

Table 6.1: Comparison of the overall sensitivity of models describing cellular oscillators. m: number of variables, r: number of reactions.

Biological rhythm	Model description	m	r	Sensitivity
Calcium oscillations	Goldbeter *et al.* [36]	2	6	1.30
	Somogyi and Stucki [117]	2	5	1.42
	Marhl *et al.* [74]	3	8	1.67
Glycolytic oscillations	Goldbeter and Lefever [35]	2	3	0.38
	Bier *et al.* [13]	2	3	0.94
	Wolf and Heinrich [146]	7	9	0.51
Circadian rhythms	Ruoff *et al.* [108]	3	6	0.24
	Goldbeter [33]	5	10	0.30
	Becker-Weimann *et al.* [9]	7	13	0.12
	Leloup and Goldbeter [69]	16	41	0.27

non-glycolytic ATP consumption in Wolf and Heinrich [146] ($C_{k_5}^{per} = -1.27$). However, the key enzyme phosphofructokinase has a negative control in all models. A detailed comparison of the models describing glycolytic oscillations was carried out in [98].
In models of circadian rhythms we find that many parameters have only a very small impact on the period (see 6.2). Exceptions are the parameters describing processes of *Bmal1* mRNA accumulation and degradation in the model of Leloup and Goldbeter [69] giving rise to control coefficients of $C_{v_{sB}}^{per} = 1.33$ and $C_{v_{mB}}^{per} = -0.93$, respectively. The high control of *Bmal1* mRNA accumulation is exceptional in particular since rates of transcription or mRNA accumulation have a very low control in the other models (k_1 in Ruoff *et al.* [108]; v_s in Goldbeter [33]; v_{1b} and v_{4b} in Becker-Weimann *et al.* [9]). However, we find all these transcriptional processes to be related to positive control coefficients. This holds true for the maximal rates of *Per* and *Cry* mRNA accumulation v_{sP} and v_{sC} in the model of Leloup and Goldbeter, [69] with the positive control coefficients $C_{v_{sP}}^{per} = 0.23$ and $C_{v_{sC}}^{per} = 0.25$. Another common characteristics of the different models is a significant negative control of the parameters characterizing the processes of mRNA degradation (k_4 in Ruoff *et al.* [108]; v_m in Goldbeter, [33]; k_{1d} in Becker-Weimann *et al.* [9]; v_{mP} and v_{mC} in Leloup and Goldbeter [69]).
The results show that there are indeed similarities in the sensitivity and robustness characteristics in models describing the same biological oscillator. Moreover, the models of different rhythms show a characteristic difference: the maximal absolute value of control coefficients differ considerably, indicating that the period of Ca^{2+} oscillations can be influenced much more strongly by parameter changes than that of glycolytic and circadian rhythms. In order to quantify this, the overall sensitivities of the models are calculated according to Eq. 6.4 and given in Table 6.1.

Apparently, the overall sensitivities of the models vary considerably. The smallest value of $\sigma = 0.12$ is shown by the model described in detail in chapter 3 [9] describing the mammalian circadian oscillator, the highest value ($\sigma = 1.67$) by the calcium model of Marhl *et al.* [74]. Interestingly, models describing the same rhythm have very

similar overall sensitivities. The highest sensitivities are shown by models for calcium oscillations, the highest robustness by models for circadian rhythms. Models for glycolytic oscillations show intermediate values (see also Fig. 6.3). Clearly, the overall sensitivities quantify and confirm the observation made on the level of single sensitivity coefficients. The fact that the overall sensitivity value of models describing the same rhythm is comparable, despite the considerable differences in the amount it detail of the model descriptions strongly supports the hypothesis that the sensitivity and robustness properties are characteristics of the cellular rhythms and depend primarily on the underlying design principles of the oscillator.
The sensitivity measure σ used here integrates the effect of independent parameter perturbations on the oscillatory period. However, it also might shed light on situations when all parameters are simultaneously varied to a different extent as it is the case for changes in temperature. In general, the influence of the temperature on the period of an oscillator can depend on various aspects, e.g. the effect of temperature changes on the individual processes, the sensitivity of the period to parameter changes or the existence of compensation mechanisms. One may ask to what extent the influence of the temperature is correlated with the period sensitivity σ. In experiments, the temperature dependence of oscillations is usually characterized by Q_{10}-values. These give the ratio of the oscillatory period at a certain temperature to that of the period at the temperature increased by $10°C$. For glycolytic and calcium oscillations Q_{10}-values of around 2.5 and 3.0, respectively, are reported [43, 109], whereas circadian rhythms are characterized by Q_{10}-value close to 1.0 (e.g. [103, 130]). In Fig. 6.3 the calculated overall sensitivities and experimentally estimated Q_{10}-values of the rhythms are plotted. This plot shows an interesting correlation between both: oscillations characterized by a high period sensitivity are strongly dependent on temperature. In contrast, circadian rhythms which were found to be very robust in the sensitivity analysis are relatively independent of temperature changes in experiments.

6.4 Dependence of the period sensitivity on design principles of the oscillator

The model comparison revealed that all circadian models are characterized by a low sensitivity. It should be emphasized that this is true irrespective of the differences in complexity of the models, e.g. the overall sensitivity of the 3-variable model (Ruoff et al. [108]) ($\sigma = 0.24$) is very similar to that of the 16-variable model of Leloup and Goldbeter [69] ($\sigma = 0.27$). This suggests that robustness is mainly determined by very basic structural mechanisms which are included in all circadian models. Up to now there are, however, only speculations as to which design principles mainly determine the robustness of an oscillator.
Design principles which are somehow central for circadian rhythms and underlie all models, are negative feedback loops with clock proteins inhibiting their own transcription and networks built on processes of transcription and translation. Thus one may ask to

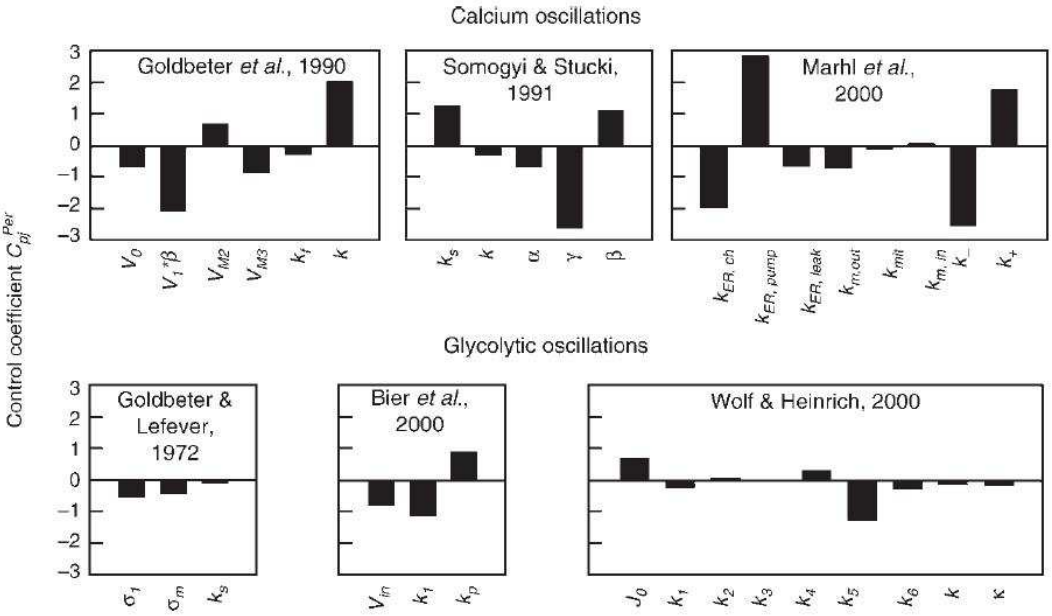

Figure 6.1: Period sensitivity for models describing calcium and glycolytic oscillations. Shown are the control coefficients for parameter variations of ±10%

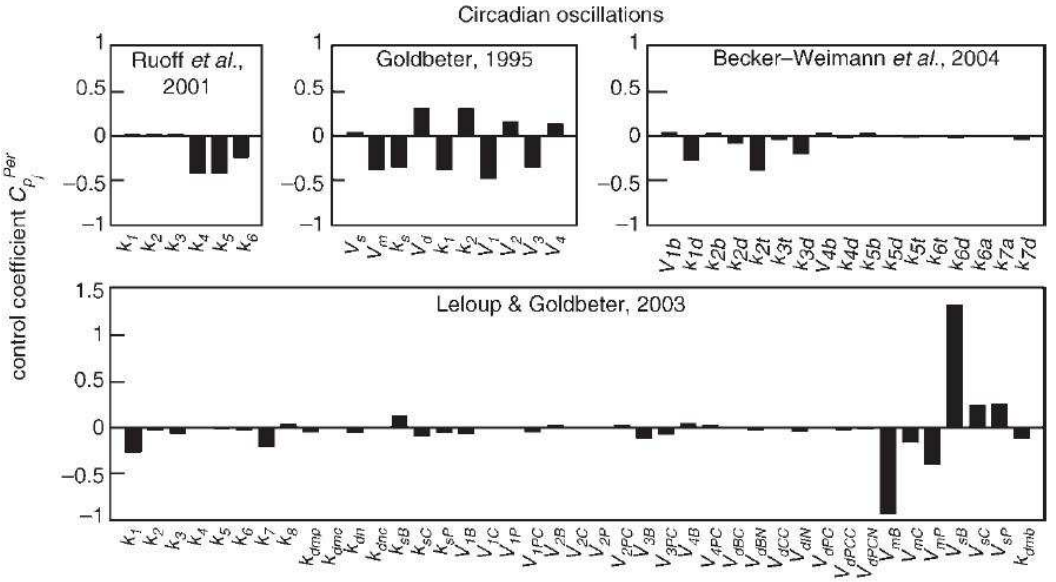

Figure 6.2: Period sensitivity of circadian models. The control coefficients are calculated for parameter variations of ±10%

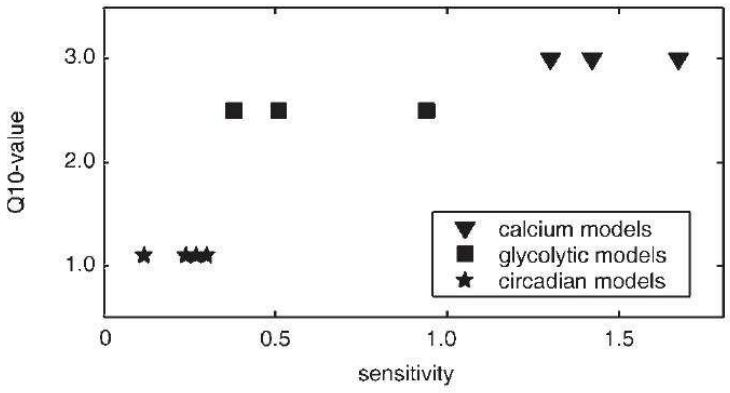

Figure 6.3: Comparison of calculated overall sensitivities of the models (see Table 6.1) and experimentally measured Q_{10}-values for the different rhythms. Q_{10}-values characterize the temperature dependency of the oscillatory period

what extent these contribute to robustness. The type of feedback might be of particular interest since in contrast, calcium oscillations are based on positive feedback regulations. Consequently, we here focus as a starting point on the question to what extent the type of feedback contributes to the robustness of an oscillator. The effect of positive and negative feedback control was analyzed in different contexts (see [119] and references therein), but its impact on the robustness of the oscillatory period is not clear. Here we use a model which is designed for a direct comparison of positive and negative feedback regulation. The model (shown in Fig. 6.4) is related to the Goodwin model. However, it describes a biochemical system characterized by a flux of matter. Moreover, the number of intermediates in the reaction chain is variable and the regulation is exerted by the last compound of the reaction chain on its second step. In such a system both feedback inhibition and feedback activation can generate oscillations.
The network with m intermediates is described by the following system of differential equations:

$$\frac{\mathrm{d}S_i}{\mathrm{d}t} = v_{2i-1} - v_{2i} - v_{2i+1}, \quad i = 1, \ldots, m \tag{6.5}$$

with the reaction rates:

$$\begin{aligned} v_1 &= const\,, \\ v_2 &= k_2 S_1\,, \\ v_3 &= k_3 S_1 N \end{aligned} \tag{6.6}$$

as well as

$$\begin{aligned} v_{2i} &= k_{2i} s\,, \\ v_{2i+1} &= k_{2i+1} S_i \;\; for \;\; i \geq 2\,. \end{aligned} \tag{6.7}$$

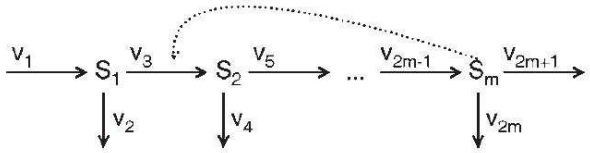

Figure 6.4: Model for the comparison of positive and negative feedback regulation. The feedback (broken line) is either inhibitory or activating, the number of intermediates in the reaction chain is arbitrary

The non-linearity term in reaction rate v_3 for a negative feedback reads

$$N = \left[1 + \left(\frac{S_m}{K_I}\right)^{n_I}\right]^{-1} . \tag{6.8}$$

A corresponding description of a positive feedback is given by

$$N = 1 + \left(\frac{S_m}{K_A}\right)^{n_A} . \tag{6.9}$$

The systems with positive and negative feedback have identical sets of parameters for all processes except reaction 3, which includes the regulation (for parameter values see the legend of Fig. 6.5). The Hill coefficients $n_I = 9$ and $n_A = 2$ may serve as reference cases for negative and positive feedback, respectively. In the system with negative feedback regulation oscillations can only occur for $i \geq 4$. By comparing systems of four to ten variables we show the period sensitivity to be dependent on the type of regulation and the length of the chain (see Fig. 6.5). Systems with positive feedback regulation have a higher sensitivity than systems with the same number of intermediates and a negative feedback. Moreover, an increase in the number of intermediates within the feedback chain increases the robustness for both types of regulation. The sensitivity of systems with a positive feedback ranges from $\sigma = 0.45$ in the 4-variable model to $\sigma = 0.26$ in the 10-variable model, and the systems with negative feedback are characterized by sensitivities between $\sigma = 0.18$ (4-variable model) and $\sigma = 0.07$ (10-variable model). Clearly, these values give only a first estimation and have to be verified by more parameter sets. However, this analysis shows that the low sensitivity values of circadian oscillators can be easily reached (and outperformed) by a negative feedback regulation. Even systems with positive feedback regulation can give rise to sensitivities in the order of those observed in circadian systems. In our example, the prerequisite is that the feedback chain reaches a critical length.

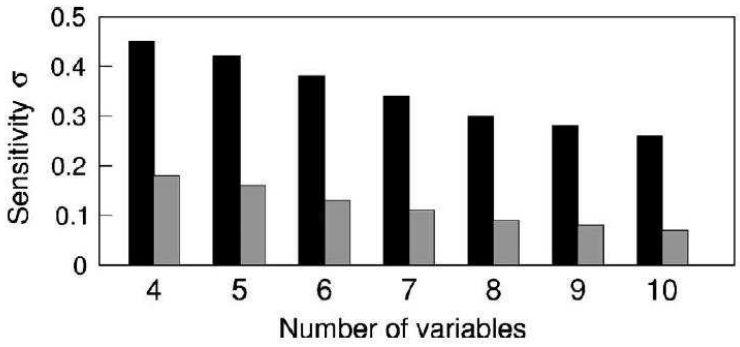

Figure 6.5: Comparison of the overall sensitivity of models with either positive (black bars) or negative (grey bars) feedback. Most kinetic parameters are identical in the systems: $v_1 = 5.0$, $k_2 = 0.01$, $K_I = K_A = 1.0$ as well as $k_{2i} = 0.1$, $k_{2i+1} = 1.0$ for $i = 2...m$.. However, the parameters of reaction 3 differ in models with both types of feedback: $k_3 = 0.02$, $n_A = 2$ in systems with positive feedback and $k_3 = 0.2$, $n_I = 9$ in systems with negative feedback

6.5 Structural design, robustness and temperature compensation

Our comparison of ten mathematical models describing three different cellular rhythms shows clear evidence that robustness properties are strongly determined by underlying oscillatory mechanisms. We demonstrate that period sensitivities differ considerably for models describing different rhythms, whereas models of the same rhythm are quite similar in that respect. In particular, we find the period of calcium oscillations to be very sensitive towards changes in parameters whereas that of circadian systems is most robust. Models for glycolytic oscillations show an intermediate sensitivity.
In our study, we compare the different models using their reference parameter sets given in the original papers. These parameter sets are most suitable for this investigation since they are optimized in order to describe the rhythm under consideration most accurate with the corresponding model. However, the use of a specific parameter set restricts our analysis to local characteristics. An extension which certainly can be carried out only for a subset of the models considered here, would be the analysis of global sensitivities of different rhythms. Such an approach was recently used for a comparison of two circadian models [120]. Interestingly, the hierarchy found in the period sensitivities of the different rhythms corresponds to that found in their temperature dependence estimated experimentally. Therefore, one may speculate as to what extent the ability of circadian rhythms to compensate temperature changes actually is the result of specific temperature-compensating mechanisms as often assumed (e.g. [107, 53]). The design of the oscillator and the resulting sensitivity characteristics might contribute to a significant extent to the small effect of temperature changes in the circadian system and

might be suited for simultaneous compensation of different disturbances. Therefore, our results support the proposition of Pittendrigh and Calderola that 'the temperature-compensation is only a special case of a general homeostatic conservation of the frequency of circadian oscillations in the face of all changes they are likely to encounter in the cell' [90]. Further insight might be given by mutants which lose the ability for temperature-compensation together with that for other compensations, e.g. pH [106].

For the discussion of circadian rhythms it might also be important to stress the fact that all models, even the core model, show a very high robustness. This strongly indicates that robustness of these oscillations depends mainly on the very basic structural mechanisms taken into account by all of the models. Here, we start to investigate the impact of the type of feedback and the length of the regulated chain. Our example shows that the robustness of circadian oscillators can be easily reached and outperformed by negative feedback regulation and is also possible in positive feedback regulation within longer reaction chains. Since our analysis concentrates on pure negative and positive feedback regulations it gives only limited insights for systems with interlocked feedbacks. However, the impact of the positive feedback on the interlocked feedback system of *Drosophila* and mammals was analyzed in [115, 9], respectively. In both cases the positive feedback has hardly any effect on the robustness of the overall circadian system. It should be emphasized that the system studied here is a biochemical rather than a genetic model since it is characterized by a flux of matter through the reaction chain. The impact of genetic processes in the network and that of other design principles remains to be investigated. Preliminary results show that the robustness of corresponding genetic and biochemical oscillators is very similar.

Of course, our comparison is far from being complete. An interesting extension would be the inclusion of other metabolic and genetic rhythms [34, 82, 58]. Several ultradian clocks of eukaryotic microbes show robustness of their periods towards temperature and other environmental factors [58] and might therefore be promising candidates.

In summary, we state that the comparison of different rhythms gives a more comprehensive picture on the impact of design principles on the robustness and sensitivity characteristics of cellular oscillators. Whereas the comparison of models describing the same rhythm can be used to reveal the impact of submodules, our approach shows the impact of the overall design of an oscillator. Clearly, the interplay of both types of studies is necessary to understand the relation between structure and robustness.

7 Discussion

7.1 Feedback loops in the circadian oscillator

Several models of the circadian oscillator that differ in their complexity and in the number of feedbacks taken into account are presented and discussed in this thesis. In order to obtain reasonable and useful results with simulations, the model has to be chosen with care. On the one hand it has to include all the details necessary to solve specific problems. On the other hand the complexity should be kept minimal since knowledge of the parameters is usually limited and a model containing many parameters gets arbitrary and unclear. In this thesis, the very simple Goodwin model [38] with only one feedback loop and three variables was used to investigate the impact of varying kinetics on the behavior of an oscillator (chapter 2). We find that only in certain cases the introduction of saturation can promote oscillations. Two new models of the circadian oscillator that are based on two and three feedback loops and contain more biological details were constructed. They were used to investigate the function and meaning of feedback loops for the oscillator and to reproduce and explain the results of mutation experiments (chapters 3 and 4). With the simpler model we could also make predictions for mutation experiments and reveal a correlation of the phase of entrainment in the synchronized state with a restriction of light-input to certain phases ('gating', chapter 5). For the investigation of robustness and the correlation with design principles, many models of different complexity were implemented (chapter 6). Comparison of the models indicates a role of the negative feedback for the robustness of a biological oscillator.

The central negative feedback loop

The circadian oscillator consists of a complex network of interlocked feedback loops. The central element is a negative feedback loop that is found even in the most simple organisms. A transcriptional activator (in mammals the BMAL1/CLOCK complex) activates the transcription of one or several inhibitors of transcription (in mammals the *Per*s and *Cry*s). After a delay, those inhibitors accumulate in the nucleus and inhibit their own synthesis, which leads to a delayed decrease of inhibitor concentration. Again, transcription can start, and so on. [100]
In experiments as well as in the models the central negative feedback determines to a large degree the dynamics of the system. In experiments, mutations in the negative feedback lead either to remarkable changes of the circadian period or to the loss of oscillations [6, 14, 31, 137]. In contrast, mutations outside the negative feedback, e.g. the mutation of *Rev-erbα*, can have a less pronounced phenotype[95]. In the models of

chapter 3 and 4 similar dynamical changes were observed if the parameters were varied corresponding to the mutations. Parameter variations in the negative feedback tended to have a stronger effect on the period than variations in the other feedbacks.
In a simple negative feedback the period of oscillations is to a good degree determined by the number and the half-lives of the components. The period of the circadian oscillator is rather long compared to usual molecular time-scales. A number of post-translational processes and regulated degradation support the long phase-shifts between transcription and nuclear accumulation that are necessary for the 24h period. The question can be asked if additional feedback loops also contribute to the long period. In our simulations we find, that even in the models with additional feedback loops the long half-lives and alternatively a higher number of components in the negative feedback are needed for oscillations with a 24h period. An additional positive or negative feedback has only a slight influence on the period. We find that complex kinetics in the negative feedback can support oscillations (chapter 2), but the correlation with the period still has to be investigated.
One possible explanation for the negative feedback as the core element of the circadian clock might be the robustness achieved with this design. If we compare circadian models and models of other biological oscillations, we find that the circadian models tend to be more robust than others towards parameter variations with respect to the period of the oscillator. The negative feedback loop is the common element of those circadian models, while some other biological oscillators investigated are based on positive feedback. In addition, simple models containing only one positive or one negative feedback were compared with respect to their robustness. The models including a negative feedback are more robust towards parameter variations with respect to the period than those including positive feedback.
Taken together this means, that even though the central negative feedback is the most sensitive part of the circadian oscillator, models based on a negative feedback are very robust compared to others. This special robustness observed in the circadian oscillator is necessary for reliable time-keeping and might even contribute to the temperature compensation observed in the circadian oscillator, but not in many other oscillators.

The function of additional feedback loops

Especially in higher organisms, in addition to the core negative feedback loop, the circadian clock contains several positive and negative feedback loops that are all interconnected. Even though the central negative feedback loop of the circadian oscillator plays such an important role for maintaining the oscillations, the effect of the additional feedback loops cannot be neglected:
In our studies we find, that a loss of oscillations that is due to a parameter variation in the negative feedback can be reversed by an additional parameter variation in a positive feedback (chapter 3). With this finding, we can explain the non-intuitive observations made in $Per2^{Brdm1}$/*Rev-erbα* double mutant mice: Oscillations are damped in the $Per2^{Brdm1}$ mice (mutation in the negative feedback) and rescued in the double

mutant (additional mutation in the positive feedback). We can predict the outcome of other double-mutants with our model, that would be similarly surprising. Our results indicate that in a certain range the positive feedback can support the stability of oscillations and the period of oscillations.
Additional feedback loops could also play a role in output pathways of the circadian oscillator.
In order to elucidate further possible functions of the different feedback loops, models containing different numbers and kinds of feedback loops could be compared with respect to their characteristics. E.g. the dynamics of the models described in chapters 3 and 4 could be compared in detail. This might reveal crucial differences with respect to period changes when parameters are varied.

7.2 Future work

Stability vs. flexibility

In this thesis, we investigate the entrainment by light (chapter 5). We find that the modulation of light-input by components of the oscillator shapes the phase-response curve, which then determines the phase between the oscillator and the input signal in the synchronized state. Investigation of this modulation and its implication for the phase can be investigated further in a broader context. The modulation of input pathways could provide for a flexibility of the phase between the oscillator and its surroundings even if the core oscillator itself is very stable. Our studies indicate a possible solution to the question how stability and flexibility of the circadian oscillator are obtained at the same time, and further investigation of this question will be interesting.

Features of circadian model families

The models introduced here contribute to the growing number of known models of the circadian oscillator. As more and more models of different complexity and size are developed, categorizing and comparing the models systematically with respect to their circadian features could give further hints on the structural features underlying those features. In the future the question "Which model represents a certain circadian feature correct?" could be converted to the question "Which KIND of model represents a certain circadian feature correct?" Therefore, having a large number of different models is of great value for the future computational circadian research. A first step in this direction was done in this thesis in chapter 6. Indeed we find a remarkable difference in sensitivity between a number of circadian models and models representing glycolysis and calcium oscillations. This difference cannot be the result of the specific structure of one of the models, as many models are taken into account.

Bibliography

[1] M. Akashi, Y. Tsuchiya, T. Yoshino, and E. Nishida. Control of intracellular dynamics of mammalian period proteins by casein kinase I epsilon (CKIepsilon) and CKIdelta in cultured cells. *Mol Cell Biol*, 22(6):1693–1703, 2002.

[2] U. Albrecht, Z. Sun, G. Eichele, and C. Lee. A differential response of two putative mammalian circadian regulators, mper1 and mper2, to light. *Cell*, 91(7):1055–64, 1997.

[3] R. Allada. Circadian clocks: a tale of two feedback loops. *Cell*, 112(3):284–286, Feb 2003.

[4] M. Antoch, E. Song, A. Chang, M. Vitaterna, Y. Zhao, L. Wilsbacher, A. Sangoram, D. King, L. Pinto, and J. Takahashi. Functional identification of the mouse circadian Clock gene by transgenic BAC rescue. *Cell*, 89(4):655–67, 1997.

[5] J. Aschoff. Circadian rhythms: influences of internal and external factors on the period measured in constant conditions. *Z Tierpsychol*, 49(3):225–49, 1979.

[6] K. Bae, X. Jin, E. Maywood, M. Hastings, S. Reppert, and D. Weaver. Differential functions of mPer1, mPer2, and mPer3 in the SCN circadian clock. *Neuron*, 30 (2):525–36, 2001.

[7] N. Bagheri, J. Stelling, and F. J. Doyle. Quantitative performance metrics for robustness in circadian rhythms. *Bioinformatics*, 23(3):358–364, Feb 2007. doi: 10.1093/bioinformatics/btl627.

[8] N. Barkai and S. Leibler. Circadian clocks limited by noise. *Nature*, 403(6767): 267–8, 2000.

[9] S. Becker-Weimann, J. Wolf, H. Herzel, and A. Kramer. Modeling feedback loops of the mammalian circadian oscillator. *Biophys J*, 87(5):3023–3034, 2004.

[10] S. Becker-Weimann, J. Wolf, A. Kramer, and H. Herzel. A model of the mammalian circadian oscillator including the REV-ERB alpha module. *Genome Inf*, 15:3–12, 2004.

[11] W. J. Belden, J. J. Loros, and J. C. Dunlap. Clock leaves its mark on histones. *Trends Biochem Sci*, 31(11):610–613, Nov 2006. doi: 10.1016/j.tibs.2006.09.009.

[12] S. Bernard, D. Gonze, B. Cajavec, H. Herzel, and A. Kramer. Synchronization-induced rhythmicity of circadian oscillators in the suprachiasmatic nucleus. *PLoS Comput Biol*, 3(4):e68, Apr 2007. doi: 10.1371/journal.pcbi.0030068.

[13] M. Bier, B. Bakker, and H. Westerhoff. How yeast cells sychronize their glycolytic oscillations: a perturbation analysis treatment. *Biophys J*, 78:1087–1093, 2000.

[14] M. K. Bunger, L. D. Wilsbacher, S. M. Moran, C. Clendenin, L. A. Radcliffe, J. B. Hogenesch, M. C. Simon, J. S. Takahashi, and C. A. Bradfield. Mop3 is an essential component of the master circadian pacemaker in mammals. *Cell*, 103(7): 1009–1017, 2000.

[15] N. Cermakian, L. Monaco, M. Pando, A. Dierich, and P. Sassone-Corsi. Altered behavioral rhythms and clock gene expression in mice with a targeted mutation in the Period1 gene. *EMBO J*, 20(15):3967–74, 2001.

[16] P. Cheng, Y. Yang, and Y. Liu. Interlocked feedback loops contribute to the robustness of the Neurospora circadian clock. *Proc Natl Acad Sci U S A*, 98(13): 7408–7413, 2001.

[17] S. Daan and C. Pittendrigh. A functional analysis of circadian pacemakers in nocturnal rodents, ii. The variability of phase response curves. *J Comp Physiol*, 106:253–266, 1976.

[18] S. Daan and C. Pittendrigh. A functional analysis of circadian pacemakers in nocturnal rodents, iii. Heavy water and constant light homeostasis of frequency? *J Comp Physiol*, 106:267–290, 1976.

[19] S. Daan, U. Albrecht, G. van der Horst, H. Illnerova, T. Roenneberg, T. Wehr, and W. Schwartz. Assembling a clock for all seasons: are there M and E oscillators in the genes? *J Biol Rhythms*, 16(2):105–16, 2001.

[20] J. Dunlap. Molecular bases for circadian clocks. *Cell*, 96(2):271–90, 1999.

[21] J. Dunlap, J. Loros, and P. DeCoursey. *Chronobiology: Biological Timekeeping.* Sunderland, MA, 2004.

[22] K. D. Edwards and A. J. Millar. Analysis of circadian leaf movement rhythms in arabidopsis thaliana. *Methods Mol Biol*, 362:103–113, 2007.

[23] E. J. Eide, E. L. Vielhaber, W. A. Hinz, and D. M. Virshup. The circadian regulatory proteins BMAL1 and cryptochromes are substrates of casein kinase Iepsilon. *J Biol Chem*, 277(19):17248–17254, 2002.

[24] J. Etchegaray, C. Lee, P. Wade, and S. Reppert. Rhythmic histone acetylation underlies transcription in the mammalian circadian clock. *Nature*, 421:177–182, 2003.

[25] D. Fell. *Understanding the control of metabolism.* Portland Press, London, UK, 1997.

[26] D. Forger and C. Peskin. A detailed predictive model of the mammalian circadian clock. *Proc Natl Acad Sci U S A*, 100(25):14806–11, 2003.

[27] W. Friesen and G. Block. What is a biological oscillator? *Am J Physiol*, 246: R847–853, 1984.

[28] O. Froy, A. L. Gotter, A. L. Casselman, and S. M. Reppert. Illuminating the circadian clock in monarch butterfly migration. *Science*, 300(5623):1303–1305, May 2003. doi: 10.1126/science.1084874.

[29] D. Gau, T. Lemberger, C. von Gall, O. Kretz, N. Le Minh, P. Gass, W. Schmid, U. Schibler, H. Korf, and G. Schutz. Phosphorylation of CREB Ser142 regulates light-induced phase shifts of the circadian clock. *Neuron*, 34(2):245–53, 2002.

[30] F. Geier, S. Becker-Weimann, A. Kramer, and H. Herzel. Entrainment in a model of the mammalian circadian oscillator. *J Biol Rhythms*, 20(1):83–93, Feb 2005. doi: 10.1177/0748730404269309.

[31] N. Gekakis, D. Staknis, H. B. Nguyen, F. C. Davis, L. D. Wilsbacher, D. P. King, J. S. Takahashi, and C. J. Weitz. Role of the CLOCK protein in the mammalian circadian mechanism. *Science*, 280(5369):1564–1569, 1998.

[32] L. Glass and M. Mackey. *From Clocks to Chaos: The Rhythms of Life.* Princeton University Press, 1988.

[33] A. Goldbeter. A model for circadian oscillations in the Drosophila period protein (PER). *Proc R Soc Lond B Biol Sci*, 261(1362):319–24, 1995.

[34] A. Goldbeter. Computational approaches to cellular rhythms. *Nature*, 420(6912): 238–245, Nov 2002.

[35] A. Goldbeter and R. Lefever. Dissipative structures for an allosteric model. Application to glycolytic oscillations. *Biophys J*, 12:1302–1315, 1972.

[36] A. Goldbeter, G. Dupont, and M. Berridge. Minimal model for signal-induced Ca2+ oscillations and for their frequency encoding through protein phosphorylation. *Proc Natl Acad Sci U S A*, 87:1461–1465, 1990.

[37] D. Gonze, J. Halloy, and A. Goldbeter. Robustness of circadian rhythms with respect to molecular noise. *Proc Natl Acad Sci U S A*, 99(2):673–8, 2002.

[38] B. Goodwin. Oscillatory behavior of enzymatic control processes. *Adv Enzyme Regul*, 3:425–439, 1965.

[39] E. Griffin, Jr, D. Staknis, and C. Weitz. Light-independent role of CRY1 and CRY2 in the mammalian circadian clock. *Science*, 286(5440):768–71, 1999.

[40] J. Griffith. Mathematics of cellular control processes. I. Negative feedback to one gene. *J Theor Biol*, 20(2):202–8, 1968.

[41] C. Grundschober, F. Delaunay, A. Puhlhofer, G. Triqueneaux, V. Laudet, T. Bartfai, and P. Nef. Circadian regulation of diverse gene products revealed by mRNA expression profiling of synchronized fibroblasts. *J Biol Chem*, 276(50):46751–8, 2001.

[42] F. Guillaumond, H. Dardente, V. Giguère, and N. Cermakian. Differential control of bmal1 circadian transcription by rev-erb and ror nuclear receptors. *J Biol Rhythms*, 20(5):391–403, Oct 2005. doi: 10.1177/0748730405277232.

[43] R. Hajjar and J. Bonventre. Oscillations of intracellular calcium induced by vasopressin in individual Fura-2-loaded mesangial cells. *J Biol Chem*, 266:21589–21594, 1991.

[44] T. Hamada, J. LeSauter, J. Venuti, and R. Silver. Expression of Period genes: rhythmic and nonrhythmic compartments of the suprachiasmatic nucleus pacemaker. *J Neurosci*, 21(19):7742–50, 2001.

[45] J. Hannibal, J. Ding, D. Chen, J. Fahrenkrug, P. Larsen, M. Gillette, and J. Mikkelsen. Pituitary adenylate cyclase-activating peptide (PACAP) in the retinohypothalamic tract: a potential daytime regulator of the biological clock. *J Neurosci*, 17(7):2637–44, 1997.

[46] G. Hardy, J. Littlewood, and G. Poyla. *Inequalities*. Cambridge University Press, Cambridge, UK, 1988.

[47] J. L. Hargrove, M. G. Hulsey, and E. G. Beale. The kinetics of mammalian gene expression. *Bioessays*, 13(12):667–674, 1991.

[48] M. H. Hastings, A. B. Reddy, and E. S. Maywood. A clockwork web: circadian timing in brain and periphery, in health and disease. *Nat Rev Neurosci*, 4(8): 649–661, Aug 2003. doi: 10.1038/nrn1177.

[49] R. Heinrich and S. Schuster. *The regulation of cellular systems*. Chapman and Hall, New York, USA, 1996.

[50] R. Heinrich and S. Schuster. *The regulation of cellular systems*. Chapman and Hall, New York, USA, 1996.

[51] T. Hofer. Model of intercellular calcium oscillations in hepatocytes: synchronization of heterogeneous cells. *Biophys J*, 77:1244–1256, 1999.

[52] C. T. Hotta, M. J. Gardner, K. E. Hubbard, S. J. Baek, N. Dalchau, D. Suhita, A. N. Dodd, and A. A. R. Webb. Modulation of environmental responses of plants by circadian clocks. *Plant Cell Environ*, 30(3):333–349, Mar 2007. doi: 10.1111/j.1365-3040.2006.01627.x.

[53] M. Izumo, C. Johnson, and S. Yamazaki. Circadian gene expression in mammalian fibroblasts revealed by real-time luminescence reporting: Temperature compensation and damping. *Proc Natl Acad Sci U S A*, 26:16089–16094, 2003.

[54] X. Jin, L. P. Shearman, D. R. Weaver, M. J. Zylka, G. J. de Vries, and S. M. Reppert. A molecular mechanism regulating rhythmic output from the suprachiasmatic circadian clock. *Cell*, 96(1):57–68, Jan 1999.

[55] C. Johnson. Forty years of PRCs–what have we learned? *Chronobiol Int*, 16(6): 711–43, 1999.

[56] C. Jones, S. Campbell, S. Zone, F. Cooper, A. DeSano, P. Murphy, B. Jones, L. Czajkowski, and L. Ptacek. Familial advanced sleep-phase syndrome: A short-period circadian rhythm variant in humans. *Nat Med*, 5(9):1062–5, 1999.

[57] I. Karatsoreos, L. Yan, J. LeSauter, and R. Silver. Phenotype matters: identification of light-responsive cells in the mouse suprachiasmatic nucleus. *J Neurosci*, 24 (1):68–75, 2004.

[58] F. Kippert and P. Hunt. Ultradian clocks in eukaryotic microbes: from behavioral observation to functional genomics. *BioEssays*, 22:16–22, 2000.

[59] R. J. Konopka and S. Benzer. Clock mutants of drosophila melanogaster. *Proc Natl Acad Sci U S A*, 68(9):2112–2116, Sep 1971.

[60] A. Kramer, F. Yang, P. Snodgrass, X. Li, T. Scammell, F. Davis, and C. Weitz. Regulation of daily locomotor activity and sleep by hypothalamic EGF receptor signaling. *Science*, 294(5551):2511–5, 2001.

[61] R. Kruger and R. Heinrich. Model reduction and analysis of robustness for the Wnt/beta-catenin signal transduction pathway. *Genome Inf*, 15(1):138–148, 2004.

[62] K. Kume, M. J. Zylka, S. Sriram, L. P. Shearman, D. R. Weaver, X. Jin, E. S. Maywood, M. H. Hastings, and S. M. Reppert. mCRY1 and mCRY2 are essential components of the negative limb of the circadian clock feedback loop. *Cell*, 98(2): 193–205, 1999.

[63] H. Kunz and P. Achermann. Simulation of circadian rhythm generation in the suprachiasmatic nucleus with locally coupled self-sustained oscillators. *J Theor Biol*, 224:63–78, 2003.

[64] G. Kurosawa, A. Mochizuki, and Y. Iwasa. Comparative study of circadian clock models, in search of processes promoting oscillation. *J Theor Biol*, 216(2):193–208, 2002.

[65] C. Lee, J. P. Etchegaray, F. R. Cagampang, A. S. Loudon, and S. M. Reppert. Posttranslational mechanisms regulate the mammalian circadian clock. *Cell*, 107 (7):855–867, 2001.

[66] E. Lee, A. Salic, R. Kruger, R. Heinrich, and M. Kirschner. The roles of APC and Axin derived from experimental and theoretical analysis of the Wnt pathway. *PLoS Biol*, 1(1):116–132, 2003.

[67] J. Leloup and A. Goldbeter. Temperature compensation of circadian rhythms: control of the period in a model for circadian oscillations of the per protein in drosophila. *Chronobiol Intern*, 14(5):511–520, 1997.

[68] J. Leloup and A. Goldbeter. A model for circadian rhythms in Drosophila incorporating the formation of a complex between the PER and TIM proteins. *J Biol Rhythms*, 13(1):70–87, 1998.

[69] J. Leloup and A. Goldbeter. Toward a detailed computational model for the mammalian circadian clock. *Proc Natl Acad Sci U S A*, 100(12):7051–6, 2003.

[70] J. Leloup and A. Goldbeter. Modeling the mammalian circadian clock: sensitivity analysis and multiplicity of oscillatory mechanisms. *J Theor Biol*, 230(4):541–62, 2004.

[71] J. C. Leloup and A. Goldbeter. Temperature compensation of circadian rhythms: control of the period in a model for circadian oscillations of the per protein in drosophila. *Chronobiol Int*, 14(5):511–520, Sep 1997.

[72] G. Lincoln, H. Andersson, and A. Loudon. Clock genes in calendar cells as the basis of annual timekeeping in mammals–a unifying hypothesis. *J Endocrinol*, 179 (1):1–13, 2003.

[73] P. Lowrey and J. Takahashi. Mammalian circadian biology: elucidating genome-wide levels of temporal organization. *Annu Rev Genomics Hum Genet*, 5:407–41, 2004.

[74] M. Marhl, T. Haberichter, M. Brumen, and R. Heinrich. Complex calcium oscillations and the role of mitochondria and cytosolic proteins. *BioSystems*, 57:75–86, 2000.

[75] E. Maywood, J. O'Brien, and M. Hastings. Expression of mCLOCK and other circadian clock-relevant proteins in the mouse suprachiasmatic nuclei. *J Neuroendocrinol*, 15(4):329–34, 2003.

[76] N. McDonald. *Delays in biological systems: Linear stability theory.* Cambridge University Press, Cambridge, UK, 1989.

[77] P. McNamara, S. P. Seo, R. D. Rudic, A. Sehgal, D. Chakravarti, and G. A. FitzGerald. Regulation of clock and mop4 by nuclear hormone receptors in the vasculature: a humoral mechanism to reset a peripheral clock. *Cell*, 105(7):877–889, Jun 2001.

[78] J. Meijer and W. Schwartz. In search of the pathways for light-induced pacemaker resetting in the suprachiasmatic nucleus. *J Biol Rhythms*, 18(3):235–49, 2003.

[79] S. Messager, A. Ross, P. Barrett, and P. Morgan. Decoding photoperiodic time through Per1 and ICER gene amplitude. *Proc Natl Acad Sci U S A*, 96(17): 9938–43, 1999.

[80] S. Messager, D. Hazlerigg, J. Mercer, and P. Morgan. Photoperiod differentially regulates the expression of Per1 and ICER in the pars tuberalis and the suprachiasmatic nucleus of the Siberian hamster. *Eur J Neurosci*, 12(8):2865–70, 2000.

[81] S. Miyake, Y. Sumi, L. Yan, S. Takekida, T. Fukuyama, Y. Ishida, S. Yamaguchi, K. Yagita, and H. Okamura. Phase-dependent responses of Per1 and Per2 genes to a light-stimulus in the suprachiasmatic nucleus of the rat. *Neurosci Lett*, 294 (1):41–4, 2000.

[82] N. Monk. Oscillatory expression of Hes1, p53, and NF-kB driven by transcriptional time delays. *Curr Biol*, 13:1409–1413, 2003.

[83] Myers M, Wager-Smith K, A. Rothenfluh-Hilfiker, and M. Young. Light-induced degradation of TIMELESS and entrainment of the Drosophila circadian clock. *Science*, 271:1736–1740, 1996.

[84] B. Nuesslein-Hildesheim, J. O'Brien, F. Ebling, E. Maywood, and M. Hastings. The circadian cycle of mPER clock gene products in the suprachiasmatic nucleus of the siberian hamster encodes both daily and seasonal time. *Eur J Neurosci*, 12 (8):2856–64, 2000.

[85] K. Oishi, K. Miyazaki, K. Kadota, R. Kikuno, T. Nagase, G. ichi Atsumi, N. Ohkura, T. Azama, M. Mesaki, S. Yukimasa, H. Kobayashi, C. Iitaka, T. Umehara, M. Horikoshi, T. Kudo, Y. Shimizu, M. Yano, M. Monden, K. Machida, J. Matsuda, S. Horie, T. Todo, and N. Ishida. Genome-wide expression analysis of mouse liver reveals clock-regulated circadian output genes. *J Biol Chem*, 278(42): 41519–41527, Oct 2003. doi: 10.1074/jbc.M304564200.

[86] H. Okamura, S. Miyake, Y. Sumi, S. Yamaguchi, A. Yasui, M. Muijtjens, J. H. Hoeijmakers, and G. T. van der Horst. Photic induction of mPer1 and mPer2 in cry-deficient mice lacking a biological clock. *Science*, 286(5449):2531–2534, 1999.

[87] H. Oster, A. Yasui, G. T. van der Horst, and U. Albrecht. Disruption of mcry2 restores circadian rhythmicity in mper2 mutant mice. *Genes Dev*, 16(20):2633–2638, Oct 2002.

[88] Y. Ouyang, C. R. Andersson, T. Kondo, S. S. Golden, and C. H. Johnson. Resonating circadian clocks enhance fitness in cyanobacteria. *Proc Natl Acad Sci U S A*, 95(15):8660–8664, Jul 1998.

[89] B. O. Palsson and T. M. Groshans. Mathematical modelling of dynamics and control in metabolic networks: Vi. dynamic bifurcations in single biochemical control loops. *J Theor Biol*, 131(1):43–53, Mar 1988.

[90] C. Pittendrigh and P. Caldarola. General homeostasis of the frequency of circadian oscillators. *Proc Natl Acad Sci USA*, 70:2697–2701, 1973.

[91] C. Pittendrigh and S. Daan. A functional analysis of circadian pacemakers in nocturnal rodents. *J Comp Physiol A*, 106:223–252, 1976.

[92] C. Pittendrigh and S. Daan. A functional analysis of circadian pacemakers in nocturnal rodents, i. The stability and lability of spontaneous frequency. *J Comp Physiol*, 106:223–252, 1976.

[93] C. Pittendrigh and S. Daan. A functional analysis of circadian pacemakers in nocturnal rodents, iv. Entrainment: Pacemaker as clock. *J Comp Physiol*, 106: 291–331, 1976.

[94] C. Pittendrigh and S. Daan. A functional analysis of circadian pacemakers in nocturnal rodents. *J Comp Physiol*, 106:223–355, 1976.

[95] N. Preitner, F. Damiola, L. Lopez-Molina, J. Zakany, D. Duboule, U. Albrecht, and U. Schibler. The orphan nuclear receptor REV-ERBalpha controls circadian transcription within the positive limb of the mammalian circadian oscillator. *Cell*, 110(2):251–260, 2002.

[96] J. Quintero, S. Kuhlman, and D. McMahon. The biological clock nucleus: a multiphasic oscillator network regulated by light. *J Neurosci*, 23(22):8070–6, 2003.

[97] M. R. Ralph and M. Menaker. A mutation of the circadian system in golden hamsters. *Science*, 241(4870):1225–1227, Sep 1988.

[98] K. Reijenga, H. Westerhoff, B. Kholodenko, and J. Snoep. Control analysis for autonomously oscillating biochemical networks. *Biophys J*, 82:99–108, 2002.

[99] S. M. Reppert and D. R. Weaver. Molecular analysis of mammalian circadian rhythms. *Annu Rev Physiol*, 63:647–676, 2001.

[100] S. M. Reppert and D. R. Weaver. Coordination of circadian timing in mammals. *Nature*, 418(6901):935–941, 2002.

[101] T. Roenneberg and M. Merrow. Circadian systems and metabolism. *J Biol Rhythms*, 14:449–459, 1999.

[102] T. Roenneberg, A. Wirz-Justice, and M. Merrow. Life between clocks: daily temporal patterns of human chronotypes. *J Biol Rhythms*, 18(1):80–90, 2003.

[103] N. Ruby, D. Burns, and H. Heller. Circadian rhythms in the suprachiasmatic nucleus are temperature-compensated and phase-shifted by heat pulses in vitro. *J Neurosci*, 19(19):8630–6, 1999.

[104] P. Ruoff and L. Rensing. The temperature-compensated goodwin model simulates many circadian clock properties. *J Theor Biol*, 179:275–285, 1996.

[105] P. Ruoff and L. Rensing. The temperature-compensated goodwin oscillator simulates many circadian clock properties. *J Theor Biol*, 179:275–285, 1996.

[106] P. Ruoff, A. Behzadi, M. Hauglid, M. Vinsjevik, and H. Havas. pH homeostasis of the circadian sporulation rhythm in clock mutants of Neurospora crassa. *Chronobiol Intern*, 17(6):733–750, 2000.

[107] P. Ruoff, M. Vinsjevik, and L. Rensing. Temperature compensation in biological oscillators: a challange for joint experimental and theoretical analysis. *Comments Theor Biol*, 5:361–382, 2000.

[108] P. Ruoff, M. Vinsjevik, C. Monnerjahn, and L. Rensing. The Goodwin model: simulating the effect of light pulses on the circadian sporulation rhythm of Neurospora crassa. *J Theor Biol*, 209(1):29–42, 2001.

[109] P. Ruoff, M. Christensen, J. Wolf, and R. Heinrich. Temperature dependency and temperature compensation in a model of yeast glycolytic oscillations. *Biophys Chem*, 106:179–192, 2003.

[110] J. Rutter, M. Reick, and S. McKnight. Metabolism and the control of circadian rhythms. *Annu Rev Biochem*, 71:307–31, 2002.

[111] S. Schuster, M. Marhl, and T. Hofer. Modelling of simple and complex calcium oscillations. From single-cell responses to intercellular signalling. *Eur J Biochem*, 269(5):1333–55, 2002.

[112] L. P. Shearman, X. Jin, C. Lee, S. M. Reppert, and D. R. Weaver. Targeted disruption of the mPer3 gene: subtle effects on circadian clock function. *Mol Cell Biol*, 20(17):6269–6275, 2000.

[113] L. P. Shearman, S. Sriram, D. R. Weaver, E. S. Maywood, I. Chaves, B. Zheng, K. Kume, C. C. Lee, G. T. van der Horst, M. H. Hastings, and S. M. Reppert. Interacting molecular loops in the mammalian circadian clock. *Science*, 288(5468): 1013–1019, 2000.

[114] Y. Shigeyoshi, K. Taguchi, S. Yamamoto, S. Takekida, L. Yan, H. Tei, T. Moriya, S. Shibata, J. Loros, J. Dunlap, and H. Okamura. Light-induced resetting of a mammalian circadian clock is associated with rapid induction of the mPer1 transcript. *Cell*, 91(7):1043–53, 1997.

[115] P. Smolen, D. A. Baxter, and J. H. Byrne. A reduced model clarifies the role of feedback loops and time delays in the drosophila circadian oscillator. *Biophys J*, 83(5):2349–2359, Nov 2002.

[116] P. Smolen, P. Hardin, B. Lo, D. Baxter, and J. Byrne. Simulation of Drosophila circadian oscillations, mutations, and light responses by a model with VRI, PDP-1, and CLK. *Biophys J*, 86(5):2786–802, 2004.

[117] R. Somogyi and J. Stucki. Hormone-induced calcium oscillations in liver cells can be explained by a simple one-pool model. *J Biol Chem*, 266:11068–11077, 1991.

[118] S. Steinlechner, B. Jacobmeier, F. Scherbarth, H. Dernbach, F. Kruse, and U. Albrech. Robust circadian rhythmicity of Per1 and Per2 mutant mice in constant light, and dynamics of Per1 and Per2 gene expression under long and short photoperiods. *J Biol Rhythms*, 17(3):202–9, 2002.

[119] J. Stelling, E. Gilles, and F. Doyle. Robustness properties of circadian clock architectures. *Proc Natl Acad Sci U S A*, 101:13210–13215, 2004.

[120] J. Stelling, U. Sauer, Z. Szallasi, F. Doyle, and J. Doyle. Robustness of cellular functions. *Cell*, 118:675–685, 2004.

[121] F. Stephan and I. Zucker. Circadian rhythms in drinking behavior and locomotor activity of rats are eliminated by hypothalamic lesions. *Proc Natl Acad Sci U S A*, 69:1583–1586, 1972.

[122] K. Storch, O. Lipan, I. Leykin, N. Viswanathan, F. Davis, W. Wong, and C. Weitz. Extensive and divergent circadian gene expression in liver and heart. *Nature*, 417 (6884):78–83, 2002.

[123] A. Sumova, M. Sladek, M. Jac, and H. Illnerova. The circadian rhythm of Per1 gene product in the rat suprachiasmatic nucleus and its modulation by seasonal changes in daylength. *Brain Res*, 947(2):260–70, 2002.

[124] A. Sumova, M. Jac, M. Sladek, I. Sauman, and H. Illnerova. Clock gene daily profiles and their phase relationship in the rat suprachiasmatic nucleus are affected by photoperiod. *J Biol Rhythms*, 18(2):134–44, 2003.

[125] A. Sumova, Z. Bendova, M. Sladek, Z. Kovacikova, and H. Illnerova. Seasonal molecular timekeeping within the rat circadian clock. *Physiol Res*, 53 Suppl 1: S167–76, 2004.

[126] T. Tamaru, Y. Isojima, T. Yamada, M. Okada, K. Nagai, and K. Takamatsu. Light and glutamate-induced degradation of the circadian oscillating protein BMAL1 during the mammalian clock resetting. *J Neurosci*, 20(20):7525–7530, 2000.

[127] K. L. Toh, C. R. Jones, Y. He, E. J. Eide, W. A. Hinz, D. M. Virshup, L. J. Ptacek, and Y. H. Fu. An hPer2 phosphorylation site mutation in familial advanced sleep phase syndrome. *Science*, 291(5506):1040–1043, 2001.

[128] B. Tournier, J. Menet, H. Dardente, V. Poirel, A. Malan, M. Masson-Pevet, P. Pevet, and P. Vuillez. Photoperiod differentially regulates clock genes' expression in the suprachiasmatic nucleus of Syrian hamster. *Neuroscience*, 118(2): 317–22, 2003.

[129] Z. Travnickova-Bendova, N. Cermakian, S. Reppert, and P. Sassone-Corsi. Bimodal regulation of mPeriod promoters by CREB-dependent signaling and CLOCK/BMAL1 activity. *Proc Natl Acad Sci U S A*, 99(11):7728–33, 2002.

[130] Y. Tsuchiya, M. Akasho, and E. Nishida. Temperature compensation and temperature resetting of circadian rhythms in mammalian cultured fibroblasts. *Genes Cells*, 8:713–720, 2003.

[131] J. J. Tyson, C. I. Hong, C. D. Thron, and B. Novak. A simple model of circadian rhythms based on dimerization and proteolysis of PER and TIM. *Biophys J*, 77 (5):2411–2417, 1999.

[132] H. Ueda, W. Chen, A. Adachi, H. Wakamatsu, S. Hayashi, T. Takasugi, M. Nagano, K. Nakahama, Y. Suzuki, S. Sugano, M. Iino, Y. Shigeyoshi, and S. Hashimoto. A transcription factor response element for gene expression during circadian night. *Nature*, 418(6897):534–9, 2002.

[133] H. R. Ueda, M. Hagiwara, and H. Kitano. Robust oscillations within the interlocked feedback model of Drosophila circadian rhythm. *J Theor Biol*, 210(4): 401–406, 2001.

[134] G. T. van der Horst, M. Muijtjens, K. Kobayashi, R. Takano, S. Kanno, M. Takao, J. de Wit, A. Verkerk, A. P. Eker, D. van Leenen, R. Buijs, D. Bootsma, J. H. Hoeijmakers, and A. Yasui. Mammalian Cry1 and Cry2 are essential for maintenance of circadian rhythms. *Nature*, 398(6728):627–630, 1999.

[135] J. Vilar, H. Kueh, N. Barkai, and S. Leibler. Mechanisms of noise-resistance in genetic oscillators. *Proc Natl Acad Sci U S A*, 99(9):5988–92, 2002.

[136] M. W. Vitalini, R. M. de Paula, C. S. Goldsmith, C. A. Jones, K. A. Borkovich, and D. Bell-Pedersen. Circadian rhythmicity mediated by temporal regulation of the activity of p38 mapk. *Proc Natl Acad Sci U S A*, 104(46):18223–18228, Nov 2007. doi: 10.1073/pnas.0704900104.

[137] M. Vitaterna, C. Selby, T. Todo, H. Niwa, C. Thompson, E. Fruechte, K. Hitomi, R. Thresher, T. Ishikawa, J. Miyazaki, J. Takahashi, and A. Sancar. Differential regulation of mammalian period genes and circadian rhythmicity by cryptochromes 1 and 2. *Proc Natl Acad Sci U S A*, 96(21):12114–9, 1999.

[138] M. H. Vitaterna, D. P. King, A. M. Chang, J. M. Kornhauser, P. L. Lowrey, J. D. McDonald, W. F. Dove, L. H. Pinto, F. W. Turek, and J. S. Takahashi. Mutagenesis and mapping of a mouse gene, clock, essential for circadian behavior. *Science*, 264(5159):719–725, Apr 1994.

[139] M. H. Vitaterna, C. H. Ko, A.-M. Chang, E. D. Buhr, E. M. Fruechte, A. Schook, M. P. Antoch, F. W. Turek, and J. S. Takahashi. The mouse clock mutation reduces circadian pacemaker amplitude and enhances efficacy of resetting stimuli and phase-response curve amplitude. *Proc Natl Acad Sci U S A*, 103(24):9327–9332, Jun 2006. doi: 10.1073/pnas.0603601103.

[140] C. von Gall, G. Duffield, M. Hastings, M. Kopp, F. Dehghani, H. Korf, and J. Stehle. CREB in the mouse SCN: a molecular interface coding the phase-adjusting stimuli light, glutamate, PACAP, and melatonin for clockwork access. *J Neurosci*, 18(24):10389–97, 1998.

[141] P. Wagner, J. Kunz, A. Koller, and M. N. Hall. Active transport of proteins into the nucleus. *FEBS Lett*, 275(1-2):1–5, 1990.

[142] D. Weinert and J. Waterhouse. The circadian rhythm of core temperature: effects of physical activity and aging. *Physiol Behav*, 90(2-3):246–256, Feb 2007. doi: 10.1016/j.physbeh.2006.09.003.

[143] D. Welsh, D. Logothetis, M. Meister, and S. Reppert. Individual neurons dissociated from rat suprachiasmatic nucleus express independently phased circadian firing rhythms. *Neuron*, 14(4):697–706, 1995.

[144] D. K. Welsh, S.-H. Yoo, A. C. Liu, J. S. Takahashi, and S. A. Kay. Bioluminescence imaging of individual fibroblasts reveals persistent, independently phased circadian rhythms of clock gene expression. *Curr Biol*, 14(24):2289–2295, Dec 2004. doi: 10.1016/j.cub.2004.11.057.

[145] A. Winfree. *The geometry of biological time*. Springer, New York, 2001.

[146] J. Wolf and R. Heinrich. Effect of cellular interaction on glycolytic oscillations in yeast: a theoretical investigation. *Biochem J*, 345:321–334, 2000.

[147] J. Wolf, S. Becker-Weimann, and R. Heinrich. Analysing the robustness of cellular rhythms. *Syst Biol (Stevenage)*, 2(1):35–41, Mar 2005.

[148] S. Yamaguchi, H. Isejima, T. Matsuo, R. Okura, K. Yagita, M. Kobayashi, and H. Okamura. Synchronization of cellular clocks in the suprachiasmatic nucleus. *Science*, 302(5649):1408–12, 2003.

[149] S. Yamazaki, R. Numano, M. Abe, A. Hida, R. Takahashi, M. Ueda, G. Block, Y. Sakaki, M. Menaker, and H. Tei. Resetting central and peripheral circadian oscillators in transgenic rats. *Science*, 288(5466):682–5, 2000.

[150] S.-H. Yoo, S. Yamazaki, P. L. Lowrey, K. Shimomura, C. H. Ko, E. D. Buhr, S. M. Siepka, H.-K. Hong, W. J. Oh, O. J. Yoo, M. Menaker, and J. S. Takahashi. Period2::luciferase real-time reporting of circadian dynamics reveals persistent circadian oscillations in mouse peripheral tissues. *Proc Natl Acad Sci U S A*, 101 (15):5339–5346, Apr 2004. doi: 10.1073/pnas.0308709101.

[151] C. Yuh, H. Bolouri, and E. Davidson. Genomic cis-regulatory logic: experimental and computational analysis of a sea urchin gene. *Science*, 279:1896–1902, 1998.

[152] B. Zheng, D. Larkin, U. Albrecht, Z. Sun, M. Sage, G. Eichele, C. Lee, and A. Bradley. The mPer2 gene encodes a functional component of the mammalian circadian clock. *Nature*, 400(6740):169–73, 1999.

[153] B. Zheng, U. Albrecht, K. Kaasik, M. Sage, W. Lu, S. Vaishnav, Q. Li, Z. S. Sun, G. Eichele, A. Bradley, and C. C. Lee. Nonredundant roles of the mPer1 and mPer2 genes in the mammalian circadian clock. *Cell*, 105(5):683–694, 2001.

[154] W. Zimmerman, C. Pittendrigh, and T. Pavlidis. Temperature compensation of the circadian oscillation in Drosophila pseudoobscura and its entrainment by temperature cycles. *J Insect Physiol*, 14:669–684, 1968.

Models

1 Models of the circadian oscillator

Goodwin, 1965 [38]/ Ruoff et al., 2001 [108]

$$\frac{dx_1}{dt} = \frac{a}{A + kx_3^p} - bx_1 \tag{1}$$

$$\frac{dx_2}{dt} = \alpha x_1 - \beta x_2 \tag{2}$$

$$\frac{dx_3}{dt} = \gamma x_2 - \delta x_3 \tag{3}$$

Parameter	Goodwin [38] (damped oscillations)	reference set Chapter 6	Griffith [40] Chapter 2
a	360	20	1
A	1	1	1
k	43	1	K_I
b	1	0.15	κ_1
α	1	0.1	1
β	0.6	0.15	κ_2
γ	1	0.1	1
δ	0.8	0.17	κ_3
p	1	9	p

Table 1: Goodwin, 1965 [38]/ Ruoff et al., 2001 [108]: Parameters

Becker-Weimann et al., 2004a [9]/ Geier et al., 2005 [30]

$$\frac{dy_1}{dt} = f_{trans(Per2/Cry)} - k_{1d} \cdot y_1 \quad (4)$$

$$\frac{dy_2}{dt} = k_{2b} \cdot y_1^q - k_{2d} \cdot y_2 - k_{2t} \cdot y_2 + k_{3t} \cdot y_3 \quad (5)$$

$$\frac{dy_3}{dt} = k_{2t} \cdot y_2 - k_{3t} \cdot y_3 - k_{3d} \cdot y_3 \quad (6)$$

$$\frac{dy_4}{dt} = f_{trans(Bmal1)} - k_{4d} \cdot y_4 \quad (7)$$

$$\frac{dy_5}{dt} = k_{5b} \cdot y_4 - k_{5d} \cdot y_5 - k_{5t} \cdot y_5 + k_{6t} \cdot y_6 \quad (8)$$

$$\frac{dy_6}{dt} = k_{5t} \cdot y_5 - k_{6t} \cdot y_6 - k_{6d} \cdot y_6 + k_{7p} \cdot y_7 - k_{6p} \cdot y_6 \quad (9)$$

$$\frac{dy_7}{dt} = k_{6p} \cdot y_6 - k_{7p} \cdot y_7 - k_{7d} \cdot y_7 \quad (10)$$

For the inclusion of light-input in chapter 5, equation 4 modifies to

$$\frac{dy_1}{dt} = f_{trans(Per2/Cry)} - k_{1d} \cdot y_1 + lightinput \quad (11)$$

Parameter	Value	Description
v_{1b}	9 nMh^{-1}	Maximal rate of *Per2/Cry* transcription
k_{1b}	1 nM	Michaelis constant of *Per2/Cry* transcription
k_{1i}	0.56 nM	Inhibition constant of *Per2/Cry* transcription
c	0.01 nM	Concentration of constitutive activator
p	8	Hill coefficient of inhibition of *Per2/Cry* transcription
k_{1d}	0.12 h^{-1}	Degradation rate of *Per2/Cry* mRNA
k_{2b}	0.3 $nM^{-1}h^{-1}$	Complex formation rate of PER2/CRY
q	2	Number of PER2/CRY complex forming subunits
k_{2d}	0.05 h^{-1}	Degradation rate of the cytoplasmatic PER2/CRY
k_{2t}	0.24 h^{-1}	Nuclear import rate of the PER2/CRY complex
k_{3t}	0.02 h^{-1}	Nuclear export rate of the PER2/CRY complex
k_{3d}	0.12 h^{-1}	Degradation rate of the nuclear PER2/CRY complex
v_{4b}	3.6 nMh^{-1}	Maximal rate of *Bmal1* transcription
k_{4b}	2.16 nM	Michaelis constant of *Bmal1* transcription
r	3	Hill coefficient of activation of *Bmal1* transcription
k_{4d}	0.75 h^{-1}	Degradation rate of *Bmal1* mRNA
k_{5b}	0.24 h^{-1}	Translation rate of BMAL1
k_{5d}	0.06 h^{-1}	Degradation rate of cytoplasmatic BMAL1

continued on next page

continued from previous page

Parameter	Value	Description
k_{5t}	0.45 h^{-1}	Nuclear import rate of BMAL1
k_{6t}	0.06 h^{-1}	Nuclear export rate of BMAL1
k_{6d}	0.12 h^{-1}	Degradation rate of nuclear BMAL1
k_{6a}	0.09 h^{-1}	Activation rate of nuclear BMAL1
k_{7a}	0.003 h^{-1}	Deactivation rate of nuclear BMAL1*
k_{7d}	0.09 h^{-1}	Degradation rate of nuclear BMAL1*

Table 2: Becker-Weimann et al., 2004a [9]: Parameters

Becker-Weimann et al., 2004b [10]

$$\frac{dy_1}{dt} = \frac{v_{1b}(y_7^s + c)}{k_{1b}^s(1 + (y_3^p/k_{1i}^p)) + (y_7^s + c)} - k_{1d}y_1 \tag{12}$$

$$\frac{dy_2}{dt} = k_{2b}y_1^q - k_{2t}y_2 + k_{3t}y_3 - k_{2d}y_2 \tag{13}$$

$$\frac{dy_3}{dt} = k_{2t}y_2 - k_{3t}y_3 - k_{3d}y_3 \tag{14}$$

$$\frac{dy_4}{dt} = \frac{v_{4b}}{k_{4b} + (y_8^u/k_{4i}^u)} - k_{4d}y_4 \tag{15}$$

$$\frac{dy_5}{dt} = k_{5b}y_4 - k_{5t}y_5 + k_{6t}y_6 - k_{5d}y_5 \tag{16}$$

$$\frac{dy_6}{dt} = k_{5t}y_5 - k_{6t}y_6 - k_{6a}y_6 + k_{7a}y_7 - k_{6d}y_6 \tag{17}$$

$$\frac{dy_7}{dt} = k_{6a}y_6 - k_{7a}y_7 - k_{7d}y_7 \tag{18}$$

$$\frac{dy_8}{dt} = \frac{v_{8b}(y_7^r + c)}{k_{8b}^r(1 + (y_3^v/k_{8i}^v)) + (y_7^r + c)} - k_{8d}y_8 \tag{19}$$

Parameter	Value	Description
v_{1b}	18 $nMhr^{-1}$	Maximal rate of *Per2/Cry* transcription
k_{1b}	1 nM	Michaelis constant of *Per2/Cry* transcription
k_{1i}	0.65 nM	Inhibition constant of *Per2/Cry* transcription
c	0.001 nM	Concentration of constitutive BMAL1*
p	8	Hill coefficient of inhibition of *Per2/Cry* transcription
s	5	Hill coefficient of activation of *Per2/Cry* transcription
k_{1d}	0.12 hr^{-1}	Degradation rate of *Per2/Cry* mRNA
k_{2b}	0.3 $nM^{-1}hr^{-1}$	Complex formation rate of PER2/CRY
q	2	Number of PER2/CRY complex forming subunits

continued on next page

continued from previous page

Parameter	Value	Description
k_{2d}	0.07 hr^{-1}	Degradation rate of the cytoplasmatic PER2/CRY
k_{2t}	0.24 hr^{-1}	Nuclear import rate of the PER2/CRY complex
k_{3t}	0.02 hr^{-1}	Nuclear export rate of the PER2/CRY complex
k_{3d}	0.12 hr^{-1}	Degradation rate of the nuclear PER2/CRY complex
v_{4b}	3.0 $nMhr^{-1}$	Maximal rate of *Bmal1* transcription
k_{4b}	1 nM	Michaelis constant of *Bmal1* transcription
k_{4i}	0.9 nM	Inhibition constant of *Bmal1* transcription
u	3	Hill coefficient of inhibition of *Bmal1* transcription
k_{4d}	1.8 hr^{-1}	Degradation rate of *Bmal1* transcription
k_{5b}	0.14 hr^{-1}	Translation rate of BMAL1
k_{5d}	0.03 hr^{-1}	Degradation rate of cytoplasmatic BMAL1
k_{5t}	0.15 hr^{-1}	Nuclear import rate of BMAL1
k_{6t}	0.06 hr^{-1}	Nuclear export rate of BMAL1
k_{6d}	0.03 hr^{-1}	Degradation rate of nuclear BMAL1
k_{6a}	0.03 hr^{-1}	Activation rate of nuclear BMAL1
k_{7a}	0.003 hr^{-1}	Deactivation rate of nuclear BMAL1
k_{7d}	0.02 hr^{-1}	Degradation rate of activated nuclear BMAL1
v_{8b}	10.6 $nMhr^{-1}$	Maximal rate of REV-ERBα synthesis
k_{8b}	1 nM	Michaelis constant of REV-ERBα synthesis
k_{8i}	1.1 nM	Inhibition constant of REV-ERBα synthesis
r	1	Hill coefficient of activation of REV-ERBα synthesis
v	2	Hill coefficient of inhibition of REV-ERBα synthesis
k_{8d}	1.5 hr^{-1}	Degradation rate of REV-ERBα

Table 3: Becker-Weimann et al., 2004b [10]: Parameters

Goldbeter, 1995 [33]

$$\frac{dM}{dt} = v_s \frac{K_I^n}{K_I^n + P_N^n} - v_m \frac{M}{K_m + M} \tag{20}$$

$$\frac{dP_0}{dt} = k_s M - V_1 \frac{P_0}{K_1 + P_0} + V_2 \frac{P_1}{K_2 + P_1} \tag{21}$$

$$\frac{dP_1}{dt} = V_1 \frac{P_0}{K_1 + P_0} - V_2 \frac{P_1}{K_2 + P_1} - V_3 \frac{P_1}{K_3 + P_1} + V_4 \frac{P_2}{K_4 + P_2} \tag{22}$$

$$\frac{dP_2}{dt} = V_3 \frac{P_1}{K_3 + P_1} - V_4 \frac{P_2}{K_4 + P_2} - k_1 P_2 + k_2 P_N - v_d \frac{P_2}{K_d + P_2} \tag{23}$$

$$\frac{dP_N}{dt} = k_1 P_2 - k_2 P_N \tag{24}$$

Parameter	Value
v_s	0.76 $\mu M h^{-1}$
v_m	0.65 $\mu M h^{-1}$
K_m	0.5 μM
k_s	0.38 h^{-1}
v_d	0.95 $\mu M h^{-1}$
k_1	1.9 h^{-1}
k_2	1.3 h^{-1}
K_I	1 μM
K_d	0.2 μM
n	4
K_1	2 μM
K_2	2 μM
K_3	2 μM
K_4	2 μM
V_1	3.2 $\mu M h^{-1}$
V_2	1.58 $\mu M h^{-1}$
V_3	5 $\mu M h^{-1}$
V_4	2.5 $\mu M h^{-1}$

Table 4: Goldbeter, 1995 [33]: Parameters

Leloup and Goldbeter, 2003 [69]

$$\frac{dM_P}{dt} = v_{sP}\frac{B_N^n}{K_{AP}^n + B_N^n} - v_{mP}\frac{M_P}{K_{mP} + M_P} - k_{dmp}M_P \tag{25}$$

$$\frac{dM_C}{dt} = v_{sC}\frac{B_N^n}{K_{AC}^n + B_N^n} - v_{mC}\frac{M_C}{K_{mC} + M_C} - k_{dmc}M_C \tag{26}$$

$$\frac{dM_B}{dt} = v_{sB}\frac{K_{IB}^m}{K_{IB}^m + B_N^m} - v_{mB}\frac{M_B}{K_{mB} + M_B} - k_{dmb}M_B \tag{27}$$

$$\frac{dP_C}{dt} = k_{sP}M_P - V_{1P}\frac{P_C}{K_p + P_C} + V_{2P}\frac{P_{CP}}{K_{dp} + P_{CP}} + k_4 PC_C - k_3 P_C C_C - k_{dn}P_C \tag{28}$$

$$\frac{dC_C}{dt} = k_{sC}M_C - V_{1C}\frac{C_C}{K_p + C_C} + V_{2C}\frac{C_{CP}}{K_{dp} + C_{CP}} + k_4 PC_C - k_3 P_C C_C - k_{dnc}C_C \tag{29}$$

$$\frac{dP_{CP}}{dt} = V_{1P}\frac{P_C}{K_p + P_C} - V_{2P}\frac{P_{CP}}{K_{dp} + P_{CP}} - v_{dPC}\frac{P_{CP}}{K_d + P_{CP}} - k_{dn}P_{CP} \tag{30}$$

$$\frac{dC_{CP}}{dt} = V_{1C}\frac{C_C}{K_p + C_C} - V_{2C}\frac{C_{CP}}{K_{dp} + C_{CP}} - v_{dCC}\frac{C_{CP}}{K_d + C_{CP}} - k_{dn}C_{CP} \quad (31)$$

$$\frac{dPC_C}{dt} = -V_{1PC}\frac{PC_C}{K_p + PC_C} + V_{2PC}\frac{PC_{CP}}{K_{dp} + PC_{CP}} - k_4 PC_C + k_3 P_C C_C + k_2 PC_N - k_1 PC_C - k_{dn}PC_C \quad (32)$$

$$\frac{dPC_N}{dt} = -V_{3PC}\frac{PC_N}{K_p + PC_N} + V_{4PC}\frac{PC_{NP}}{K_{dp} + PC_{NP}} - k_2 PC_N + k_1 PC_C - k_7 B_N PC_N + k_8 I_N - k_{dn}PC_N \quad (33)$$

$$\frac{dPC_{CP}}{dt} = V_{1PC}\frac{PC_C}{K_p + PC_C} - V_{2PC}\frac{PC_{CP}}{K_{dp} + PC_{CP}} - v_{dPCC}\frac{PC_{CP}}{K_d + PC_{CP}} - k_{dn}PC_{CP} \quad (34)$$

$$\frac{dPC_{NP}}{dt} = V_{3PC}\frac{PC_N}{K_p + PC_N} - V_{4PC}\frac{PC_{NP}}{K_{dp} + PC_{NP}} - v_{dPCN}\frac{PC_{NP}}{K_d + PC_{NP}} - k_{dn}PC_{NP} \quad (35)$$

$$\frac{dB_C}{dt} = k_{sB}M_B - V_{1B}\frac{B_C}{K_p + B_C} + V_{2B}\frac{B_{CP}}{K_{dp} + B_{CP}} - k_5 B_C + k_6 B_N - k_{dn}B_C \quad (36)$$

$$\frac{dB_{CP}}{dt} = V_{1B}\frac{B_C}{K_p + B_C} - V_{2B}\frac{B_{CP}}{K_{dp} + B_{CP}} - v_{dBC}\frac{B_{CP}}{K_d + B_{CP}} - k_{dn}B_{CP} \quad (37)$$

$$\frac{dB_N}{dt} = -V_{3B}\frac{B_N}{K_p + B_N} + V_{4B}\frac{B_{NP}}{K_{dp} + B_{NP}} + k_5 B_C - k_6 B_N - k_7 B_N PC_N + k_8 I_N - k_{dn}B_N \quad (38)$$

$$\frac{dB_{NP}}{dt} = V_{3B}\frac{B_N}{K_p + B_N} - V_{4B}\frac{B_{NP}}{K_{dp} + B_{NP}} - v_{dBN}\frac{B_{NP}}{K_d + B_{NP}} - k_{dn}B_{NP} \quad (39)$$

$$\frac{dI_N}{dt} = -k_8 I_N + k_7 B_N PC_N - v_{dIN}\frac{I_n}{K_d + I_N} - k_{dn}I_N \quad (40)$$

Parameter	Value	Parameter	Value
k_1	0.4 h^{-1}	n	4
k_2	0.2 h^{-1}	v_{1b}	0.5 $nM^{-1}h^{-1}$
k_3	0.4 $nM^{-1}h^{-1}$	v_{1c}	0.6 $nM^{-1}h^{-1}$
k_4	0.2 h^{-1}	v_{1p}	0.4 $nM^{-1}h^{-1}$
k_5	0.4 h^{-1}	v_{1pc}	0.4 $nM^{-1}h^{-1}$
k_6	0.2 h^{-1}	v_{2b}	0.1 $nM^{-1}h^{-1}$
k_7	0.5 $nM^{-1}h^{-1}$	v_{2c}	0.1 $nM^{-1}h^{-1}$
k_8	0.1 h^{-1}	v_{2p}	0.3 $nM^{-1}h^{-1}$
k_{ap}	0.7 nM	v_{2pc}	0.1 $nM^{-1}h^{-1}$
k_{ac}	0.6 nM	v_{3b}	0.5 $nM^{-1}h^{-1}$
k_{ib}	2.2 nM	v_{3pc}	0.4 $nM^{-1}h^{-1}$
k_{dmb}	0.01 h^{-1}	v_{4b}	0.2 $nM^{-1}h^{-1}$
k_{dmc}	0.01 h^{-1}	v_{4pc}	0.1 $nM^{-1}h^{-1}$
k_{dmp}	0.01 h^{-1}	v_{dbc}	0.5 $nM^{-1}h^{-1}$
k_{dn}	0.01 h^{-1}	v_{dbn}	0.6 $nM^{-1}h^{-1}$
k_{dnc}	0.12 h^{-1}	v_{dcc}	0.7 $nM^{-1}h^{-1}$
k_d	0.3 nM	v_{din}	0.8 $nM^{-1}h^{-1}$
k_{dp}	0.1 nM	v_{dpc}	0.7 $nM^{-1}h^{-1}$
k_p	0.1 nM	v_{dpcc}	0.7 $nM^{-1}h^{-1}$
k_{mb}	0.4 nM	v_{dpcn}	0.7 $nM^{-1}h^{-1}$
k_{mc}	0.4 nM	v_{mb}	0.8 $nM^{-1}h^{-1}$
k_{mp}	0.31 nM	v_{mc}	1.0 $nM^{-1}h^{-1}$
k_{sb}	0.12 h^{-1}	v_{mp}	1.1 $nM^{-1}h^{-1}$
k_{sc}	1.6 h^{-1}	v_{sb}	1.0 $nM^{-1}h^{-1}$
k_{sp}	0.6 h^{-1}	v_{sc}	1.1 $nM^{-1}h^{-1}$
m	2	v_{sp}	1.5 $nM^{-1}h^{-1}$

Table 5: Leloup and Goldbeter, 2003 [69]: Parameters

2 Models describing glycolytic oscillations

Goldbeter and Lefever, 1972 [35]

$$\frac{d\alpha}{dt} = \sigma_1 - \sigma_M \Phi \tag{41}$$

$$\frac{d\gamma}{dt} = \sigma_M \Phi - k_s \gamma \tag{42}$$

$$\Phi = \frac{\alpha e(1+\alpha e)(1+\gamma)^2 + L\Theta\alpha ce'(1+\alpha ce')}{L(1+\alpha ce')^2 + (1+\gamma)^2(1+\alpha e)^2} \tag{43}$$

Parameter	Value
σ_1	0.7
σ_M	4
k_s	0.1
L	10^6
c	10^{-5}
e	0.9090909
e'	0.9090909
Θ	1.0

Table 6: Goldbeter and Lefever, 1972 [35]: Parameters

Bier et al., 2000 [13]

$$\frac{dG}{dt} = V_{in} - k_1 GT \tag{44}$$

$$\frac{dT}{dt} = 2k_1 GT - k_p \frac{T}{K_m + T} \tag{45}$$

Parameter	Value
V_{in}	0.36
k_1	0.02
k_p	6.0
K_M	13.0

Table 7: Bier et al., 2000 [13]: Parameters

Wolf and Heinrich, 2000 [146]

$$\frac{dS_1}{dt} = J_0 - \frac{k_1 S_1 A_3}{1 + (A_3/K_I)^q} \tag{46}$$

$$\frac{dS_2}{dt} = \frac{2k_1 S_1 A_3}{1 + (A_3/K_I)^q} - k_2 S_2 (N - N_2) - k_6 S_2 N_2 \tag{47}$$

$$\frac{dS_3}{dt} = k_2 S_2 (N - N_2) - k_3 S_3 (A - A_3) \tag{48}$$

$$\frac{dS_4}{dt} = k_3 S_3 (A - A_3) - k_4 S_4 N_2 - \kappa (S_4 - S_4^{ex}) \tag{49}$$

$$\frac{dN_2}{dt} = k_2 S_2 (N - N_2) - k_4 S_4 N_2 - k_6 S_2 N_2 \tag{50}$$

$$\frac{dA_3}{dt} = -\frac{2k_1 S_1 A_3}{1 + (A_3/K_I)^q} + 2k_3 S_3 (A - A_3) - k_5 A_3 \tag{51}$$

$$\frac{dS_4^{ex}}{dt} = \varphi\kappa \left(S_4 - S_4^{ex}\right) - k S_4^{ex} \tag{52}$$

Parameter	Value
J_0	$2.5\mathrm{m}Mmin^{-1}$
k_1	$100.0\mathrm{m}M^{-1}min^{-1}$
k_2	$6.0\mathrm{m}M^{-1}min^{-1}$
k_3	$16.0\mathrm{m}M^{-1}min^{-1}$
k_4	$100.0\mathrm{m}M^{-1}min^{-1}$
k_5	$1.28\mathrm{m}in^{-1}$
k_6	$12.0\mathrm{m}M^{-1}min^{-1}$
k	$1.8\mathrm{m}in^{-1}$
κ	$13.0\mathrm{m}in^{-1}$
q	4.0
K_I	$0.52\mathrm{m}M$
N	$1.0\mathrm{m}M$
A	$4.0\mathrm{m}M$
φ	0.1

Table 8: Wolf and Heinrich, 2000 [146]: Parameters

3 Models describing Calcium oscillations

Goldbeter et al., 1990 [36]

$$\frac{dZ}{dt} = \nu_0 + \nu_1\beta - V_{M2}\frac{Z^n}{K_2^n + Z^n} + V_{M3}\frac{Y^m}{K_R^m + y^m}\frac{Z^p}{K_A^p + Z^p} + k_f Y - k_Z \quad (53)$$

$$\frac{dY}{dt} = V_{M2}\frac{Z^n}{K_2^n + Z^n} - V_{M3}\frac{Y^m}{K_R^m + y^m} - k_f Y \quad (54)$$

Parameter	Value
ν_0	$1\ \mu Ms^{-1}$
k	$10\ \mathrm{s}^{-1}$
k_f	$1\ \mathrm{s}^{-1}$
ν_1	$7.3\ \mu Ms^{-1}$
V_{M2}	$65\ \mu Ms^{-1}$
V_{M3}	$500\ \mu Ms^{-1}$
K_2	$1\ \mu M$
K_R	$2\ \mu M$
K_A	$0.9\ \mu M$
m	2

continued on next page

continued from previous page

Parameter	Value
n	2
p	4
β	0.4

Table 9: Goldbeter et al., 1990 [36]: Parameters

Somogyi and Stucki, 1991 [117]

$$\frac{dx}{dt} = k_s y - kx - \alpha x \frac{y^n}{a^n + y^n} \tag{55}$$

$$\frac{dy}{dt} = kx - k_s y + \alpha x \frac{y^n}{a^n + y^n} + \gamma - \beta y \tag{56}$$

Parameter	Value
n	4
k	0.01
k_s	2
α	4.5
β	1
γ	1
a	2

Table 10: Somogyi and Stucki, 1991 [117]: Parameters

Marhl et al., 2000 [74]

$$\frac{dCa_{cyt}}{dt} = J_{ch} + J_{leak} - J_{pump} + J_{out} - J_{in} + k_{-}CaPr - k_{+}Ca_{cyt}Pr \tag{57}$$

$$\frac{dCa_{ER}}{dt} = \frac{\beta_{ER}}{\rho_{ER}}(J_{pump} - J_{ch} - J_{leak}) \tag{58}$$

$$\frac{dCa_m}{dt} = \frac{\beta_m}{\rho_m}(J_{in} - J_{out}) \tag{59}$$

with

$$J_{pump} = k_{pump} Ca_{cyt} \tag{60}$$

$$J_{ch} = k_{ch} \frac{Ca_{cyt}^2}{K_1^2 + Ca_{cyt}^2} (Ca_{ER} - Ca_{cyt}) \tag{61}$$

$$J_{leak} = k_{leak} (Ca_{ER} - Ca_{cyt}) \tag{62}$$

$$J_{in} = k_{in} \frac{Ca_{cyt}^8}{K_2^8 + Ca_{cyt}^8} \tag{63}$$

$$J_{out} = \left(k_{out} \frac{Ca_{cyt}^2}{K_3^2 + Ca_{cyt}^2} + k_m \right) Ca_m \tag{64}$$

and

$$Ca_{tot} = Ca_{cyt} + \frac{\rho_{ER}}{\beta_{ER}} Ca_{ER} + \frac{\rho_m}{\beta_m} Ca_m + CaPr \tag{65}$$

$$Pr_{tot} = Pr + CaPr \tag{66}$$

Parameter	Value
Total concentration	
Ca_{tot}	$90\mu M$
Pr_{tot}	$120\mu M$
Geometric parameters	
ρ_{ER}	0.01
ρ_m	0.01
β_{ER}	0.0025
β_m	0.0025
Kinetics parameters	
k_{ch}	800 s^{-1}
k_{pump}	20 s^{-1}
k_{leak}	0.05 s^{-1}
k_{in}	300 $\mu M s^{-1}$
k_{out}	125 s^{-1}
k_m	0.00625 s^{-1}
k_+	0.1 $\mu M^{-1} s^{-1}$
k_-	0.01 s^{-1}
K_1	5 μM
K_2	0.8 μM
K_3	5 μM

Table 11: Marhl et al., 2000 [74]: Parameters

Danksagung

In erster Linie möchte ich mich bei Herrn Prof. Dr. Hanspeter Herzel bedanken, der es mir ermöglichte, meine Doktorarbeit am Institut für Theoretische Biologie anzufertigen. Ich fand hier die perfekte Kombination von Unterstützung und Freiheit für meine Arbeit.

Vielen Dank an Prof. Dr. Achim Kramer, der immer ein offenes Ohr hatte für meine biologischen Fragen und Probleme. Dadurch konnte ich nicht nur von seinem immensen Wissen über circadiane Uhren profitieren, sondern auch viel über das wissenschaftliche Arbeiten an sich lernen.

Many thanks to Frank Doyle who gave me the opportunity to spend part of my time as a PhD student in his lab in Santa Barbara. Learning the point of view of engineers on biological systems was a great experience.

Jana, vielen Dank für die zahllosen Diskussionen über Rückkopplungen, Oszillationen und Robustheit, die ich immer sehr hilfreich und inspirierend fand. Und einfach vielen Dank für die wundervolle Atmosphäre in unserem Büro und die netten Kaffeepäuschen, die mir immer die Arbeit versüßt haben.

Vielen Dank, Florian, für Deinen engagierten Einsatz bei der Modelierung von Synchronization, und vor allem für Deine Hilfe bei so manchem Computerproblem.

Thank you, Didier, for many interesting discussions about oscillations and the circadian clock. I enjoyed working with you very much.

Tausend Dank auch an Niels Bluethgen, Jürgen Neubauer und Andreas Hanschmann, die mir mit ihrem unermüdlichem Einsatz und ihrem Computerwissen immer wieder auf die Sprünge halfen.

Many thanks to everybody in the Herzel, Kramer and Doyle groups. Because of you I will always remember the years as a PhD student as a very enriching experience and a wonderful time with a lot of fun.

Danke Tanja, danke, Bettina, füer die vielen motivierenden Worte in den Durststrecken, ohne die die Arbeit möglicherweise in einer Schublade verschwunden wäre.

Vielen, vielen Dank auch meiner ganzen Familie. Ihr habt mich nicht nur bis hierher gebracht, ohne Euch und Euren großartigen Einsatz in den letzten Wochen wäre die Arbeit nie fertig geworden.

Vielen Dank, Holger, daß Du für mich da bist. Ich liebe Dich.

Selbständigkeitserklärung

Hiermit erkläre ich, die vorliegende Arbeit selbständig und ausschließlich unter Verwendung der angegebenen Literatur und Hilfstmittel angefertigt zu haben.